

ASPECTS OF THE LIFE HISTORY, ECOPHYSIOLOGY, BIOENERGETICS, AND
POPULATION DYNAMICS OF THE COWNOSE RAY, *RHINOPTERA BONASUS*,
IN THE NORTHERN GULF OF MEXICO

A Dissertation

Submitted to the Graduate Faculty of the
Louisiana State University and
Agricultural and Mechanical College
In partial fulfillment of the
Requirements for the degree of
Doctor of Philosophy

in

The Department of Oceanography and Coastal Sciences

by

Julie Ann Neer

B.S., California State University – Long Beach, 1993

M.S., San Jose State University, 1998

August 2005

ACKNOWLEDGEMENTS

First, I must thank my major professors, Kenny Rose and Bruce Thompson, for without their guidance this research would not have been completed. Thanks to Kenny for introducing and educating me on the fine art of modeling. Thanks to Bruce for all the long discussions on my research, elasmobranchs in general, and nothing in particular. Thanks also to the rest of my Committee. Jay Geaghan helped me over my statistical obstacles. Enric Cortés provided invaluable assistance with the matrix modeling. Thanks to Mark Mitchell for bringing a veterinarian's viewpoint to the research. Additionally, Greg Stone and Andy Nyman offered insightful comments that greatly improved the quality of this work. Thanks go to I. E. Baremore, D. Bethea, J. K. Carlson, and all the Shark Population Assessment Group interns with assistance in collection and maintenance of the rays. Special thanks to John Carlson for educating me in the wonderful world of ecophysiology. This research was partially funded by the National Marine Fisheries Service/National Sea Grant Joint Fellowship Program in Population Dynamics and Marine Resource Economics. Additional thanks go to the National Marine Fisheries Service – Panama City, Florida Laboratory for providing logistical support without which this research would not have been possible. Thanks to the secretarial and administrative staff of the Coastal Fisheries Institute, Department of Oceanography, Louisiana Sea Grant, and the Graduate School for guidance and support with all aspects of my paper trail through the University. Thanks to Shaye Sable for all of her time spent with the modeling novice. Ted Switzer provided invaluable statistics help. Special thanks to Jason Blackburn for time on the water, nights in the lab, and Anders Osborne. I thank my parents, Carol and David, for putting up with me for one more degree. (I think I'm done now!). Finally, thanks to Fred Martin for constant unwavering support,

logistically, financially, personally, and emotionally. You are the love of my life and I cannot wait for our wedding and the chance to begin the rest of our lives together, whatever that may bring.

TABLE OF CONTENTS

	Page
ACKNOWLEDGEMENTS -----	ii
LIST OF TABLES -----	vi
LIST OF FIGURES -----	vii
ABSTRACT -----	ix
CHAPTER I. INTRODUCTION -----	1
Literature Cited -----	6
CHAPTER II. LIFE HISTORY OF THE COWNOSE RAY, <i>RHINOPTERA BONASUS</i> , IN THE NORTHERN GULF OF MEXICO, WITH COMMENTS ON GEOGRAPHIC VARIABILITY IN LIFE HISTORY TRAITS -----	8
Introduction -----	8
Materials and Methods -----	9
Results -----	16
Discussion -----	27
Literature Cited -----	31
CHAPTER III. OXYGEN CONSUMPTION OF THE COWNOSE RAY, <i>RHINOPTERA BONASUS</i> : THE EFFECT OF TEMPERATURE AND SALINITY -----	35
Introduction -----	35
Materials and Methods -----	36
Results -----	39
Discussion -----	43
Literature Cited -----	48
CHAPTER IV. MODELING THE EFFECTS OF TEMPERATURE ON INDIVIDUAL AND POPULATION GROWTH OF THE COWNOSE RAY, <i>RHINOPTERA BONASUS</i> : A BIOENERGETICS APPROACH -----	52
Introduction -----	52
Materials and Methods -----	56
Results -----	76
Discussion -----	95
Literature Cited -----	105
CHAPTER V. SUMMARY -----	112
Literature Cited -----	119

APPENDIX: LETTER OF PERMISSION FROM ENVIRONMENTAL BIOLOGY OF
FISHES -----121

VITA -----124

LIST OF TABLES

Table 2.1. Summary of goodness-of-fit of four models fitted to observed size-at-age data for the cownose ray from the northern Gulf of Mexico.-----	22
Table 3.1. Experimental trials for the cownose ray summarizing weight, temperature, salinity, and oxygen consumption rate (MO_2). Standard errors are shown in parentheses.-----	40
Table 3.2. Summary of repetitive oxygen consumption (MO_2) trials at differing salinities. Standard errors are shown in parentheses. -----	44
Table 3.3. Summary of oxygen consumption rates (MO_2) for select elasmobranch species. All rates reported were determined at 20 °C using flow-through respirometry, except noted. Standard errors are shown in parentheses when available. *determined using static respirometry.-----	46
Table 4.1. Bioenergetics parameter values used in the cownose ray bioenergetics model. --	62
Table 4.2. Percent change in age-specific p-values in relation to the Baseline scenario.-----	80
Table 4.3. Percent change in age-specific daily consumption (%BW/day in g ray/g ray/day) in relation to the Baseline scenario.-----	82
Table 4.4. Reproductive output by age (m_i ; number of female pups/female) for the Baseline, cooler, and warmer scenarios under the Temperature Effect simulations. -----	84
Table 4.5. Percent of the population reproducing by age for the Baseline, cooler, and warmer scenarios under the Temperature Effect simulations.-----	85
Table 4.6. Demographic parameters calculated from the matrix projection model configured with bioenergetics outputs under the Baseline and four Temperature Effect simulations. λ = population growth rate; r = intrinsic rate of change; R_0 = net reproductive rate; \bar{A} = mean age of the parents of the offspring produced by a population at the stable age distribution.-----	88

LIST OF FIGURES

Figure 1.1. Organizational flowchart of this dissertation. Dotted shapes indicate data measured as part of this dissertation.-----	4
Figure 2.1 Location of three main collections sites for cownose rays off Florida in the northwest portion of the Gulf of Mexico. -----	10
Figure 2.2. Sagittal section from an 860 mm female cownose ray vertebra used for age determination. This ray was estimated to be 11 ⁺ years old.-----	12
Figure 2.3. Length frequency histogram for cownose rays examined during this study (n = 227).-----	17
Figure 2.4. Mean marginal increment analysis for cownose rays (n = 169) by a) month and b) season. Vertical bars are ± one standard deviation.-----	19
Figure 2.5. Mean marginal increment analysis for young-of-the-year cownose rays (n = 20) by a) month and b) season. Vertical bars are ± one standard deviation.-----	20
Figure 2.6. Growth functions fitted to the combined sexes observed size-at-age data for cownose rays (n = 227).-----	23
Figure 2.7. Relationship between maturity and disk width for the cownose ray. A logistic regression model was fitted to the binominal maturity data (0 = immature, 1 = mature). -----	25
Figure 2.8. Relationship between outer clasper length and disk width for the cownose ray (n = 99). -----	26
Figure 3.1. Standard mass-dependent oxygen consumption rates (mg O ₂ kg ⁻¹ hr ⁻¹) determined for the cownose ray. Mean (± standard error) are presented for the four temperature groups (19, 22, 25, and 28 °C ± one degree), along with the raw data.-----	41
Figure 3.2. Relationship of mass and standard mass-dependent oxygen consumption rates (mg O ₂ kg ⁻¹ hr ⁻¹) for the four temperature groups (19, 22, 25, and 28 °C ± one degree) determined for the cownose ray. -----	42
Figure 4.1. Average daily temperature experienced by the rays in the bioenergetics model for the four altered temperature scenarios. Baseline is shown on all graphs. Day 1 represents May 1 st . -----	66
Figure 4.2. Comparison of model-predicted average weights-at-age with the Gompertz growth curve determined from cownose ray weight-at-age field data. Error bars represent plus or minus one standard deviation from the mean of the model-predicted data. -----	77

Figure 4.3. Comparison of model-predicted individual weight-at-age data with the observed cownose ray weight-at-age field data. The model-predicted average weights-at-age and the Gompertz growth curve are also shown. -----78

Figure 4.4. Average weight of all individuals alive on Day 365 of each year of the simulation. -----79

Figure 4.5. Predicted survivorship curves for the Baseline scenario and four alternative temperature scenarios for the Temperature Effect simulations. -----87

Figure 4.6. Predicted stable age distributions for the Baseline and four temperature scenarios. -----90

Figure 4.7. Predicted reproductive values for the Baseline and four alternative temperature scenarios. Fifty percent maturity, determined from field data, is also shown.-----91

Figure 4.8. The elasticity of age-specific survival ($e(P_i)$), and elasticity of age-specific fertility ($e(f_i)$) for the Baseline and four alternative temperature scenarios.-----93

Figure 4.9. The elasticity of λ to fertility ($e(f)$), juvenile survival ($e(P_j)$) and adult survival ($e(P_a)$) examined by life stage for each scenario.-----94

ABSTRACT

The cownose ray, *Rhinoptera bonasus*, is an elasmobranch commonly observed throughout the Gulf of Mexico. Cownose rays appear to be sensitive to water temperature. I performed laboratory experiments and collected field data to obtain basic life history information, and used the information to configure an individual-based bioenergetics model. The bioenergetics model was coupled to a matrix projection model, and the coupled models were used to predict how warmer and cooler water temperatures, compared to current conditions, would affect the growth and population dynamics of the cownose rays. The life history study determined weight at age, maturity by weight, and fecundity for cownose rays. Verified vertebral age estimates ranged from 0⁺ to 18⁺ years. Likelihood ratio tests indicated that a combined sexes Gompertz model best described the growth of cownose rays. A relationship between maturity and weight was estimated; annual fecundity was determined to be one pup. The laboratory experiments resulted in the estimation of standard oxygen consumption rate as a function of weight and temperature, and a Q₁₀ value of 2.33. The bioenergetics model predicted that rays would have a slower growth rate and reach smaller average weights at age (9.6-16.8% smaller) if they inhabited 2°C warmer water than baseline (current) conditions, while individuals would grow faster and attain heavier weights at age (13.4-17.2% heavier) under a 2°C cooler scenario. Changes in growth rates under the warmer and cooler conditions also lead to changes in age-specific survivorship, maturity, and pup production, which I used as inputs to a matrix projection model. Faster growth of individuals under the cooler scenarios translated into an increased population growth rate (4.4-4.7%/year versus 2.7%/year under baseline), shorter generation time, and higher net reproductive rates, while slower growth under the warmer scenarios translated into slower population growth rate

(0.05-1.2%/year), longer generation times, and lower net reproductive rates. Elasticity analysis indicated that population growth rate was most sensitive to adult survival.

Reproductive values by age were highest for intermediate ages. The combination of coordinated laboratory experiments, field data collection, and coupled individual-based bioenergetics and matrix projection models provides a powerful approach for relating physiology to demographic responses.

CHAPTER I.

INTRODUCTION

Understanding the underlying factors contributing to population fluctuations is necessary for the adequate conservation and management of long-lived species. The cownose ray, *Rhinoptera bonasus*, is a marine elasmobranch commonly observed throughout the Gulf of Mexico (McEachran and Fechhelm 1998). Elasmobranchs (sharks, skates, and rays) are long-lived, late reproducing, low fecundity organisms, with many species having complex reproductive cycles and movement patterns (Compagno 1990, Hoenig and Gruber 1990, Castro 1993). The "K-selected" life history characteristics of these species make them extremely susceptible to overfishing (Holden 1974), and to variation in other natural and anthropogenic factors (Heppell et al. 1999, Russell 1999).

Cownose ray abundance and distribution seems to be determined, at least in part, by water temperature (Smith and Merriner 1987, Schwartz 1990). Cownose rays appear in the Chesapeake Bay when water temperatures reach 16°C in the spring, and usually begin their southward migration when water temperatures cool to 22°C in the fall (Smith and Merriner 1987, Schwartz 1990). Along the northwest Florida shelf, rays begin to depart the area when the summer water temperatures are between 28°C and 30°C, and very few rays are captured at temperatures warmer than 30°C (John Carlson, personal communication). These movements in response to temperature suggest that cownose rays may behaviorally thermoregulate.

The overall objectives of my research were to obtain basic life history information on cownose rays in the northern Gulf of Mexico and to simulate the effects of water temperatures warmer and cooler than current conditions on the growth rates and population dynamics of cownose rays. Warmer and cooler water temperatures can result from interannual variation in

environmental conditions and from global climate change. I performed laboratory experiments and collected field data to provide site-specific information on size- and weight-at-age, growth rates, reproduction (Chapter II), and metabolic rates (Chapter III) of cownose rays. In addition to these results providing useful information on the life history of cownose rays, I also used the information to help refine and calibrate an individual-based cownose ray bioenergetics model.

The life history study (Chapter II) focused on obtaining basic biological information on the cownose ray. Chapter II consisted of two parts: 1) a vertebral ageing study to determine estimates of age, growth rate, and longevity, and 2) a reproductive component focusing on the determination of size at maturity, fecundity, gestation length, and timing of parturition. Age estimates were determined using vertebral sections and the timing of the band deposition was verified using marginal increment ratio analysis. I then fitted the size-at-age data to four different growth models, and used likelihood ratio tests to determine which model best described the data and whether there were sex differences in growth patterns. Male and female reproductive status was determined using multiple physiological criteria, and a logistic function was fitted to the binomial maturity data to estimate median size at 50% maturity. Gravid females also provided information on litter size and the seasonal reproductive cycle.

The metabolism component of my dissertation (Chapter III) was directed at obtaining estimates of standard oxygen consumption rate (MO_2) and the determination of Q_{10} , a measure of temperature sensitivity. Flow-through respirometry experiments were conducted on seasonally acclimated cownose rays to determine MO_2 rates. Multiple regression analysis

was used to examine how temperature, salinity, and body mass affected these rates. I also used the MO_2 estimates to calculate a Q_{10} value.

The modeling strategy (Chapter IV) consisted of coupling an individual-based bioenergetics model to a matrix projection model, which were then used in combination to predict how water temperatures warmer and cooler than current conditions would affect the growth and population dynamics of the cownose ray in the northern Gulf of Mexico (Figure 1.1). In Figure 1.1, hatched diamonds represent the models used, dotted shapes represent data measured as part of this dissertation, and open squares or rectangles represent model outputs. The metabolism-related parameters of the bioenergetics model were estimated from laboratory experiments on metabolism (Chapter III), fecundity and maturity at age parameters used in the bioenergetics model were estimated from the age and growth field study (Chapter II), and the bioenergetics model was calibrated to weights-at-age also measured in the field study (Chapter II). Warmer and cooler water temperature scenarios were simulated, each under two alternative assumptions about whether rays could find cooler water if conditions got too warm. The bioenergetics model followed the daily growth, survival, and reproduction of individuals from birth to age 25 years. The bioenergetics model was run in two modes: Temperature Effect and Consumption Effect. Temperature Effect mode allowed for rays to grow differently in response to warmer and cooler water temperatures than baseline (field-based) weights-at-age, while the Consumption Effect allowed for estimation of the changes in food intake needed for rays to maintain their baseline weights-at-age under the warmer and cooler conditions. The outputs of age-specific survival and reproductive rates from the bioenergetics model under the Temperature Effects mode were then used to estimate the parameters (inputs) of an age-based matrix projection model. The matrix model was then

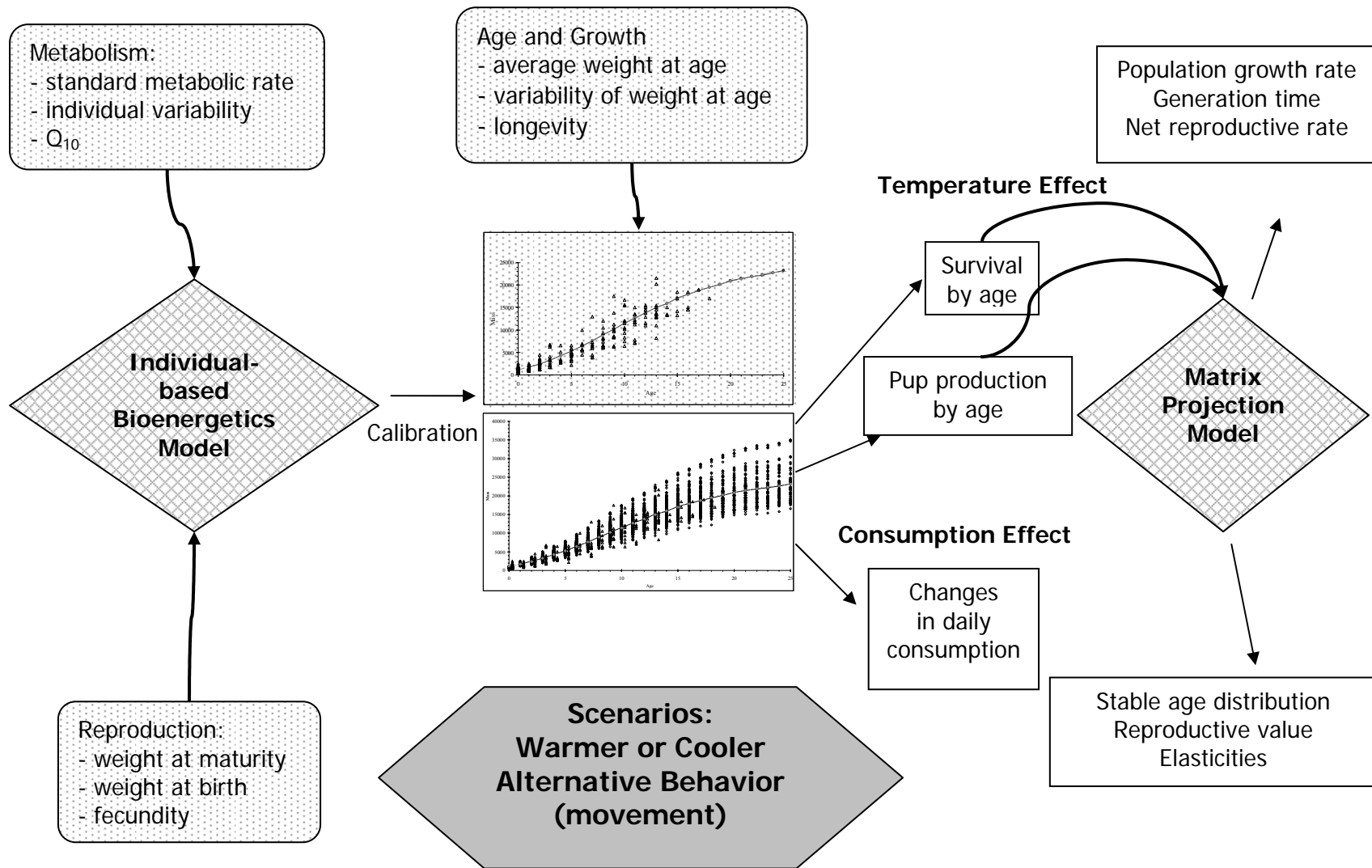


Figure 1.1. Organizational flowchart of this dissertation. Dotted shapes indicate data measured as part of this dissertation.

analyzed to obtain estimates of population growth rate, stable age-distributions, net reproductive rate, generation times, and elasticities (sensitivity of growth rate to survival and reproduction).

Bioenergetics and matrix projection models have been widely used for teleost fishes (Ney 1993, Hanson et al. 1997, Caswell 2001), but much less so for elasmobranchs (Du preez et al. 1990, Cortés 2002, Frisk et al. 2002, Schindler et al. 2002). Bioenergetics modeling is appealing as it provides a link between fish physiology and environmental conditions, and provides a means for quantifying the relative importance of various environmental factors on individual growth or consumption (Adams and Breck 1990, Brandt and Hartman 1993). Matrix projection models provide a link between the growth, survival, and reproduction of an individual and the long-term population dynamics of the species (Caswell 2001).

In this dissertation, I used laboratory experiments, field data collection, and simulation modeling to provide some basic information about cownose ray life history, and to improve our understanding of cownose ray responses to changes in water temperature. Chapter II presents the results of the field data study on age, growth, and reproduction, and Chapter III presents the results of the metabolic experiments. Chapter IV presents the results of the coupled individual-based bioenergetics and matrix projection models, and discusses the likely individual and population consequences of warmer and cooler water temperatures on cownose rays, future areas of research to improve the models, and the implications of the modeling results to resource management. The final chapter (Chapter V) summarizes the major results of this dissertation.

Literature Cited

- Adams, S.M. and J.E. Breck. 1990. Bioenergetics. Pages 389-415 in C.B. Schreck and P.B. Moyle, editors. Methods for fish biology. American Fisheries Society, Bethesda, Maryland.
- Brandt, S.B. and K.J. Hartman. 1993. Innovative approaches with bioenergetics models: future applications to fish ecology and management. Transactions of the American Fisheries Society 122:731-735.
- Castro, J. I. 1993. The shark nursery of Bulls Bay, South Carolina, with a review of the shark nurseries of the southeastern coast of the United States. Environmental Biology of Fishes 38: 37-48.
- Caswell, H. 2001. Matrix population models: construction, analysis, and interpretation. 2nd Ed. Sinauer Associates, Inc., Sunderland, Massachusetts.
- Cortés, E. 2002. Incorporating uncertainty into demographic modeling: application to shark populations and their conservation. Conservation Biology 16(4): 1048-1062.
- Compagno, L. J. V. 1990. Alternative life history styles of cartilaginous fishes in time and space. Environmental Biology of Fishes 28:33-75.
- Du Preez, H.H., A. McLachlan, J.F.K. Marais, and A.C. Cockcroft. 1990. Bioenergetics of fishes in a high-energy surf-zone. Marine Biology 106: 1-12.
- Frisk, M.G., T.J. Miller, and M.J. Fogarty. 2002. The population dynamics of little skate *Leucoraja erinacea*, winter skate *Leucoraja ocellata*, and barndoor skate *Dipturus laevis*: predicting exploitation limits using matrix analyses. ICES Journal of Marine Science 59: 576-586.
- Hanson, P.C., T.B. Johnson, D.E. Schindler, and J.F. Kitchell. 1997. Fish Bioenergetics 3.0. University of Wisconsin-Madison Center for Limnology. Wisconsin Sea Grant Institute.
- Heppell, S.S., L.B. Crowder, and T.R. Menzel. 1999. Life table analysis of long-lived marine species with implications for conservation and management. Pages 137-146 in J. A. Musick, editor. Life in the slow lane: ecology and conservation of long-lived marine animals. American Fisheries Society Symposium 23, Bethesda, Maryland.
- Hoenig, J.M. and S.H. Gruber. 1990. Life-history patterns in the elasmobranch: implications for fisheries management. Pages 1-16 in H.L. Pratt, S.H. Gruber, and T. Taniuchi, editors. Elasmobranchs as living resources: Advances in the biology, ecology, systematics, and the status of the fisheries. U.S. Department of Commerce. NOAA Technical Report NMFS 90.

- Holden, M.J. 1974. Problems in the rational exploitation of elasmobranch populations and some suggested solutions. Pages 117-137 *in* Sea fisheries research. F.R. Harden-Jones, editor. John Wiley and Sons, New York.
- McEachran, J.D. & J.D. Fechhelm. 1998. Fishes of the Gulf of Mexico. Volume 1. University of Texas Press.
- Ney, J.J. 1993. Bioenergetics modeling today: growing pains on the cutting edge. *Transactions of the American Fisheries Society* 122:736-748.
- Russell, R.W. 1999. Comparative demography and life history tactics of seabirds: implications for conservation and marine monitoring. Pages 51-76 *in* J. A. Musick, editor. *Life in the slow lane: ecology and conservation of long-lived marine animals*. American Fisheries Society Symposium 23, Bethesda, Maryland.
- Schindler, D.E., T.E. Essington, J.F. Kitchell, C. Boggs, and R. Hilborn. 2002. Sharks and tunas: Fisheries impacts on predators with contrasting life histories. *Ecological Applications* 12(3):735-748.
- Schwartz, F.J. 1990. Mass migratory congregations and movements of several species of cownose rays, Genus *Rhinoptera*: a world-wide review. *Journal of the Elisha Mitchell Scientific Society* 106:10-13.
- Smith, J.W. and J.V. Merriner 1987. Age and growth, movements and distribution of the cownose ray, *Rhinoptera bonasus*, in Chesapeake Bay. *Estuaries* 10(2): 153-164.

¹CHAPTER II.

LIFE HISTORY OF THE COWNOSE RAY, *RHINOPTERA BONASUS*, IN THE NORTHERN GULF OF MEXICO, WITH COMMENTS ON GEOGRAPHIC VARIABILITY IN LIFE HISTORY TRAITS.

Introduction

Variability in life history traits for geographically separated populations of the same species has been documented for several species of elasmobranchs. Driggers et al. (2004) found differences in growth parameters and theoretical longevity between the Gulf of Mexico and the western Atlantic Ocean for the blacknose shark, *Carcharhinus acronotus*. Carlson et al. (2003) determined that the finetooth shark, *C. isodon*, obtained a smaller size at maturation in the Gulf of Mexico versus the Atlantic Ocean. Latitudinal variation in life history traits for the bonnethead shark, *Sphyrna tiburo*, in the eastern Gulf of Mexico has also been documented (Parsons 1993, Lombardi-Carlson et al. 2003). To date, no studies examining the variability of life history traits between the Gulf of Mexico and the western Atlantic Ocean have been published on batoids (skates and rays).

The cow-nosed rays (Family Rhinopteridae) are aplacental viviparous elasmobranchs occurring worldwide in tropical and warm temperate seas, and estuaries (McEachran and Fechhelm 1998). They are semi-pelagic and gregarious, often forming large schools (McEachran and Capapé 1984). Currently, there are five recognized species occupying a single genus (Schwartz 1990).

¹ Reprinted with kind permission of Springer Science and Business Media. Minor editorial changes were made in response to the comments of the dissertation committee.

The cownose ray, *Rhinoptera bonasus*, ranges from southern New England to southern Brazil within the western Atlantic Ocean as well as throughout the Gulf of Mexico and off Cuba (Bigelow and Schroeder 1953, McEachran and Fechhelm 1998). They are most often encountered on continental and insular shelves where they feed primarily on bivalve mollusks and crustaceans (Smith and Merriner 1985; McEachran and Fechhelm 1998). Information on the age and growth and reproduction of the cownose ray in the Chesapeake Bay can be found in Smith and Merriner (1986, 1987). Additional preliminary information on the reproductive biology of cownose rays in the Atlantic Ocean has been presented in an abstract by Schwartz (1967). Smith and Merriner (1987) and Blaylock (1993) presented information on the distribution and movement of the cownose ray in the Chesapeake Bay, while Schwartz (1990) reported on the migratory movements of several species in the genus.

Whereas information exists regarding geographic variability in life history traits for sharks between the western Atlantic Ocean and the Gulf of Mexico, no evidence is available for batoids. Additionally, no published information is available on the age and growth of any batoid within the Gulf of Mexico. To address this lack of information, I sought to: 1) estimate age and growth for the cownose ray; 2) ascertain size and age at maturity, fecundity, and gestation for the cownose ray; and 3) compare these estimates with those derived for cownose rays from the western North Atlantic Ocean.

Materials and Methods

Specimen Collection and Laboratory Processing

Cownose ray specimens were collected from fishery-independent sources in the northern Gulf of Mexico (Figure 2.1). Samples were collected from June 1999 through

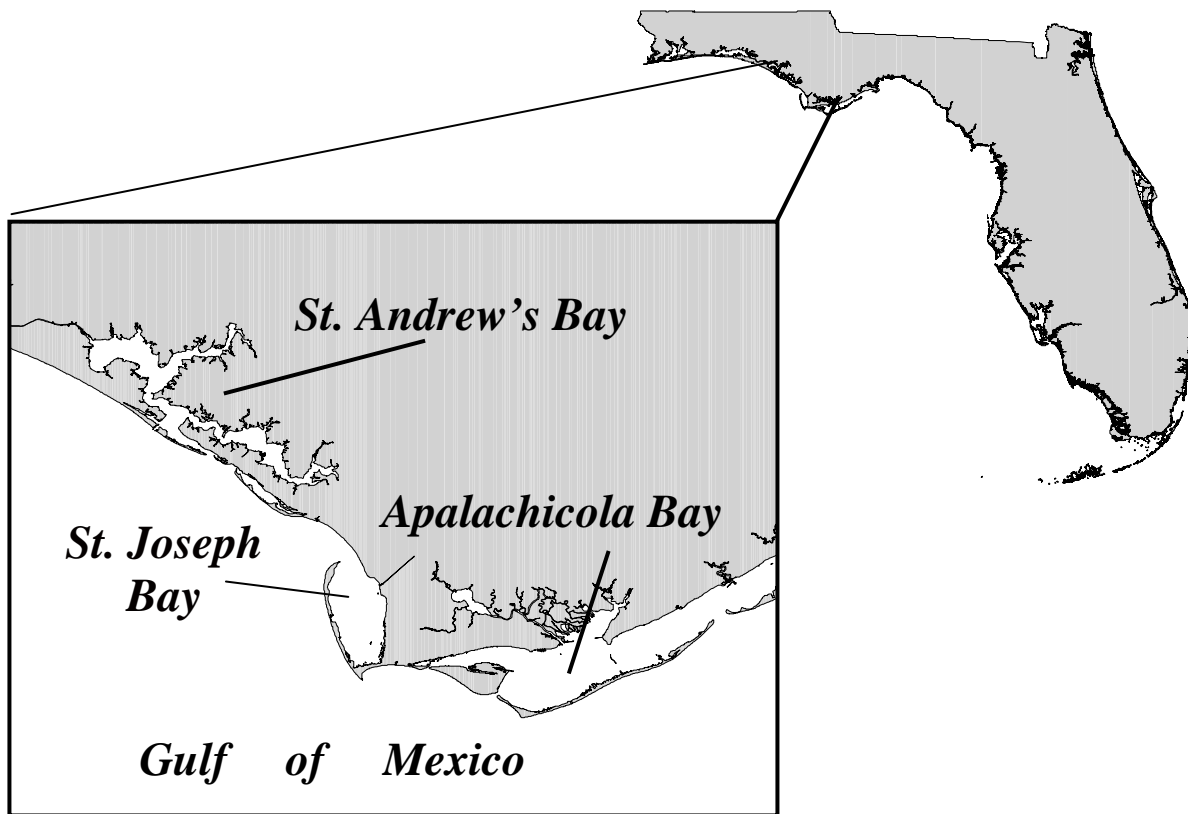


Figure 2.1 Location of three main collections sites for cownose rays off Florida in the northwest portion of the Gulf of Mexico.

November 2003. Details of the fishery-independent gillnet surveys can be found in Neer et al. (In press) and Carlson and Brusher (1999).

External examinations were conducted for all specimens. Rays were sexed, weighed to the nearest 0.1 kg, and measures to the nearest disk width (DW, mm). Outer clasper length (from free tip of clasper to where clasper meets the pelvic fin; Compagno 1984) was recorded for males. A detailed internal reproductive examination was also completed for all specimens (see Reproduction).

Five to seven vertebral centra were removed from the 15th through 25th vertebrae and prepared for age estimation following techniques outlined in Neer and Cailliet (2001). Sex-

specific relationships between disk width and centrum diameter (CD) were calculated to assess the appropriateness of using vertebrae as an ageing structure. Centrum diameter (mm) was measured using digital calipers for each specimen before sectioning. As no difference was found between sexes (ANCOVA: $F = 3.596$, $df = 1$, $p > 0.05$), I combined the log transformed data to generate a linear relationship: $\log DW = 0.779 * \log CD + 5.370$ ($p < 0.0001$; $r^2 = 0.96$; $n = 227$).

Sagittal vertebral sections 0.3 mm in thickness were cut from the vertebrae using a Buhler Isomet low speed saw. Sections were stained with a 0.01% crystal violet solution following Carlson et al. (2003). Each section was mounted on a glass microscope slide with clear resin and age estimates were determined by examining the sections under a dissecting microscope with transmitted light (Figure 2.2).

Age Assessment and Verification

I counted each specimen twice without knowledge of its size or sex. Each growth cycle included a broad band representing summer growth and a narrow band representing winter growth (Cailliet and Goldman 2004). The narrow bands were counted for age determination. If the band counts did not agree between the first two readings, the specimen was counted a third time to reach a consensus with one of the previous band counts. If no consensus was reached, the sample was discarded. An index of average percent error (APE; Beamish and Fournier 1981), percent error (D; Chang 1982), and percentage of disagreements by $\pm i$ rings (Cailliet et al. 1990) between counts were computed. Only the first two band counts were used in the precision analysis, as not all specimens were counted a third time.

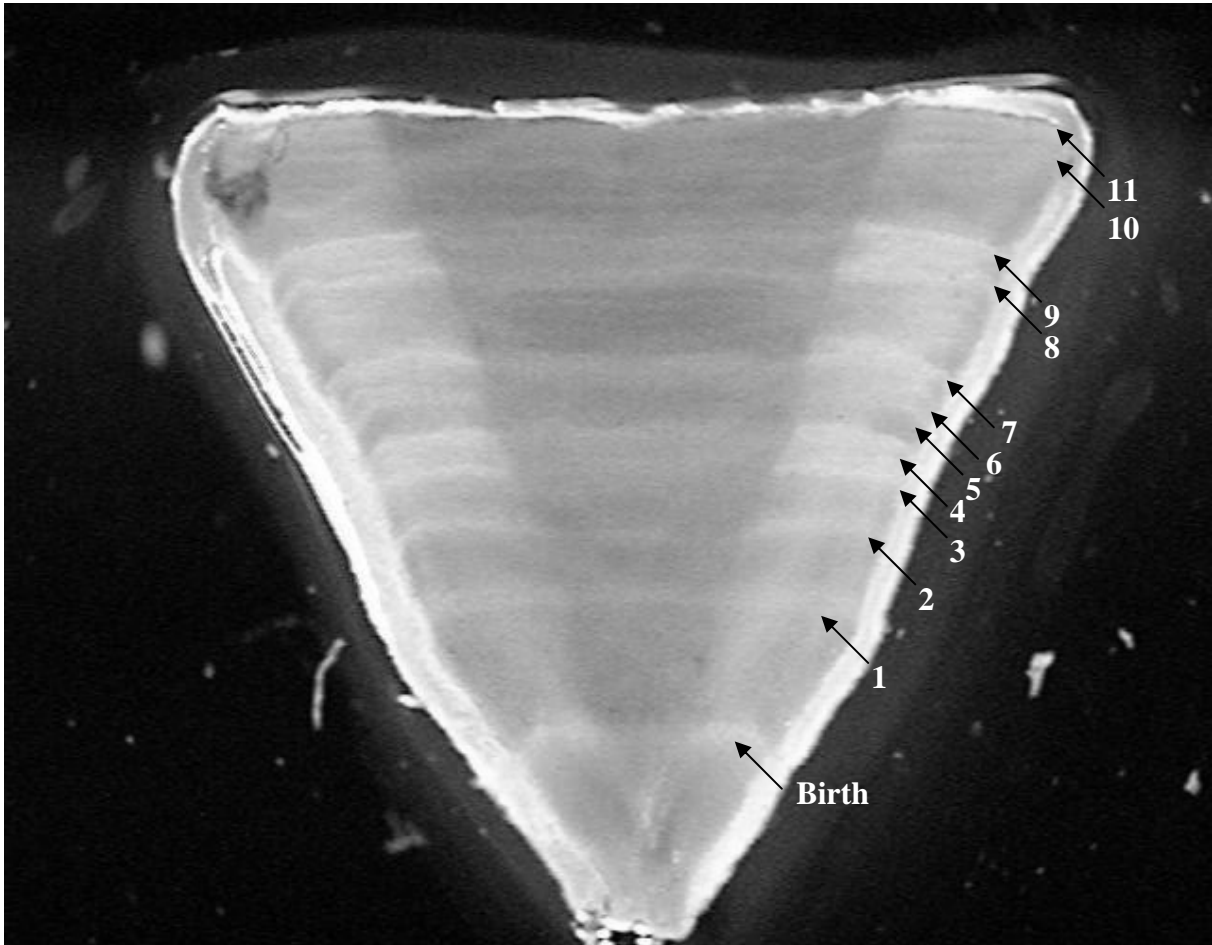


Figure 2.2. Sagittal section from an 860 mm DW female cownose ray vertebra used for age determination. This ray was estimated to be 11⁺ years old.

In order to examine the annual periodicity of the band formation, verification was accomplished using the relative marginal increment analysis following Natanson et al. (1995):

$$MIR = \frac{VR - R_n}{R_n - R_{n-1}}$$

where MIR = the marginal increment ratio; VR = the vertebral radius; R_n = the last complete narrow band; and R_{n-1} = the next-to-last complete narrow band. The distances from the centrum origin to the distal edge of the last two growth bands and from the centrum origin to

the centrum edge were measured using the Image Tools Version 3 Software Package (Department of Dental Diagnostics Science, University of Texas Health Center, Austin, TX). Mean MIR was plotted against month and season (Spring = March – May; Summer = June – August; Fall = September – November; Winter = December - February) to examine trends in band formation. A one-way analysis of variance was used on the arcsine-transformed MIR data to examine for differences between month and season (Zar 1984). This analysis was completed for rays of all size classes and for rays only displaying two bands in the vertebral section (young-of-the-year individuals; YOY) to examine potential differences in conducting the analysis over all age classes or restricting it to a single age class, as recommended by Campana (2001).

Growth Curve Analysis

In using theoretical growth models, I assumed that (1) the birth mark is the band associated with a change in angle in the intermedialia and (2) growth bands are deposited annually. Age estimates were calculated using the algorithm presented in Carlson et al. (2003): age = the birth mark + number of narrow bands – 1. If only the birth mark was present, the ray was considered a 0+ year-old individual.

Four growth models were fitted to the observed size-at-age data. The von Bertalanffy growth model (von Bertalanffy 1938) was fitted using the equation:

$$DW_t = DW_\infty (1 - e^{-K(t-t_0)}),$$

where DW_t = mean disk width at time t ; DW_∞ = theoretical asymptotic length; K = growth coefficient; and t_0 = theoretical age at zero length.

A Gompertz growth model (Ricklefs 1967, Ricker 1975), which is an asymmetric sigmoid double exponential growth model, was also fitted using the equation:

$$DW_t = DW_\infty e^{-e^{K(t-t_0)}},$$

where DW_t = mean disk width at time t ; DW_∞ = theoretical asymptotic length; K = growth coefficient; and t_0 = theoretical age at zero length.

A logistic model (Ricker 1975) was also considered in the form:

$$DW_t = \frac{DW_\infty}{1 + e^{-K(t-t_0)}},$$

where DW_t = mean disk width at time t ; DW_∞ = theoretical asymptotic length; K = growth coefficient; and t_0 = theoretical age at zero length.

Finally, a four parameter Richards or “Generalized von Bertalanffy” (Richards 1959, Gulland 1969) growth model was fitted to the observed size-at-age data in the form:

$$DW_t = DW_\infty (1 - L_0 * e^{-K*t})^p$$

where DW_t = mean disk width at time t ; DW_∞ = theoretical asymptotic length; K = growth coefficient; L_0 = y-intercept, and p is a shape parameter. This model is useful as a selection tool and can generate the other three models by varying the value of p : von Bertalanffy if $p = 1$, logistic if $p = -1$, and Gompertz as p goes to infinity.

All growth model parameters were estimated using Marquardt least-squares non-linear regression and implemented using SAS statistical software (SAS V.8, SAS Institute, Inc). The goodness-of-fit of each model was assessed by examining residual mean square error (MSE), coefficient of determination (r^2), and level of significance ($p < 0.05$; Neer and Cailliet 2001, Carlson and Baremore 2005). To aid in model selection, likelihood ratio tests

implemented using SAS (Kimura 1980, Devore 2000). A likelihood ratio test was also implemented using the solver add-in in Excel (Haddon 2001) to determine whether growth models differed between sexes (Kimura 1980, Cerrato 1990). Theoretical longevity was estimated as the age at which 95% of DW_{∞} is reached: $(\frac{5 * \ln(2)}{K})$; Fabens 1965; Cailliet et al. 1992).

In order to investigate the potential of geographic variability in growth parameters, we compared data obtained from the current study for the Gulf of Mexico with the original data of Smith and Merriner (1987) from the western Atlantic Ocean. Growth models were fitted to observed size-at-age data for the sexes separately and combined, with the resulting models compared using a likelihood ratio test (Kimura, 1980; Cerrato, 1990). A likelihood ratio test was used to compare the Smith and Merriner growth curves to those generated in the current study.

Reproduction

Male reproductive status was based on three criteria: 1) the ratio of clasper length to disk width (Smith and Merriner 1986); 2) clasper calcification (Yano 1993); and 3) vas deferens coiling (none, partial, or complete; Neer and Cailliet 2001). Outer clasper length was measured for males as the distance from the free tip of clasper to where the clasper meets the pelvic fin (Compagno 1984). Clasper calcification was subjectively assigned to one of three categories based on ease of clasper bending: not calcified, partially calcified, and calcified. I considered a specimen mature if it met at least two of the three following criteria: calcified claspers, coiled vas deferens, and a clasper length – disk width ratio, expressed as a percentage, greater than or equal to 4%.

I based the reproductive status of female specimens on two criteria: 1) diameter of ova (Smith and Merriner 1986), and 2) uterine width (Neer and Cailliet 2001). Females were considered mature if they contained ovarian ova >10 mm in diameter or the uteri were differentiated from the oviducts and measured at least 10 mm in width at its widest point. The diameter of the largest ova was measured to the nearest 0.1 mm. I considered gravid females mature, regardless of ova size. I recorded the number, size, weight, and sex for all pups observed.

Median size at maturity (DW_{50}) was determined following Mollet et al. (2000). A logistic regression model was fitted to the binomial maturity data (immature=0, mature=1) using the logit function for males and females separately. Median size at maturity was calculated using the equation $DW_{50} = \frac{-(a)}{b}$, where a and b are the parameter estimates obtained from the logistic regression analysis.

Results

Specimen Collection

A total of 227 cownose rays were examined during this study. Males ranged in size from 338 to 960 mm DW (n = 106), while females ranged from 336 to 1025 mm DW (n = 121; Figure 2.3). The disk width-weight relationship was best described by a power curve of the form: $y = 5E-09x^{3.1936}$ ($r^2=0.99$; n = 222).

Rays were collected from all months except December, January, and February, although not from all months in every year. Temperature at time of collection ranged from 20 to 32 °C, and salinity ranged from 22.1 to 36 ppt.

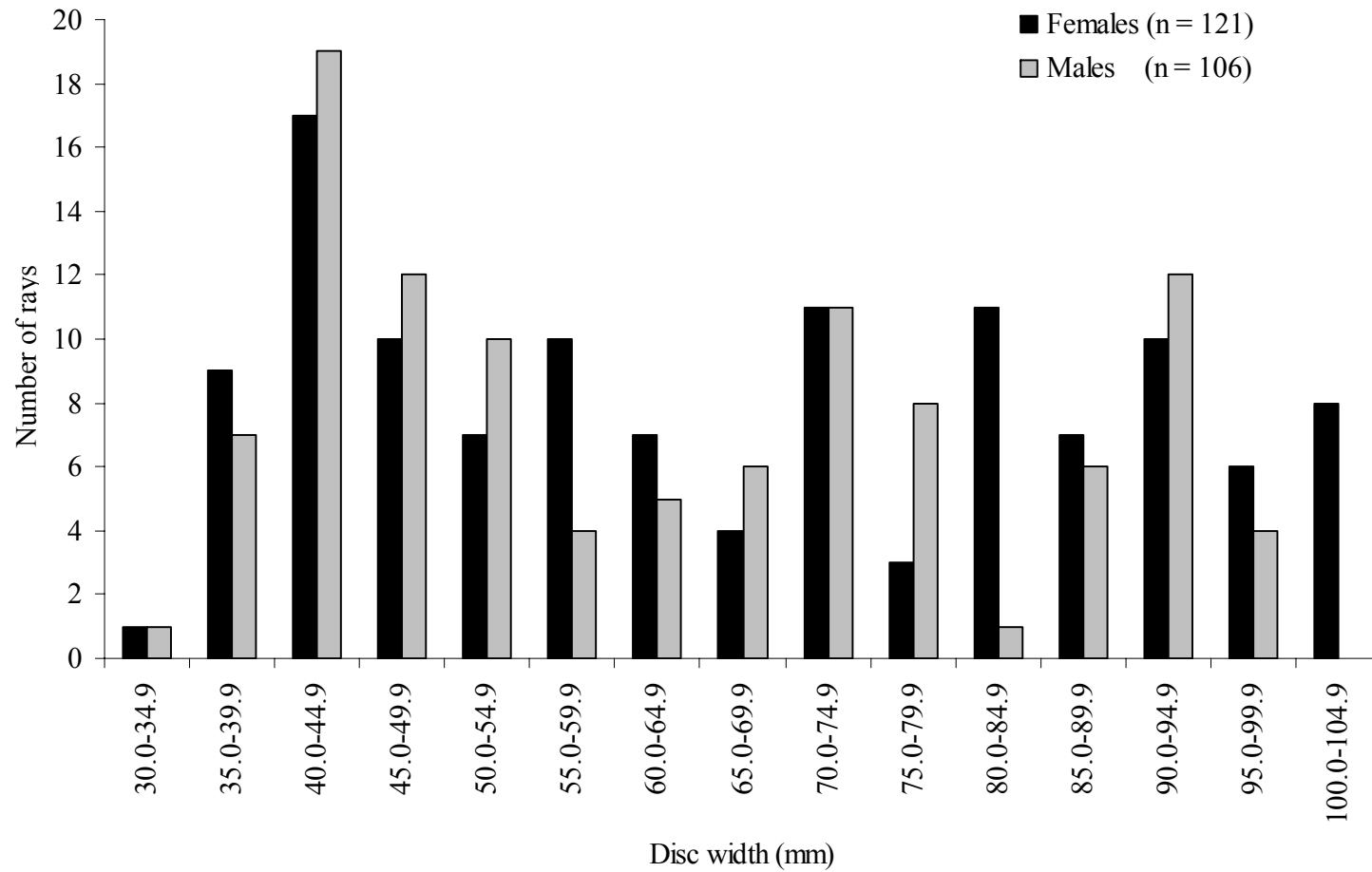


Figure 2.3. Length frequency histogram for cownose rays examined during this study (n = 227).

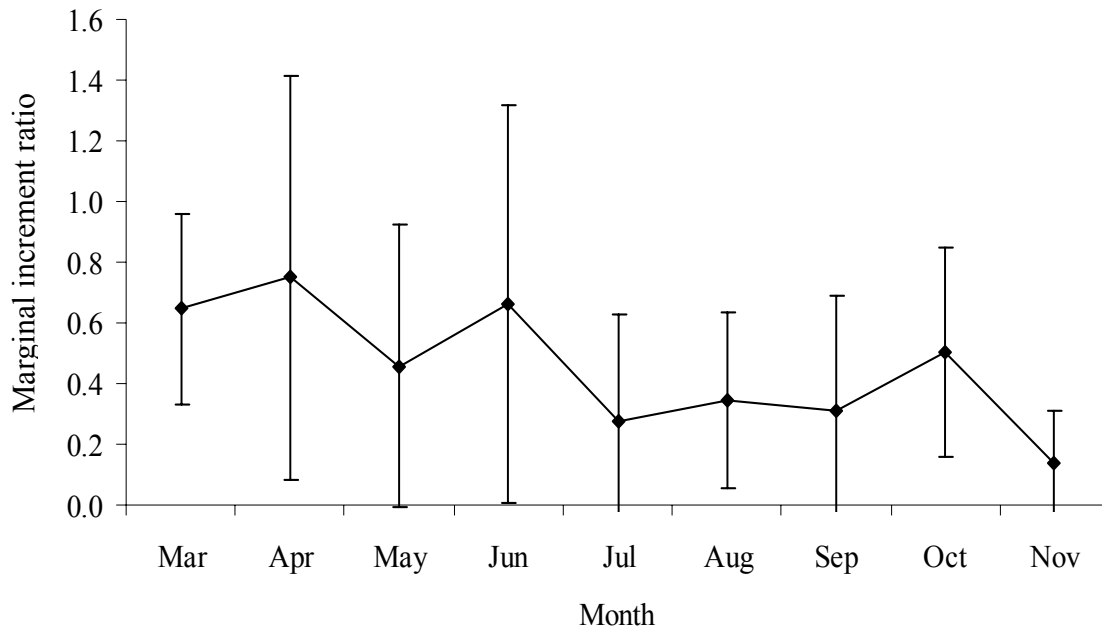
Age Assessment and Verification

I derived age estimates for all 227 specimens processed for age assessment. Age estimates ranged from 0⁺ to 18⁺ years for females (n = 121) and from 0⁺ to 16⁺ for males (n = 106). The precision of band counts was high between the first two sets of band counts, resulting in an APE of 3.81% and D (percent error) of 3.45%. Percent agreement between the first two sets of band counts was 62.6% exact count, 89.9% within 1 band, and 99.6% within 2 bands.

Significant differences were found in marginal increment analysis between seasons for all cownose ray age classes combined (single factor ANOVA by season: F-ratio = 3.721, df = 2, $p < 0.05$, n = 169; Figure 2.4). Post-hoc pairwise comparisons found that Spring was significantly different from Fall (Tukey pairwise post-hoc test: $p < 0.05$), and that Spring did not differ from Summer and Fall did not differ from Summer (Tukey pairwise post-hoc test: $p > 0.1$). Significant differences were also found in the analysis by month for all cownose ray age classes combined (single factor ANOVA by month: F-ratio = 2.422, df = 8, $p < 0.05$, n = 169; Figure 2.4). All monthly pairwise comparisons were not different with the exception of April and November (Tukey pairwise post-hoc test: $p < 0.05$).

Although monthly and seasonal changes in marginal increment analysis observed in the YOY-only analysis displayed a similar pattern as all age classes combined, the peaks with the YOY analysis were not statistically different (single factor ANOVA by month: F-ratio = 0.754, df = 4, $p > 0.10$; by season: F-ratio = 0.794, df = 2, $p > 0.10$, Figure 2.5). This lack of significance may be due to the small sample size available for the YOY only analysis (n = 20).

a.



b.

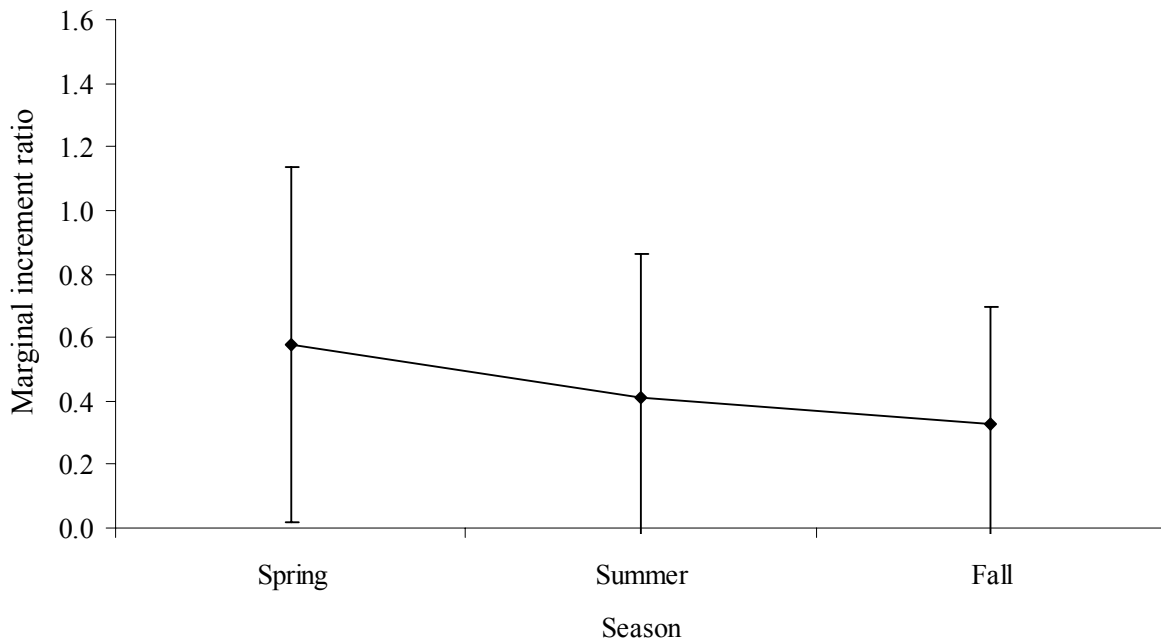
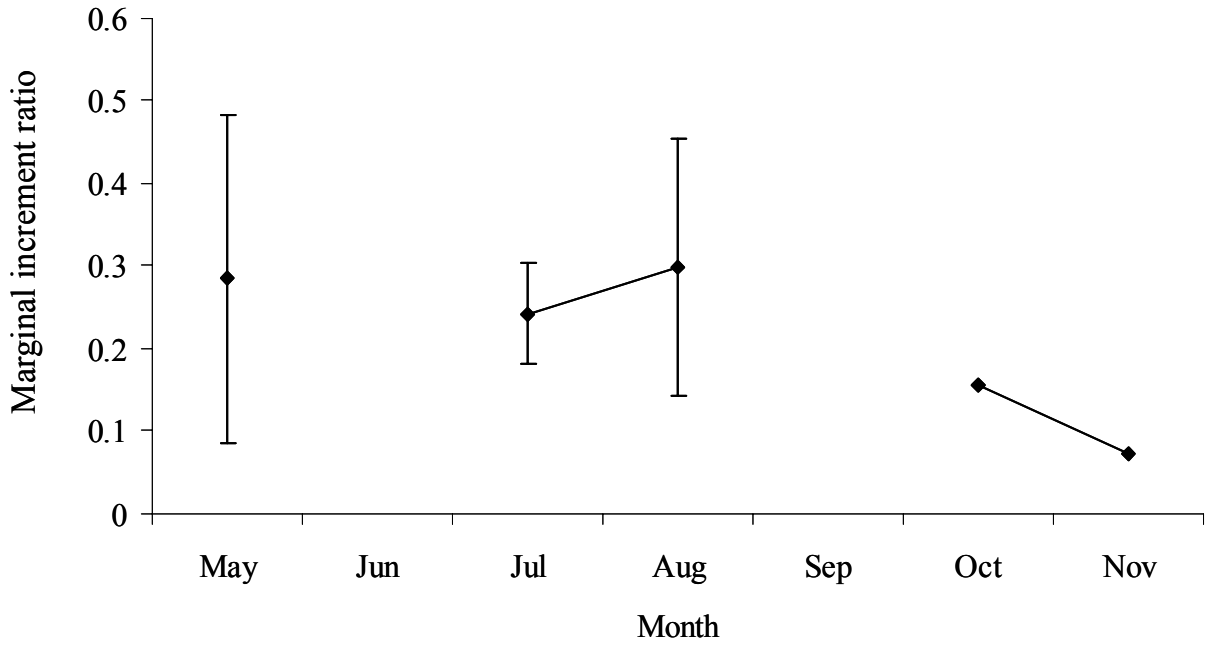


Figure 2.4. Mean marginal increment analysis for cownose rays (n = 169) by a) month and b) season. Vertical bars are \pm one standard deviation.

a.



b.

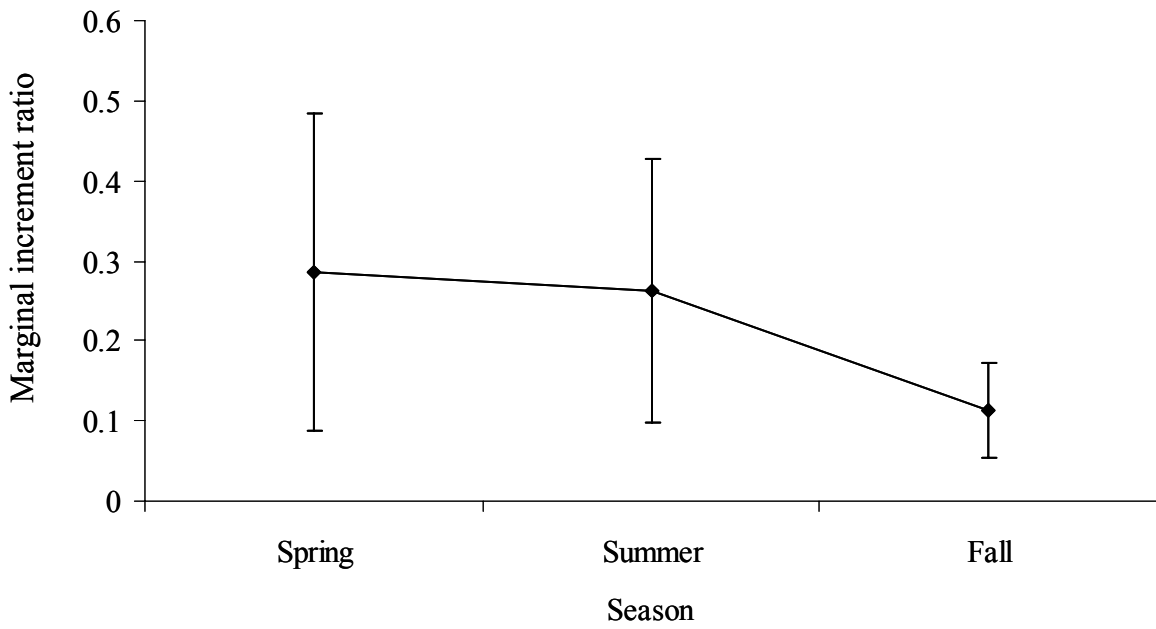


Figure 2.5. Mean marginal increment analysis for young-of-the-year cownose rays ($n = 20$) by a) month and b) season. Vertical bars are \pm one standard deviation.

Growth Curve Analysis

All four growth models fitted the observed size-at-age data well and were highly significant ($p < 0.0001$; Table 2.1). According to the criteria used, the Gompertz model best described the data. The model had the lowest MSE and the highest r^2 value of the three parameter models, and the same r^2 value as the four parameter Richards model (Table 2.1). The likelihood ratio test also indicates that the Gompertz model provides the best reduction from the four parameter Richards model, without being significantly different from the Richards model (Table 2.1). To allow for comparison to the literature, results are presented for both the Gompertz and von Bertalanffy growth models.

Likelihood ratio tests indicate that the observed size-at-age data are better described as one combined-sexes model than for the sexes separately (Gompertz: $\chi^2 = 3.23$, $df = 3$, $p > 0.10$; von Bertalanffy: $\chi^2 = 3.27$, $df = 3$, $p > 0.10$; Figure 2.6). The combined sexes Gompertz model predicted a DW_∞ of 1100.2 mm, a K value of 0.1332 per year, and a t_0 of - 0.2573 years. The von Bertalanffy model for sexes combined predicted a DW_∞ of 1238.3 mm, a K value of 0.0746 per year, and a t_0 of - 5.4799 years. Theoretical longevity was estimated to be 26.1 years for the Gompertz model and 46.2 years for the von Bertalanffy model.

Likelihood ratio tests indicate that the Smith and Merriner data were also best described using one model for the sexes combined (Gompertz: $\chi^2 = 5.52$, $df = 3$, $p > 0.10$; von Bertalanffy: $\chi^2 = 4.50$, $df = 3$, $p > 0.10$). The von Bertalanffy model for combined sexes predicted a DW_∞ of 1389.6 mm, a K value of 0.0878 per year, and a t_0 of - 4.6530 years. The combined sexes Gompertz model predicted a DW_∞ of 1195.1 mm, a K value of 0.1667 per year, and a t_0 of - 0.3990 years. Theoretical longevity was estimated to be 39.5 years for the von Bertalanffy model and 20.8 years for the Gompertz model. Significant differences were found

Table 2.1. Summary of goodness-of-fit of four models fitted to observed size-at-age data for the cownose ray from the northern Gulf of Mexico.

Model	df	SS	MSE*	r ²	p	ratio	-ln(ratio)*n	df	P>Chi ²
von Bertalanffy	224	747222	3291.73	0.920	<0.0001	0.998	0.555098396	1	0.4562419
Gompertz	224	745559	3284.4	0.921	<0.0001	1.000	0.049329424	1	0.8242343
Logistic	224	749427	3301.44	0.920	<0.0001	0.995	1.223973145	1	0.2685825
Richards	223	745397	3283.69	0.921	<0.0001				
Corrected Total	226	9380890							

* calculated with total number of observations, not df

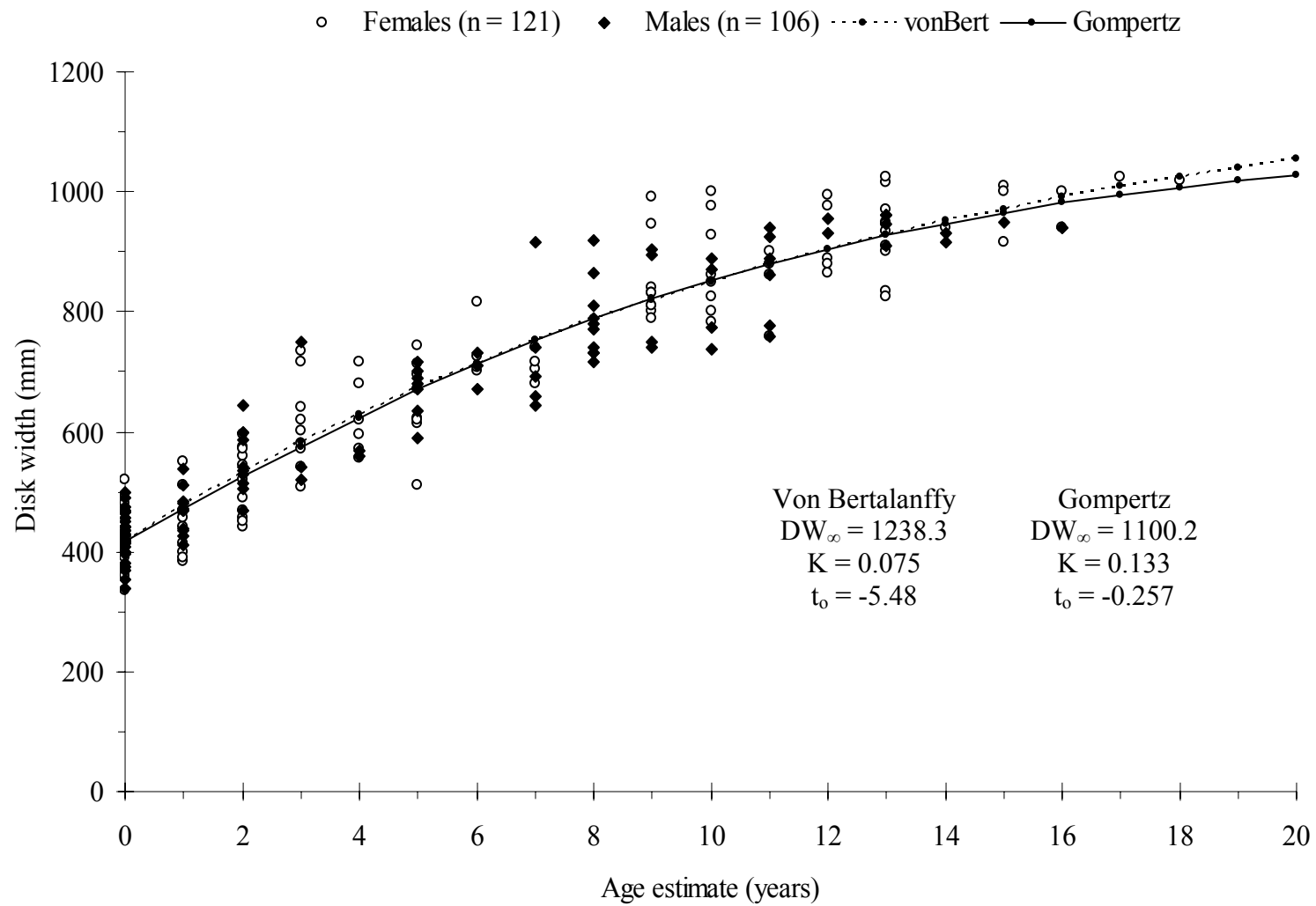


Figure 2.6. Growth functions fitted to the combined sexes observed size-at-age data for cownose rays (n = 227).

between growth models for the Gulf of Mexico and the western Atlantic Ocean ($\chi^2 = 216.17$, $df = 3$, $p < 0.0001$).

Reproduction

Reproductive status was determined for 218 rays during this study (104 males, 114 females). Median size at maturity for male cownose rays was 642 mm (Figure 2.7), which corresponds to an age at DW_{50} of ~4-5 years. An abrupt change in the clasper length – disk width relationship begins at ~600 mm DW (Figure 2.8). Seventy-one percent of males > 642 mm DW ($n = 45$) displayed complete coiling of the vas deferens and 77% ($n = 47$) had calcified claspers. The smallest mature male observed was 635 mm DW and the largest immature male was 750 mm DW.

Female cownose rays had a DW_{50} of 653 mm (Figure 2.7). The smallest mature female was 623 mm DW and the largest immature female was 713 mm DW. Ninety-eight percent of females > 653 mm DW ($n = 53$) displayed a uterine width greater than 10 mm. For females larger than 653 mm DW for which ova size data were available ($n = 42$), fifty percent possessed ovarian ova greater than 10 mm diameter. Age at DW_{50} was estimated to be approximately 4 - 5 years.

I observed 33 gravid females during this study. The smallest gravid female collected measured 760 mm DW. In all cases, only one pup was observed in the left uterus. No ovary or uterine development was observed in the right reproductive tract in any of the females rays examined ($n = 108$); thus only the left reproductive tract is functional in cownose rays. Embryos ranged in size from 205 – 395 mm DW and were observed in April, May, and September through November. The sex ratio of embryos was one to one (males to females).

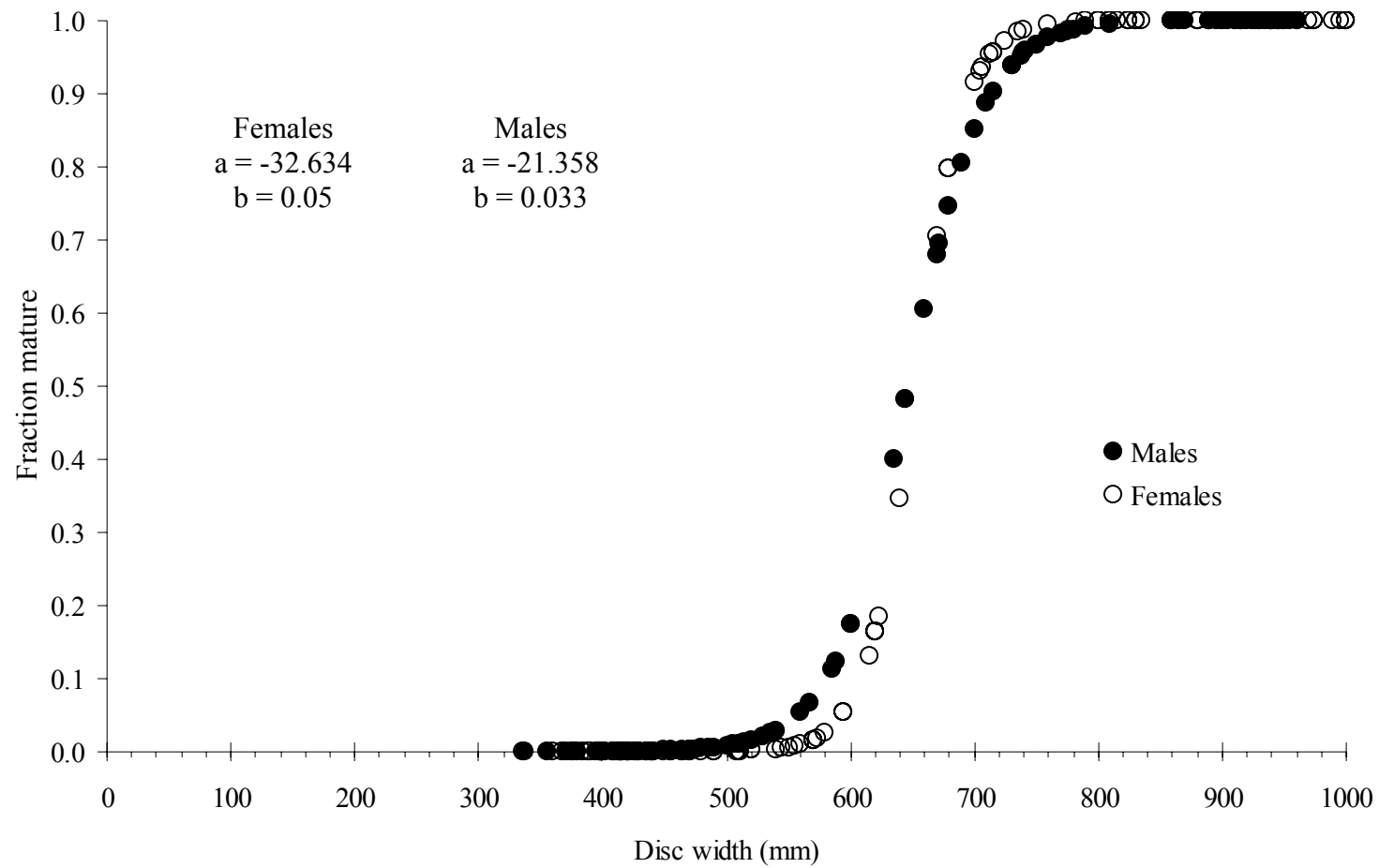


Figure 2.7. Relationship between maturity and disk width for the cownose ray. A logistic regression model was fitted to the binominal maturity data (0 = immature, 1 = mature).

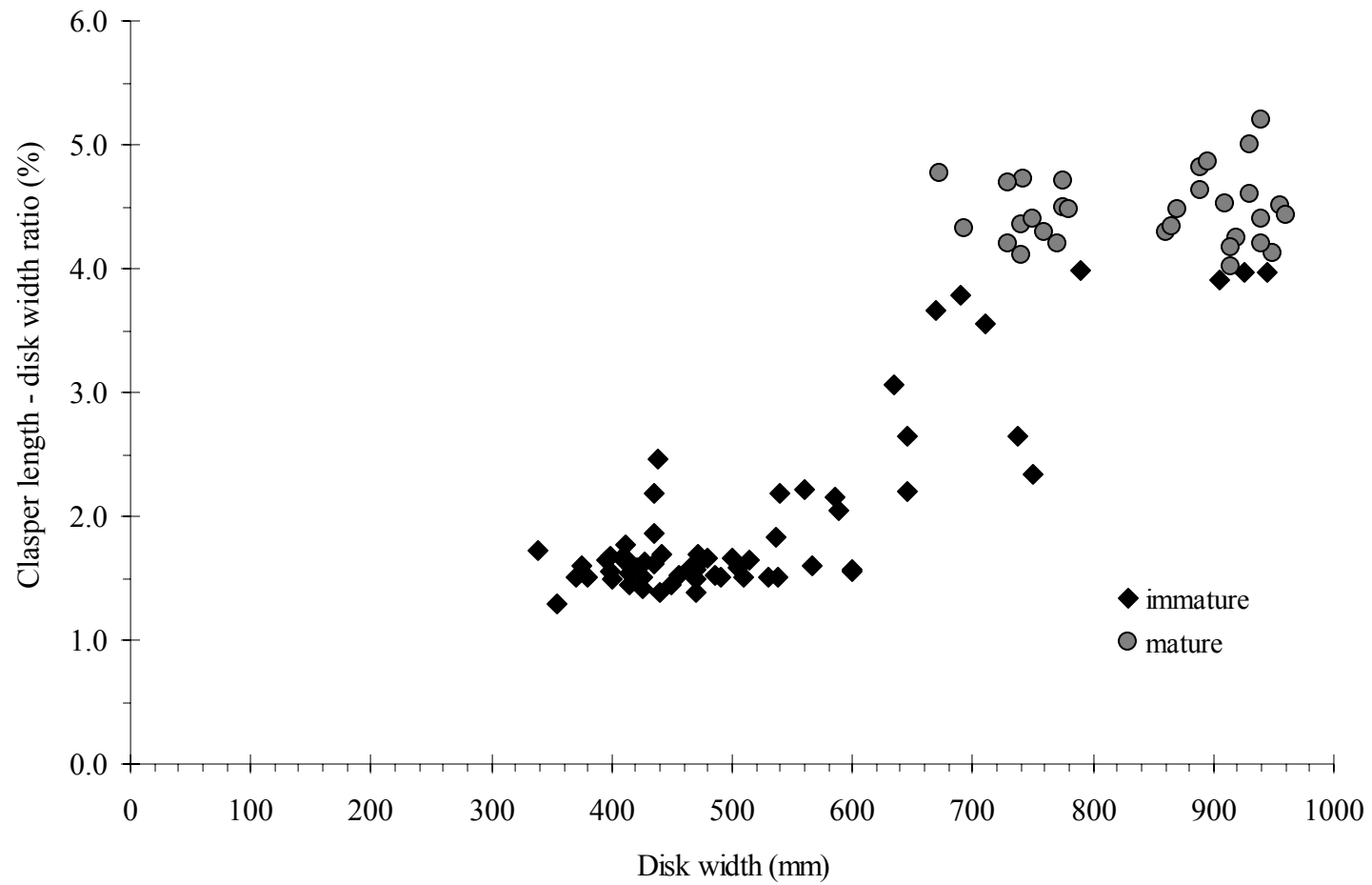


Figure 2.8. Relationship between outer clasper length and disk width for the cownose ray (n = 99).

The smallest free-swimming individual I observed measured 336 mm DW and was collected in July. The largest embryos were collected in mid-April through mid-May (285 – 395 mm DW), indicating that pupping may be occurring at this time. Gestation appears to take 11 to 12 months based on embryos sizes collected throughout the year; however, lack of samples from every month precludes further examination.

Discussion

The Gompertz growth curve best described the growth of the cownose ray. Traditionally, the von Bertalanffy growth function (VBGF) has been applied to describe the growth of elasmobranch species (see review in Cailliet and Goldman 2004). However, recent studies have indicated that the Gompertz function may better describe the growth of animals who continue to increase in weight and bulk over time, but not greatly in length, once they reach large size (Cailliet and Goldman 2004). This may be especially true for the batoids. Mollet et al. (2002) suggested that the Gompertz model best described the captive growth of the pelagic stingray, *Dasyatis violacea*, indicating that the Gompertz model provided more realistic estimates of size at birth and growth rate than the VBGF. Neer and Cailliet (2001) also suggested that the Gompertz model provided the best fit for the size-at-age data for the Pacific electric ray, *Torpedo californica*. However, they did not provide parameter estimates for the Gompertz model, but rather reported parameter values from the VBGF to allow for comparison to previously published studies.

The Gompertz model also produced more biologically realistic parameter estimates than the von Bertalanffy model for the cownose ray. The largest ray I encountered during the study was a 1025 mm DW female, close to the DW_{∞} of 1100.2 mm predicted by the Gompertz model. The DW_{∞} predicted using the VBGF (1238 mm) seems to be an

overestimate, based on the size of rays observed during this study. The estimates of longevity produced using the parameter estimates of K from the two models also indicate that the Gompertz model is likely more biologically realistic. The oldest animal aged in this study was a 18+ year old female. The theoretical longevity estimate of 26.1 years determined from the Gompertz model is possible, while it seems doubtful that this species lives to 46 years in nature, as estimated from the VBGF, based on the data currently available.

My results verified of the assumption that narrow bands are formed annually in the winter months in the cownose ray. Smith and Merriner (1987) also concluded annual band formation based on the lack of what they termed a “hyaline band” in neonates, and the presence of only one hyaline band in rays they determined to be approximately one year old. These findings lead them to suggest that this “hyaline” band is formed in the winter months. Despite this corroboration, further validation of the annual periodicity of the banding pattern observed in the cownose ray is necessary through techniques such as chemical marking or tag-recapture studies.

Results of this study indicate that geographic variation in life history traits does occur for the cownose ray. The observed differences in growth model parameters between the Gulf of Mexico and the Atlantic Ocean may be due to several factors. Differences in preparation technique (Cailliet et al. 1990) and the age-classes included in the analysis (Cailliet and Goldman 2004). can also confound comparisons among studies. The Smith and Merriner age estimates were determined using cross-sectioned vertebrae, while those determined in the current study used sagittally thin sectioned samples. The oldest rays included in the western Atlantic Ocean data set were a 13 year old female and an eight year old male. The oldest female I observed was 18+ years old, while the oldest male was 16+ years old. In addition,

the Atlantic study was published in 1987 and differences in growth between the Atlantic Ocean and my study may be partially due to historical changes in growth in the Atlantic (i.e., growth measured now in the Atlantic would be similar to the Gulf of Mexico). Although researchers have suggested that changes in life history parameters over time may be the result of compensatory changes in response to anthropogenic factors such as fishing (Walker and Hislop 1998, Carlson and Baremore 2003), I do not believe that is the case for the cownose ray as no directed fishery exists for this species. Cownose rays are taken as bycatch in several fisheries, although the magnitude of the bycatch and its effects on cownose ray life history traits are unknown. Finally, my results may truly reflect differences in regional growth patterns. Driggers et al (2004) found statistically significant differences in growth models between the western Atlantic Ocean and the Gulf of Mexico for the blacknose shark, and Carlson et al. (2003) found similar results for the finetooth shark.

Differences in reproduction also exist between cownose rays from the Gulf of Mexico and the western Atlantic Ocean. Smith and Merriner (1986) suggested that male cownose rays < 75 cm DW were immature and males > 80 cm were mature, while females begin sexual maturation at 85 – 90 cm and are mature at disk widths > 90 cm. This study found the median disk width at maturity for males in the Gulf of Mexico to be roughly 10 cm smaller and 1 – 2 years earlier than those in the Atlantic Ocean. Female cownose rays in the Gulf of Mexico also reach DW_{50} at a smaller size (~20 cm smaller) and earlier age (2 -3 years earlier) than their counterparts in the western Atlantic Ocean. Carlson et al. (2003) reported similar trend for the finetooth shark. Holden (1974) suggested that elasmobranchs mature after reaching approximately 60% of their theoretical asymptotic size. This assumption is supported by my data. Male and female cownose rays mature at ~ 58% of their estimated

maximum disk width. Smith and Merriner (1986) suggested that cownose rays in the western Atlantic Ocean mature after reaching 70-75% of their predicted maximum disk width.

Size-at-birth and timing of parturition may also differ between the Atlantic Ocean and Gulf of Mexico populations. I estimated a mean size-at-birth to be approximately 350 mm DW, although my smallest free swimming individual measured 336 mm DW. This estimate falls within the previous estimates of size-at-birth of approximately 400 mm DW from Smith and Merriner (1986) and approximately 300 mm DW proposed by Schwartz (1967).

Schwartz (1967) further defined the parturition and breeding cycle to occur June through October in the Chesapeake Bay. Smith and Merriner (1986) reported a similar seasonal reproductive cycle. My study supports this protracted pupping and mating season, although the pupping season may begin slightly earlier in the Gulf of Mexico. I observed young-of-the-year individuals less than or equal to 400 mm DW from May through November.

Additionally, I observed gravid females with embryos greater than 400 mm DW in April and May. This longer pupping season may be due to the warmer waters of the Gulf of Mexico relative to the Chesapeake Bay.

Fecundity and gestation estimates for the Gulf of Mexico population agree with the published literature. Smith and Merriner (1986) reported a fecundity estimate of one pup per litter and suggested an 11 to 12 month gestation period, both of which agree with the current study. The possibility that cownose rays may have two litters per year has been suggested (Smith and Merriner 1986); however, the current data and information on reproductive hormonal cycling in captive animals do not support this (Alan Henningsen, Baltimore Aquarium, personal communication).

This study provides the first published age and growth estimates for a batoid from the Gulf of Mexico. Cownose rays appear to be similar to other elasmobranchs in being relatively long-lived, having low fecundity, and a relatively old age at sexual maturity. However, more detailed information regarding age validation, parturition season, reproductive cycles, and migration patterns is needed to refine the estimates presented here. Demographic analysis would also be helpful for conservation and management of cownose rays.

Literature Cited

- Beamish, R.J. and D.A. Fournier. 1981. A method for comparing the precision of a set of age determinations. *Canadian Journal of Fisheries and Aquatic Science* 38:982-983.
- Bigelow, H.B. and W.C. Schroeder. 1953. *Fishes of the Western North Atlantic. Part I, Lancets, cyclostomes and sharks.* Memoir Sears Foundation for Marine Research.
- Blaylock, R.A. 1993. Distribution and abundance of the cownose ray, *Rhinoptera bonasus*, in lower Chesapeake Bay. *Estuaries* 16:255-263.
- Cailliet, G.M. and K.J. Goldman. 2004. Age determination and validation in chondrichthyan fishes. Pages 399-447 *in* *Biology of sharks and their relatives.* Carrier, J.C., J.A. Musick, and M.R. Heithaus, editors. CRC Press, Boca Raton.
- Cailliet, G.M., K.G. Yudin, S. Tanaka, and T. Taniuchi. 1990. Growth characteristics of two populations of *Mustelus manazo* from Japan based on cross-readings of vertebral bands. Pages 167-176 *in* Pratt Jr., H.L., S. H. Gruber and T. Taniuchi, editors. *Elasmobranchs as living resources: advances in the biology, ecology, systematics, and the status of the fisheries.* U.S. Department of Commerce. NOAA Technical Report NMFS 90.
- Cailliet, G.M., Mollet, H.F., Pittenger, G.G., Bedford, D., and Natanson, L. J. 1992. Growth and demography of the Pacific angel shark (*Squatina californica*), based upon tag returns off California. *Australian Journal of Marine and Freshwater Research* 43:1313-1330.
- Campana, S.E. 2001. Accuracy, precision and quality control in age determination, including a review of the use and abuse of age validation methods. *Journal of Fish Biology* 59:197-242.

- Carlson, J.K. and J.H. Brusher. 1999. An index of abundance for coastal species of juvenile sharks from the northeast Gulf of Mexico. *Marine Fisheries Review* 61(3):37-45.
- Carlson, J.K. and I.E. Baremore. 2005. Growth dynamics of the spinner shark, *Carcharhinus brevipinna*, off the Southeast United States and Gulf of Mexico: a comparison of methods. *Fishery Bulletin* 103:208-291.
- Carlson, J. K. and I. E. Baremore. 2003. Changes in biological parameters of Atlantic charrnose shark *Rhizoprionodon terraenovae* in the Gulf of Mexico: evidence for density-dependent growth and maturity? *Marine and Freshwater Research* 54:227-234.
- Carlson, J.K., E. Cortés, and D. Bethea. 2003. Life history and population dynamics of the finetooth shark, *Carcharhinus isodon*, in the northeastern Gulf of Mexico. *Fishery Bulletin* 101:281-292.
- Cerrato, R. M. 1990. Interpretable statistical tests for growth comparisons using parameters in the von Bertalanffy equation. *Canadian Journal of Fisheries and Aquatic Science* 47:1416-1426.
- Chang, W.Y.B. 1982. A statistical method for evaluating the reproducibility of age determination. *Canadian Journal of Fisheries and Aquatic Science* 39:1208-1210.
- Compagno, L.J.V. 1984. FAO species catalogue. Vol.4 Sharks of the World. An annotated and illustrated catalogue of sharks species known to date. Part 1. Hexanchiformes to Lamniformes. FAO Fisheries Synopsis 125(4).
- Devore, J.L. 2000. Probability and statistics for engineering and the sciences. 5th edition. Duxbury Australia.
- Driggers, W.B. III, J.K. Carlson, D. Oakley, G. Ulrich, B. Cullum, and J.M. Dean. 2004. Age and growth of the blacknose shark, *Carcharhinus acronotus*, in the western North Atlantic Ocean with comments on regional variation in growth rates. *Environmental Biology of Fishes* 71(2):171-178.
- Fabens, A. J. 1965. Properties and fitting of the von Bertalanffy growth curve. *Growth* 29, 265-289.
- Gulland, J.A. 1969. Manual of Methods for Fish Stock Assessment. Part 1. Fish population analysis. FAO of the United Nations, Rome.
- Haddon, M. 2001. Modelling and Quantitative Methods in Fisheries. Chapman and Hall/CRC. Boca Raton. 406 pages.

- Holden, M.J. 1974. Problems in the rational exploitation of elasmobranch populations and some suggested solutions. Pages 117-137 in Sea fisheries research. F.R. Harden-Jones, editor. John Wiley and Sons, New York.
- Kimura, D.K. 1980. Likelihood methods for the von Bertalanffy growth curve. Fishery Bulletin 77(4):765-776.
- Lombardi-Carlson, L. A., E. Cortés, G. R. Parsons, and C. A. Manire. 2003. Latitudinal variation in life-history traits of bonnethead sharks, *Sphyrna tiburo*, (Carcharhiniformes:Sphyrnidae) from the eastern Gulf of Mexico. Marine and Freshwater Research 54:875-883.
- McEachran, J.D. and C. Capapé. 1984. Rhinopteridae. Page 208 in Whitehead, P.J.P., M.-L. Bauchot, J.-C. Hureau, J. Nielsen, and E. Tortonese, editors. Fishes of the North-eastern Atlantic and Mediterranean. Volume 1. UNESCO.
- McEachran, J.D. and J.D. Fechhelm. 1998. Fishes of the Gulf of Mexico. Volume 1. University of Texas Press.
- Mollet, H.F., G. Cliff, H.L. Pratt, Jr., and J.D. Stevens. 2000. Reproductive biology of the female shortfin mako, *Isurus oxyrinchus* Rafinesque, 1810, with comments on the embryonic development of lamnoids. Fishery Bulletin 98:299-318.
- Mollet, H.F., Ezcurra, J.M. and O'Sullivan, J.B. 2002. Captive biology of the pelagic stingray, *Dasyatis violacea* (Bonaparte, 1832). Marine and Freshwater Research 53:531-541.
- Natanson, L. J., J.G. Casey, and N.E. Kohler. 1995. Age and growth estimates for the dusky shark, *Carcharhinus obscurus*, in the western North Atlantic Ocean. Fishery Bulletin 93: 116-126.
- Neer, J.A., J.K. Blackburn, B.A. Thompson. In press. Shark nursery areas of central Louisiana's nearshore coastal waters. Pages X - XX in C.T. McCandless, N.E. Kohler, and H.L. Pratt, Jr., editors. Shark nursery grounds of the Gulf of Mexico and the East Coast waters of the United States. American Fisheries Society, Symposium XX, Bethesda, Maryland.
- Neer, J.A. and G.M. Cailliet. 2001. Aspects of the Life history of the Pacific electric ray, *Torpedo californica* (Ayres). Copeia 3(2001):842-847.
- Parsons, G.R. 1993. Geographic variation in reproduction between two populations of the bonnethead shark, *Sphyrna tiburo*. Environmental Biology of Fishes 38: 25-35.
- Richards, J. 1959. A flexible growth function for empirical use. Journal of Experimental Botany 10:290-300.

- Ricker, W.E. 1975. Computation and interpretation of biological statistics of fish populations. Bulletin of the Fisheries Research Board of Canada 191:1-382.
- Ricklefs, R.E. 1967. A graphical method of fitting equations to growth curves. Ecology 48(6):978-983.
- Schwartz, F.J. 1967. Embryology and feeding behavior of the Atlantic cownose ray, *Rhinoptera bonasus*. Association of Island Marine Laboratories of the Caribbean - 7th Meeting, Barbados, West Indies.
- Schwartz, F.J. 1990. Mass migratory congregations and movements of several species of cownose rays, Genus *Rhinoptera*: a world-wide review. Journal of the Elisha Mitchell Scientific Society 106:10-13.
- Smith, J.W. and J.V. Merriner 1985. Food habits and feeding behavior of the cownose ray, *Rhinoptera bonasus*, in lower Chesapeake Bay. Estuaries 8(3): 305-310.
- Smith, J.W. and J.V. Merriner 1986. Observations on the reproductive biology of the cownose ray, *Rhinoptera bonasus*, in Chesapeake Bay. Fishery Bulletin 84(4): 871-877.
- Smith, J.W. and J.V. Merriner 1987. Age and growth, movements and distribution of the cownose ray, *Rhinoptera bonasus*, in Chesapeake Bay. Estuaries 10(2): 153-164.
- von Bertalanffy, L. 1938. A quantitative theory of organic growth (inquiries on growth laws II.) Human Biology 10(2), 181-213.
- Walker, P.A. and J.R.G. Hislop. 1998. Sensitive skates or resilient rays? Spatial and temporal shifts in ray species composition in the central and north-western North Sea between 1930 and present day. ICES Journal of Marine Science 55: 392-402.
- Yano, K. 1993. Reproductive biology of the slender smoothhound, *Gollum attenuatus*, collected from New Zealand waters. Environmental Biology of Fishes 38:59-71.
- Zar, J.H. 1984. Biostatistical Analysis Second Edition. Prentice-Hall. New Jersey.

CHAPTER III.

OXYGEN CONSUMPTION OF THE COWNOSE RAY, *RHINOPTERA BONASUS*: THE EFFECT OF TEMPERATURE AND SALINITY

Introduction

Metabolism is one of the major components of an organism's daily energy budget, and although highly variable, may account for the largest portion (Lowe 2001). Information on metabolism is vital for constructing accurate energy budgets and for developing bioenergetics models (Carlson et al. 1999). Early metabolic studies of elasmobranchs (sharks, skates, and rays) primarily focused on cool water, relatively inactive species of sharks such as spiny dogfish, *Squalus acanthias*, spotted dogfish, *Scyliorhinus canicula*, and swell shark, *Cephaloscyllium ventriosum* (Brett and Blackburn 1978, Metcalf and Butler 1984, Ferry-Graham and Gibb 2001). Recent work has focused on more active, warmer water species such as the blacknose shark, *Carcharhinus acronotus*, and the scalloped hammerhead shark, *Sphyrna lewini* (Carlson et al. 1999, Lowe 2001).

The effect of salinity and temperature on oxygen consumption rates of elasmobranchs has received little attention (see review by Carlson et al. 2004). For example, salinity effects have only been examined on bat rays, *Myliobatis californica*, and the lip shark, *Hemiscyllium plagiosum* (Chan and Wong 1977, Meloni et al. 2002), while studies examining the effects of temperature are limited to animals acclimated to acute changes in the laboratory (e.g. bull ray, *Myliobatos aquila*, Du Preez et al. 1988, bat ray, Hopkins and Cech 1994, leopard shark, *Triakis semifasciata*, Miklos et al. 2003). Only Carlson and Parsons (1999) have examined seasonal differences in routine oxygen consumption rates on acclimatized animals for the bonnethead shark, *S. tiburo*. As pointed out by Carlson et al. (2004), the length of acclimation

(e.g. acute or seasonal) at the experimental temperature may result in an increased or decreased temperature sensitivity of oxygen consumption rate. Moreover, if results are to be applied to animals in the wild, then estimates obtained on seasonally acclimatized animals may be more valid than those obtained for animals exposed in the laboratory. There are currently no published studies on the effect of temperature and salinity on oxygen consumption rate for seasonally acclimatized batoids (skates and rays).

The cownose ray, *Rhinoptera bonasus*, ranges from southern New England to southern Brazil within the western Atlantic Ocean as well as throughout the Gulf of Mexico and off Cuba (Bigelow and Schroeder 1953, McEachran and Fechhelm 1998). Cownose rays are semi-pelagic and gregarious; often forming large schools, and are known to undertake long migratory movements (McEachran and Capapé 1984, Schwartz 1990). In the northern Gulf of Mexico, cownose rays were encountered at temperatures from 15.5 to 33.6° C, and salinities ranging from 17 to 37 parts per thousand (ppt), suggesting that they are both eurythermal and euryhaline (John Carlson, personal communication). The objectives of this research were to 1) determine the standard metabolic rate of the cownose ray, 2) examine the effect temperature and salinity on standard metabolic rate, and 3) determine an estimate of temperature sensitivity (Q_{10}) for the species.

Materials and Methods

Fish Collection and Holding

Cownose rays were captured using gillnets from one of three bays (St. Andrew Bay system, St. Joseph Bay, or Apalachicola Bay) along the northwest Florida coast and transported to the National Marine Fisheries Service Laboratory, Panama City, Florida. At the laboratory, rays were held under natural lighting conditions in circular outdoor, shaded,

3000-liter tanks, with a flow-through seawater system for a minimum of five days. Following Hopkins and Cech (1994), rays were fasted for a minimum of five days (maximum of eight days) prior to experimentation to ensure all experiments were conducted on animals in a post-absorptive state. I did not manipulate water temperature or salinity (i.e. experiments were conducted on acclimatized rays).

Respirometry

Oxygen consumption measurements (MO_2) were determined using rectangular flow-through respirometers. Two respirometers were used: 148-liter unit for rays less than 55 cm disk width (DW), and a 236-liter unit for rays larger than 55 cm DW. The respirometers were constructed of plexiglass, with a removable plexiglass lid to allow placement of the rays in the respirometer.

The respirometer was filled with filtered, ultraviolet-sterilized seawater pumped from a 1500-liter water reservoir adjacent to the respirometer. The water reservoir was filled from water pumped from the adjacent bay at the existing environmental temperature and salinity. Individual rays were placed in the respirometer and the respirometer covered with black plastic to minimize external stimuli. Rays were allowed to acclimate to the respirometer for a minimum of 12 hours before the experimental trial was begun. During the acclimation period, the flow-through design of the system was maintained, with fresh seawater flowing through the filter and UV sterilizer to the water reservoir, and then into the respirometer. An aerator was placed in the water reservoir during the acclimation period to ensure the oxygen concentration of the inflowing water never dropped below 5.5 mg/liter. All experimental trials were begun within two hours of sunrise to exclude any exogenous or endogenous effect

of time-of-day. Just prior to beginning an experimental trial, the inflowing water to the water reservoir was shut off and the aerator removed.

I recorded inflow and outflow water oxygen concentrations (mg/liter) and temperature (°C) every ten minutes using a Yellow Springs Instruments (YSI) 85 multi-sensor probe or an YSI 95 oxygen meter. Salinity was recorded once at the start of the experiment.

Measurements were recorded for a minimum of two hours for each ray. The experimental duration was determined by the volume of water available in the water reservoir and flow rate during the experiment. Flow rate was determined by timed water collection several times during each experiment.

Standard mass-dependent oxygen consumption rate was determined using the general equation:

$$MO_2 = \frac{(O_{2in} - O_{2out}) * (flowrate * 60)}{Mass}$$

where MO_2 is oxygen consumption rate in $mg\ O_2\ kg^{-1}\ hr^{-1}$, O_{2in} is the inflow water oxygen concentration in mg/liter, O_{2out} is the outflow water oxygen concentration in mg/liter, flow rate is water flow in liters/min, and mass is the wet weight of the ray in kilograms. Oxygen consumption rate was calculated for each measurement, and an overall average was determined for each ray. Data were categorized into temperature groups (19, 22, 25, and 28 °C ± 1 degree) for graphical comparisons. Q_{10} , a measure of temperature sensitivity, was calculated as specified in Schmidt-Nielsen (1983).

To further examine the effect of salinity on oxygen consumption rate, additional experiments using repetitive oxygen consumption trials at salinities ranging from 17.1 to 26.5 ppt were conducted. The standard mass-dependent MO_2 was determined for three rays

following the procedure above. After initial experimentation, the rays were placed in a 3000-liter holding tank and fed a diet of squid for 12 days. The rays were then fasted for five days and a second oxygen consumption experiment conducted. The differences in salinities between the first and second trials were due to natural fluctuations in the inflowing seawater.

Statistical Analyses

Multiple regression analysis was used to examine the effect of temperature, salinity, and mass on standard mass-independent MO_2 (in $mg\ O_2\ hr^{-1}$) from all initial experiments. A single-factor ANOVA was used to test for differences in MO_2 among temperature groups. A paired two-sample t-test was used to examine differences between mass-dependent MO_2 (in $mg\ O_2\ kg^{-1}\ hr^{-1}$) at differing salinities. Statistical analyses were conducted on the individual ray MO_2 averages. The Shapiro-Wilk statistic was used to evaluate the residuals of the regression analysis for normality. If they did not meet the assumptions of normality, the data were log transformed (Sheskin 2003). Statistical significance was assigned using an $\alpha = 0.05$. All statistical analyses were conducted in SAS v9 (SAS Institute, Cary, NC, USA).

Results

Oxygen consumption rate estimates were obtained for 19 cownose rays. Rays ranged in mass between 0.40 and 8.25 kg wet weight and from 35 – 79 cm DW. Respirometry experiments were conducted on quiescent rays between April and December. Experimental temperatures ranged from 19.0 – 28.8 °C and salinities ranged from 17.1 – 30.8 ppt. Estimates of mass-dependent MO_2 ranged from 55.88 $mg\ O_2\ kg^{-1}\ hr^{-1}$ for an 8.25 kg ray to 332.75 $mg\ O_2\ kg^{-1}\ hr^{-1}$ for a 2.2 kg animal at 22-25 °C (Table 3.1).

Standard mass-dependent MO_2 of cownose rays increased with increasing temperature (Figure 3.1) and decreased with increasing mass (Figure 3.2). Multiple regression analysis

Table 3.1. Experimental trials for the cownose ray summarizing weight, temperature, salinity, and oxygen consumption rate (MO₂). Standard errors are shown in parentheses.

Ray Number	Temperature (°C)	Salinity (ppt)	Mass (kg)	VO ₂ range (mg O ₂ kg ⁻¹ hr ⁻¹)	Mean VO ₂ (mg O ₂ kg ⁻¹ hr ⁻¹)
1	19	29.1	1.3	74.8 – 108.0	91.4 (2.6)
2	19.4	28.5	0.5	79.2 – 122.4	96.0 (3.2)
3	20	29	0.8	42.0 - 94.5	74.3 (5.1)
4	19.9	29.2	0.8	89.3 - 131.25	116.7 (5.2)
5	21	26.7	2.8	84.9 - 114.4	98.6 (3.4)
6	22.8	30.1	8.25	44.8 - 70.8	55.9 (2.5)
7	23.1	30.8	7.5	81.1 - 97.2	87.8 (1.2)
8	21.4	30.1	4.75	89.3 - 101.8	97.9 (1.2)
9	21.8	30.1	3.75	104.8 - 185.5	131.3 (7.0)
10	21	30.7	1.9	114.9 - 163.6	127.0 (4.4)
11	25.8	24.3	2.5	151.3 - 308.02	204.3 (12.8)
12	26	23.9	3.8	165.8 - 300.32	215.4 (10.4)
13	25.8	25.1	1.1	294.0 - 343.6	327.3 (4.9)
14	25.4	24.2	0.6	105.0 - 273.0	225.9 (14.9)
15	26.5	24.4	2.2	294.3 - 364.8	332.8 (5.5)
16	28.8	28.1	1.1	187.1 - 316.9	232.6 (10.5)
17	28.6	18.3	0.5	72.0 - 172.8	128.4 (14.2)
18	27.8	17.1	0.6	204.0 - 300.0	232.2 (8.0)
19	28.7	19.8	0.4	179.4 - 282.9	217.1 (9.3)

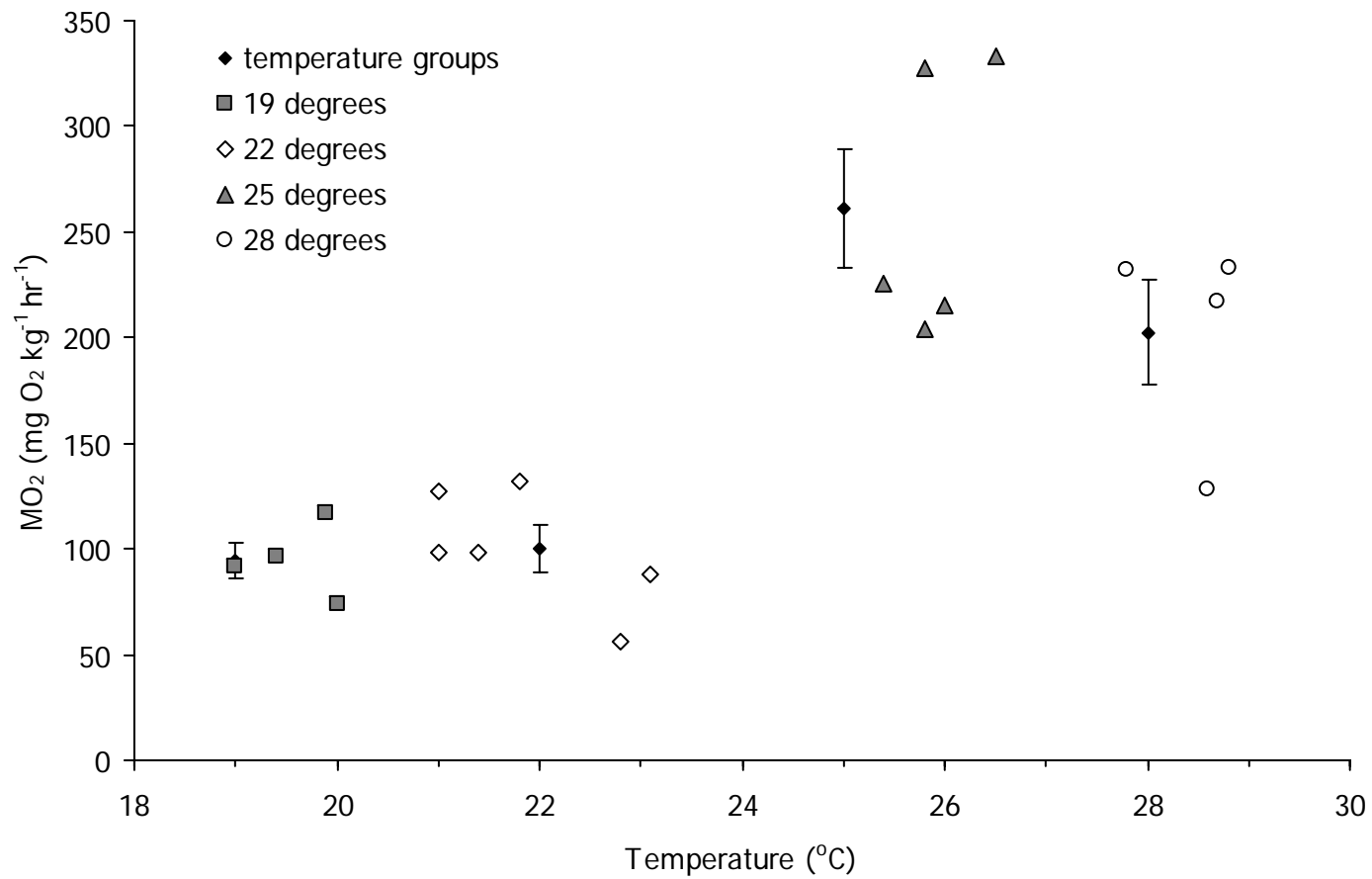


Figure 3.1. Standard mass-dependent oxygen consumption rates (mg O₂ kg⁻¹ hr⁻¹) determined for the cownose ray. Mean (\pm standard error) are presented for the four temperature groups (19, 22, 25, and 28 °C \pm one degree), along with the raw data.

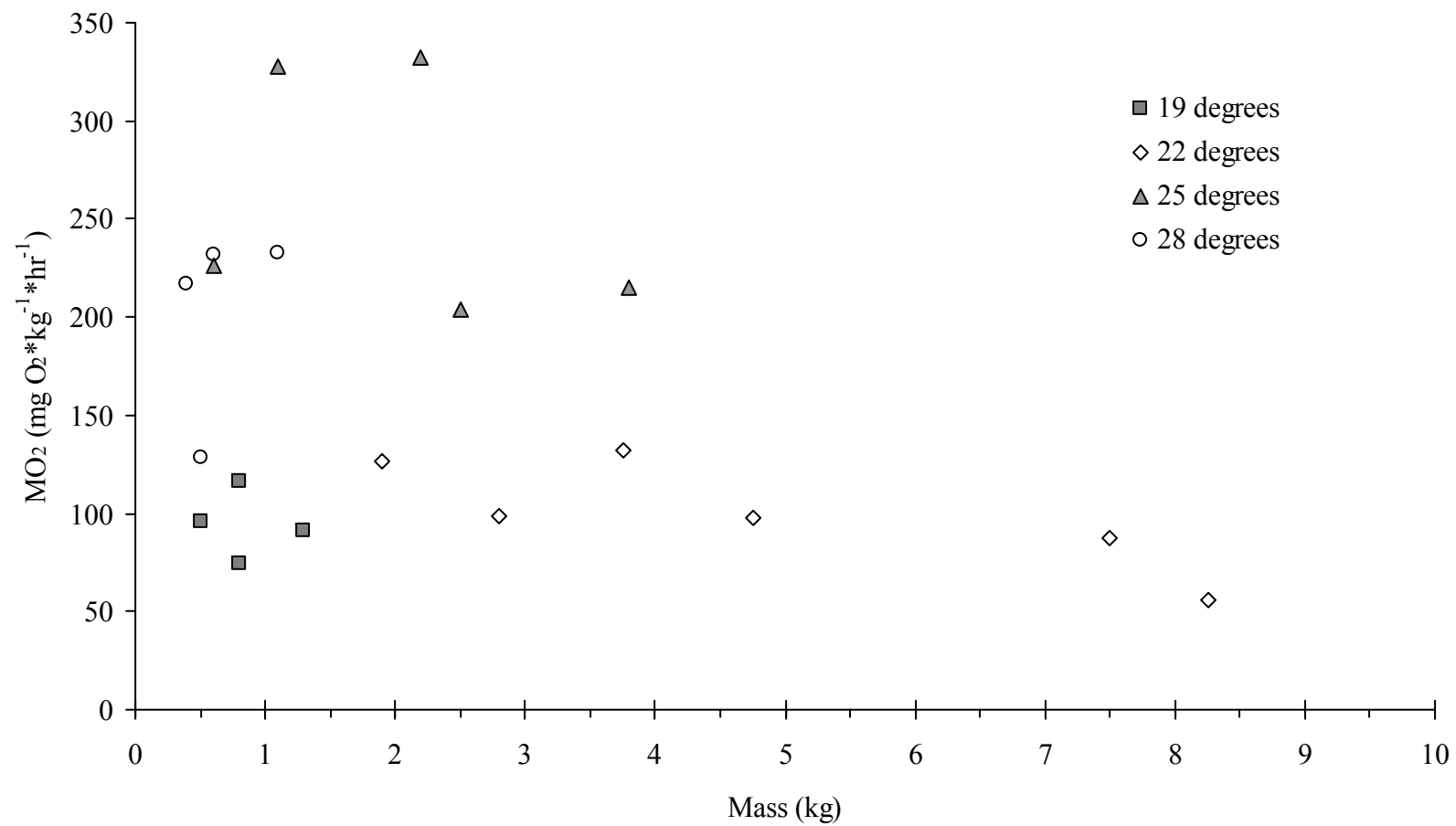


Figure 3.2. Relationship of mass and standard mass-dependent oxygen consumption rates ($\text{mg O}_2 \text{ kg}^{-1} \text{ hr}^{-1}$) for the four temperature groups (19, 22, 25, and 28 °C \pm one degree) determined for the cownose ray.

between log-transformed mass-independent MO_2 (in $mg\ O_2\ hr^{-1}$) and the log-transformed variables of salinity, temperature, and mass, indicated that temperature and mass were highly significant (temperature $p < 0.01$; mass $p < 0.0001$) while salinity was not significant ($p > 0.05$). Additionally, the model was highly significant overall (ANOVA: F-value = 32.23, $df = 3$, $p < 0.0001$, $r^2 = 0.84$). After excluding the non-significant variable salinity, the final regression model was: $\log(MO_2) = \log(\text{temperature}) * 2.48 + \log(\text{mass}) * 0.90 + 0.295$ ($p < 0.0001$; adjusted $r^2 = 0.84$).

Standard oxygen consumption rates were significantly different among temperature groups (single factor ANOVA: F-ratio = 17.728, $df = 3$, $p < 0.001$). Oxygen consumption rate ($\pm SE$) was $94.6 \pm 8.7\ mg\ O_2\ kg^{-1}\ hr^{-1}$ for the $19\ ^\circ C$ group ($n = 4$), $99.9 \pm 11.4\ mg\ O_2\ kg^{-1}\ hr^{-1}$ for the $22\ ^\circ C$ group ($n = 6$), $261.1 \pm 28.3\ mg\ O_2\ kg^{-1}\ hr^{-1}$ for the $25\ ^\circ C$ group ($n = 5$), and $202.6 \pm 25.0\ mg\ O_2\ kg^{-1}\ hr^{-1}$ for the $28\ ^\circ C$ group ($n = 4$). Tukey post-hoc pairwise comparisons found the lower temperatures (19 and $22\ ^\circ C$) were significantly different from upper temperatures (25 and $28\ ^\circ C$; $p < 0.01$) while the 19 and $22\ ^\circ C$ temperature groups and the 25 and $28\ ^\circ C$ temperature groups were not significantly different from each other ($p > 0.01$). The overall Q_{10} ($19 - 28\ ^\circ C$) was 2.33.

No significant differences in mass-dependent MO_2 were found between the repetitive oxygen consumption trials (paired two-sample t-test: $t_{calc} = -0.77$, t_{crit} (two-tailed) = 4.30, $df = 2$, $p > 0.10$). The average salinity difference between the two trials was 5.5 ppt and the average temperature difference was $1.1\ ^\circ C$ (Table 3.2).

Discussion

In ectothermic vertebrates, temperature is often one of the key environmental variables controlling many physiological functions, including oxygen consumption rate

Table 3.2. Summary of repetitive oxygen consumption (MO_2) trials at differing salinities. Standard errors are shown in parentheses.

Ray No.	Mass (kg)	Trial 1			Trial 2			Difference*	
		Mean VO_2 (mg O_2 kg^{-1} hr^{-1})	Temperature ($^{\circ}C$)	Salinity (ppt)	Mean VO_2 (mg O_2 kg^{-1} hr^{-1})	Temperature ($^{\circ}C$)	Salinity (ppt)	Temperature ($^{\circ}C$)	Salinity (ppt)
1	0.5	128.4 (14.2)	28.6	18.3	211.6 (8.3)	27.6	23.7	1	5.4
2	0.6	232.2 (8.0)	27.8	17.1	265.2 (7.1)	26.7	21.5	1.1	4.4
3	0.4	217.1 (9.3)	28.7	19.8	181.0 (10.3)	27.4	26.4	1.3	6.6

* average temperature difference = 1.1 $^{\circ}C$; average salinity difference = 5.5 ppt

(Schmidt-Nielsen 1983). Previous research on elasmobranchs has determined that MO_2 rate increases as temperature increases (Du Preez et al. 1988, Hopkins and Cech 1994, Carlson and Parsons 1999, Miklos et al. 2003). MO_2 rate continuously increased with water temperature with no indications of leveling off for the leopard shark (Miklos et al. 2003) and the bonnethead shark (Carlson and Parsons 1999). Hopkins and Cech (1994), however, reported a steady increase in MO_2 rate over the first three temperatures for the bat ray, but observed a slight leveling off at the highest temperature tested (26 °C). The MO_2 data for the cownose ray more closely follow the pattern observed by Hopkins and Cech (1994); mean oxygen consumption rate of the cownose rays increased slightly between the 19 °C and 22 °C temperature groups, with a large increase between the 22 °C and 25 °C temperature groups.

The drop in average MO_2 rate between the 25 °C and 28 °C temperature groups for the cownose rays was unexpected, but may be due to the small sample size available at the highest experimental temperature. Four data points were available to determine the average rate at 28 °C and these four values showed considerable variability. The large amount of variability in MO_2 rate observed within this temperature group indicates that a larger sample size may be necessary to obtain a more realistic estimate. Additionally, it is important to note that the 28 °C temperature group may represent the upper thermal range over which cownose rays are commonly encountered in the field (John Carlson, personal communication). Furthermore, bioenergetics modeling indicates that cownose rays decrease in weight at temperatures above 30 °C, due mainly to the high metabolic costs associated with higher water temperatures (Chapter IV).

Rates of oxygen consumption determined for the cownose ray were similar to those reported for other batoids (Table 3.3). Ezcurra (2001) determined an average oxygen

Table 3.3. Summary of oxygen consumption rates (MO_2) for select elasmobranch species. All rates reported were determined at 20 °C using flow-through respirometry, except noted. Standard errors are shown in parentheses when available. *determined using static respirometry.

Species	Mass (kg)	VO_2 (mg O_2 kg^{-1} hr^{-1})	Reference
<i>Rhinobatos annulatus</i>	1.1	81.3	Du Preez et al. (1988)
<i>Myliobatis aquila</i>	1.1	77.0	Du Preez et al. (1988)
<i>Myliobatis californica</i>	4.3 - 6.8	261.5 (30.8)	Hopkins and Cech (1994)
<i>Dasyatis americana</i>	0.3	164.3 (8.9)	Fournier (1996)
<i>Dasyatis violacea</i> *	5.3 - 32.6	101.7 (53.4)	Ezcurra (2001)
<i>Rhinoptera bonasus</i>	0.5 - 4.75	104.3 (6.1)	current study

consumption rate of 101.7 mg O_2 kg^{-1} hr^{-1} at 20 °C for 5.3 – 32.6 kg pelagic stingrays (*Dasyatis violacea*) using static respirometry. Du Preez et al. (1988) reported a MO_2 at 20 °C for a 1.1 kg bull ray of 77.0 mg O_2 kg^{-1} hr^{-1} . Cownose ray oxygen consumption rate at 20 °C was 104.3 mg O_2 kg^{-1} hr^{-1} for 0.5 – 4.75 kg rays.

Salinity did not affect oxygen consumption rate in cownose rays. This was surprising because Meloni et al. (2002) observed a significant increase in MO_2 for the bat ray between two seawater salinities (33 and 35 ppt) and two brackish water salinities (15 and 25 ppt). However, that study was designed specifically to examine the effect of salinity on oxygen consumption. My experiments were not designed to specifically examine the effect of salinity

on MO_2 . It is possible that cownose rays may experience a similar effect; however the greater effects of temperature and mass may mask the detection of a salinity effect.

Increasing osmoregulatory costs could raise standard metabolic rates (Brett and Groves 1979). Janech and Piermarini (1997) and Piermarini and Evans (1998) suggested energetic costs of osmoregulation, associated with changes in renal function, with decreases in salinity for the Atlantic stingray, *Dasyatis sabina*. The range of salinities experienced by the cownose rays in my experiments (17 to 30.8 ppt) was smaller than the range they normally experience in their natural environment (17 to 37 ppt), which may have contributed to the lack of a statistically significant salinity effect. Additional information demonstrates that they can tolerate much lower salinities than experienced during this study. Cownose rays have been collected in Lake Pontchartrain, LA at salinities as low as 5.2 ppt (Thompson and Verret 1980), indicating they are able to tolerate low salinity environments. The degree to which this affects their ability to osmoregulate, and its associated metabolic costs, needs further study.

Acclimation can result in metabolic compensation, leading to smaller differences in MO_2 between temperatures, and consequently lower Q_{10} values (Schmidt-Nielsen 1983, Burggren and Roberts 1991). Among batoids, Du Preez et al. (1988) reported an overall Q_{10} of 1.87 (10 – 25 °C) for bull rays exposed to gradual changes (1 °C per 24 hr) of temperature in the laboratory and holding the animals at the desired temperature for eight days prior to experimentation. In contrast, Hopkins and Cech (1994) examined the effect of rapid changes in temperature (0.5 °C per hr) on standard MO_2 in the bat ray acclimated for only 12 hours before oxygen consumption measurements were recorded. Bay rays displayed an overall Q_{10} (8 – 26 °C) of 3.00 (Hopkins and Cech 1994). The overall Q_{10} (19 – 28 °C) determined for

the acclimatized cownose ray was 2.33, falling between the estimates of the bull ray (1.87) and the bat ray (3.00).

Bat rays, bull rays, and cownose rays have similar autecologies in that they are specialized for active swimming (McEachran 1990), all forage in bays and estuaries for invertebrate fauna (Ridge 1963, van der Elst 1981, Smith and Merriner 1985), and all are known to inhabit environments with widely fluctuating temperatures (Du Preez et al. 1990, Smith and Merriner 1987, Matern et al. 2000). Given the similarity among species, the expectation would be that they would have similar Q_{10} values. The fact that our estimate of Q_{10} for the cownose ray falls between those of the other ray species may reflect the difference between acclimated and acclimatized rays. The high Q_{10} estimate of 3.00 obtained by Hopkins and Cech (1994) likely reflects the rapid temperature fluctuations (acclimated vs. acclimatized) on oxygen consumption rate, while the lower Q_{10} estimate of 1.87 for the bull ray (Du Preez et al., 1988) may be a consequence of the acclimation procedure. The bull rays may have been overcompensating to the change in temperature as the temperature changes still occurred more rapidly than the animals would most likely experience in the natural environment (Schmidt-Nielsen 1983). Interestingly among elasmobranchs, the Q_{10} rate measured for cownose ray was most similar to the bonnethead shark (2.3; Carlson and Parsons 1999), which was also exposed to seasonal changes in temperature.

Literature Cited

- Bigelow, H.B. and W.C. Schroeder. 1953. Fishes of the Western North Atlantic. Part I, Lancets, cyclostomes and sharks. Memoirs of the Sears Foundation of Marine Research.
- Brett, J.R. and J.M. Blackburn. 1978. Metabolic rate and energy expenditure of the spiny dogfish, *Squalus acanthias*. Journal of the Fisheries Research Board of Canada. 35: 816-821.

- Brett, J.R. and T.D.D. Groves. 1979. Physiological energetics. Pages 279-352 in W.E.S. Hoar and D.J. Randall, editors. Fish Physiology Volume VII. Academic Press, New York.
- Burggren, W.W. and J.L. Roberts. 1991. Respiration and metabolism. Pages 353-436 in C.L. Prosser, editor. Environmental and metabolic animal physiology. Wiley-Liss Inc, New York, New York.
- Carlson, J.K. and G.R. Parsons. 1999. Seasonal differences in routine oxygen consumption rates of the bonnethead shark. *Journal of Fish Biology* 55: 876-879.
- Carlson, J.K., C.L. Palmer, and G.R. Parsons. 1999. Oxygen consumption rate and swimming efficiency of the blacknose shark, *Carcharhinus acronotus*. *Copeia* 1999(1): 34-39.
- Carlson, J.K., K. J. Goldman, and C.G. Lowe. 2004. Metabolism, energetic demand, and endothermy. Pages 201- 222 in Carrier, J.C., J.A. Musick, and M.R. Heithaus, editors. Biology of sharks and their relatives. CRC Press, Boca Raton.
- Chan, D.K.O. and T.M. Wong. 1977. Physiological adjustments to dilution of the external medium in the lip-shark, *Hemiscyllium plagiosum* (Bennett). *Journal of Experimental Zoology* 200: 97-102.
- Du Preez, H. H., A. McLachlan, and J.F.K. Marais. 1988. Oxygen consumption of two nearshore marine elasmobranchs, *Rhinobatos annulatus* (Muller & Henle, 1841) and *Myliobatus aquila* (Linnaeus, 1758). *Comparative Biochemistry and Physiology* 89A(2): 283-294.
- Du Preez, H. H., A. McLachlan, J.F.K. Marais, and A.C. Cockcroft. 1990. Bioenergetics of fishes in a high-energy surf-zone. *Marine Biology* 106: 1-12.
- Ezcurra, J.M. 2001. The mass-specific routine metabolic rate of captive pelagic stingrays, *Dasyatis violacea*, with comments on energetics. Masters thesis. Moss Landing Marine Laboratories. Stanislaus, California State University, Stanislaus. 51 pages.
- Ferry-Graham, L. and A.C. Gibb. 2001. Comparison of fasting and postfeeding metabolic rates in a sedentary shark, *Cephaloscyllium ventriosum*. *Copeia* 2001(4): 1108-1113.
- Fournier, A.P. 1996. The metabolic rates of two species of benthic elasmobranchs, nurse sharks and southern stingrays. Masters thesis. Hofstra University. Hempstead, New York. 29 pages.
- Hopkins, T.E. and J.J. Cech, Jr. 1994. Effect of temperature on oxygen consumption of the bat ray, *Myliobatis californica* (Chondrichthyes, Myliobatidae). *Copeia* 1994(2): 529-532.

- Janech, M.G. and P.M. Piermarini. 1997. Urine flow rate and urine composition of freshwater Atlantic stingrays, *Dasyatis sabina*, from the St. Johns River, Florida. *American Zoologist* 37:147A.
- Lowe, C.G. 2001. Metabolic rates of juvenile scalloped hammerhead sharks (*Sphyrna lewini*). *Marine Biology* 139: 447-453.
- Matern, S.A., J.J. Cech, Jr., and T. Hopkins. 2000. Diel movements of bat rays, *Myliobatis californica*, in Tomales Bay, California: evidence for behavioral thermoregulation? *Environmental Biology of Fishes* 58: 173-182.
- McEachran, J. D. 1990. Diversity of rays: why are there so many species? *Chondros* 2:1-6.
- McEachran, J.D. and C. Capapé. 1984. Rhinopteridae. Page 208 in Whitehead, P.J.P., M.-L. Bauchot, J.-C. Hureau, J. Nielsen, & E. Tortonese, editors. *Fishes of the North-eastern Atlantic and Mediterranean*. Volume 1. UNESCO.
- McEachran, J.D. and J.D. Fechhelm. 1998. *Fishes of the Gulf of Mexico*. Volume 1. University of Texas Press.
- Meloni, C.J., J.J. Cech, Jr., and S.M. Katzman. 2002. Effect of brackish salinities on oxygen consumption of bat rays (*Myliobatis californica*). *Copeia* 2: 462-465.
- Metcalf, J.D. and P.J. Butler. 1984. Changes in activity and ventilation in response to hypoxia in unrestrained, unoperated dogfish (*Scyliorhinus canicula* L.). *Journal of Experimental Biology* 108: 411-418.
- Miklos, P., S.M. Katzman, and J.J. Cech, Jr. 2003. Effect of temperature on oxygen consumption of the leopard shark, *Triakis semifasciata*. *Environmental Biology of Fishes* 66:15-18.
- Neer, J.A., J.K. Blackburn, B.A. Thompson. In press. Shark nursery areas of central Louisiana's nearshore coastal waters. Pages X - XX in C.T. McCandless, N.E. Kohler, and H.L. Pratt, Jr., editors. *Shark nursery grounds of the Gulf of Mexico and the East Coast waters of the United States*. American Fisheries Society, Symposium XX, Bethesda, Maryland.
- Piermarini, P.M. and D.H. Evans. 1998. Osmoregulation of the Atlantic stingray (*Dasyatis sabina*) from the freshwater Lake Jesup of the St. Johns River, Florida. *Physiological Zoologist* 71(5): 553-560.
- Ridge, R.M. 1963. Food habits of the bat ray, *Myliobatis californica*, from Tomales Bay, California. Masters Thesis. University of California, Berkley.

- Schmidt-Nielsen, K. 1983. *Animal Physiology: adaptation and environment*. Cambridge Univ. Press, Cambridge, United Kingdom.
- Schwartz, F.J. 1990. Mass migratory congregations and movements of several species of cownose rays, Genus *Rhinoptera*: a world-wide review. *Journal of the Elisha Mitchell Scientific Society* 106:10-13.
- Sheskin, D.J. 2003. *Handbook of parametric and nonparametric statistical procedures*. 3rd Edition. CRC Press. Boca Raton, Florida.
- Smith, J.W. and J.V. Merriner. 1985. Food habits and feeding behavior of the cownose ray, *Rhinoptera bonasus*, in lower Chesapeake Bay. *Estuaries* 8(3): 305-310.
- Smith, J.W. and J.V. Merriner. 1987. Age and growth, movements and distribution of the cownose ray, *Rhinoptera bonasus*, in Chesapeake Bay. *Estuaries* 10(2): 153-164.
- Thompson, B.A. and J.S. Verret. 1980. Nekton of Lake Pontchartrain, Louisiana, and its surrounding wetlands. Pages 711-864 *in* Environmental analysis of Lake Pontchartrain, Louisiana, its surrounding wetlands, and selected land Uuses. Volume 2, Prepared for U.S. Army Engineer District, New Orleans.
- van der Elst, R. 1981. *A guide to the common sea fishes of Southern Africa*. Struik Publishers, Cape Town, South Africa.

CHAPTER IV.

MODELING THE EFFECTS OF TEMPERATURE ON INDIVIDUAL AND POPULATION GROWTH OF THE COWNOSE RAY, *RHINOPTERA BONASUS*: A BIOENERGETICS APPROACH

Introduction

The cownose ray, *Rhinoptera bonasus*, is a marine elasmobranch commonly observed throughout the Gulf of Mexico (McEachran and Fechhelm 1998). Elasmobranchs (sharks, skates, and rays) are long-lived, late reproducing, low fecundity organisms, with many species having complex reproductive cycles and movement patterns (Compagno 1990, Hoenig and Gruber 1990, Castro 1993). The "K-selected" life history characteristics of these species make them extremely susceptible to overfishing (Holden 1974; Rose et al. 2001), and potentially to variation in other natural and anthropogenic factors (Heppell et al. 1999, Russell 1999).

Cownose ray abundance and distribution seems to be determined, at least in part, by water temperature (Smith and Merriner 1987, Schwartz 1990). Cownose rays appear in the Chesapeake Bay when water temperatures reach 16°C in the spring, and usually begin their southward migration when water temperatures cool to 22 °C in the fall (Smith and Merriner 1987, Schwartz 1990). Along the northwest Florida shelf, rays begin to depart the area when the summer water temperatures are between 28 °C and 30 °C, and very few rays are captured at temperatures warmer than 30 °C (J. Carlson, personal communication). These movements in response to temperature suggest that cownose rays may behaviorally thermoregulate in order to facilitate their growth or some other biological process.

Changes in water temperature can arise from natural seasonal and interannual fluctuations or from human induced shifts related to global climate change. The global

climate is predicted to experience an average gradual warming of 1.4 – 5.8 °C over the next half century because of a buildup of greenhouse gases, primarily carbon dioxide (Smith 2004). The average temperature in the United States could increase by 2 – 8 °C due to the large amount of greenhouse gases produced in the region; however, the increase will most likely be less than 4 °C (Smith 2004). Mean daily coastal water temperatures along the northwest Florida coast in areas inhabited by cownose rays varied by approximately 0.5-3 °C during 2000-2002 (National Ocean Services Center for Operational Oceanography Products and Services).

Increases in temperature due to global warming could have significant effects on aquatic ecosystems (Hill and Magnuson 1990). Kennedy et al. (2002) state that, although summer temperatures in tropical waters may not increase much higher than they are currently due to evaporative cooling, temperate and boreal regions may experience temperature increases that will be stressful or lethal for some organisms. Sub-lethal effects of warmer temperatures may include changes in metabolism, growth, and distribution (Kennedy et al. 2002). I used an individual-based bioenergetics model coupled to a matrix projection model to predict how water temperatures warmer than current conditions and cooler than current conditions would affect the growth and population dynamics of the cownose ray in the northern Gulf of Mexico. The outputs of the bioenergetics model are used to estimate the parameters (inputs) of the matrix projection model.

Bioenergetics models use a balanced energy budget equation to estimate growth or production, or to predict consumption rates. Bioenergetics models have been widely used for teleosts fishes (Ney 1993, Hanson et al. 1997). These models have been used to examine predator-prey relationships (Ney 1990, Hartman and Margraf 1992), study pollutant levels in

fishes (Borgmann and Whittle 1992), quantify trophic-based processes such as nutrient cycling and energy flow across trophic levels (He et al. 1993, Schindler et al. 1993), and compare production and species growth across systems (Rand et al. 1993). Bioenergetics modeling is appealing as it provides a link between fish physiology and environmental conditions, and provides a means for quantifying the relative importance of various environmental factors on individual growth or consumption (Adams and Breck 1990, Brandt and Hartman 1993).

Bioenergetic studies on elasmobranchs have been limited compared to the widely studied teleost fishes. Physiological experiments necessary to configure a bioenergetics model are often difficult to obtain for many species of elasmobranchs. Many elasmobranchs are large and exhibit migratory behavior, which makes them difficult to maintain in captivity (Carlson et al. 2004, Lowe and Goldman 2001). For most elasmobranchs, bioenergetic studies have focused on static energy budgets typically based on the direct measurement of a few of the components, with the remaining components estimated from other studies reported in the literature. For example, Sundstrom and Gruber (1998) produced an energy budget for the lemon shark, *Negaprion brevirostris*, using speed-sensing transmitters to determine metabolism. In another study of lemon sharks, Wetherbee and Gruber (1993) constructed an energy budget for the lemon shark after they determined absorption efficiency. Based on direct determination of metabolism, energy budgets of the bull shark, *Carcharhinus leucas* (Schmid and Murru 1994), the pelagic stingray, *Dasyatis violacea* (Ezcurra 2001), and juvenile scalloped hammerhead sharks, *Sphyrna lewini* (Lowe 2002) have been produced.

Several studies have produced energy budgets using experimentally derived estimates of several of the major bioenergetics components. Du preez et al. (1988 and 1990) produced

both species-specific and a generalized elasmobranch energy budget for the lesser guitarfish, *Rhinobatus annulatus*, and the bull ray, *Myliobatus aquila* by directly measuring standard oxygen consumption rate and specific dynamic action. Parsons (1987) produced sex-specific energy budgets for the bonnethead shark, *S. tiburo*, in two different locations by measuring consumption, standard oxygen consumption rate, and activity patterns along with information regarding reproductive and somatic growth rates.

While bioenergetics-based energy budgets of elasmobranchs have been developed, few of these have used this information to estimate or examine how ecological or time-varying environmental factors would affect consumption or growth. Notable exceptions include Medved et al. (1988), who used a bioenergetics model to estimate daily ration for young sandbar sharks, *Carcharhinus plumbeus*, and Schindler et al. (2002), who modeled the predator-prey interactions between the blue shark, *Prionace glauca*, and yellowfin tuna, *Thunnus albacares*.

Matrix projection models have been widely used to examine the equilibrium and temporal dynamics of animal populations. Just as bioenergetics models provide a link between the environment and individual growth, matrix population projection models provide a link between the individual and the population (Caswell 2001). Matrix projection models are based on a description of the species life cycle. Vital rates, such as growth, maturation, reproduction, and mortality, describe the progression of individuals through their life cycle, and the magnitudes of these rates determine the dynamics of the population over time. Matrix projection models may be age-based or staged-based, depending on the life cycle and the available data, and can be used to derive equilibrium characteristics of the population (e.g., stable age distribution) or to simulate long-term population dynamics (Caswell 2001).

Age-structured matrix models have a long history in fisheries and wildlife population dynamics, and have recently been used to examine the population dynamics of several elasmobranch species (Kingsland 1985, Cortés 2004). Life tables, which are directly related to matrix projection models, have been used to examine the demographics of the sandbar shark in the western North Atlantic (Sminkey and Musick 1996), and the effects of fishing on the dusky shark, *C. obscurus*, in southwestern Australia (Simpfendorfer 1999). More recently, Cortés (2002) examined the effects of incorporating uncertainty into the estimates of vital rates used in an age-structured matrix projection modeling approach, and utilized elasticity analysis to examine the sensitivity of population growth rate to survival and fecundity among 38 species of sharks. Frisk et al. (2002) used age- and stage-based matrix projection model analysis to examine the equilibrium (long-term) population dynamics of three species of skates occurring in the western Atlantic Ocean.

The objectives of this research were to: 1) develop a bioenergetics model for the cownose ray in the northern Gulf of Mexico using, as much as possible, species-specific laboratory and field-derived parameter estimates, 2) predict the growth, survival, and reproductive output of individual rays over their lifetime, 3) predict the relative effects of warmer and cooler than baseline water temperatures on cownose ray growth, survival, and reproductive output, and 4) extrapolate the growth, survival, and reproductive responses to warmer and cooler temperatures to the population level using a matrix projection model.

Materials and Methods

Species Description

The cownose ray ranges from southern New England to southern Brazil within the western Atlantic Ocean as well as throughout the Gulf of Mexico and off the coast of Cuba

(Bigelow and Schroeder, 1953; McEachran and Fechhelm, 1998). Rays are semi-pelagic and gregarious; often forming large schools, and are known to undertake long migratory movements (McEachran and Capapé, 1984; Schwartz, 1990). Cownose rays are most often encountered on continental and insular shelves where they feed primarily on bivalve mollusks and crustaceans (Smith & Merriner 1985; McEachran & Fechhelm 1998).

The life history of the cownose ray in the northern Gulf of Mexico has been described by Neer and Thompson (in press; Chapter II). Verified age estimates indicate that cownose rays live in nature for at least 18 years, with a predicted theoretical longevity of 26 years. Both male and female cownose rays reach 50% maturity at 4-5 years of age (~4.6 – 4.9 kg wet weight). Females produce one pup/litter, with a gestation time of 11-12 months. Cownose rays have few natural predators with the exception of some large shark species such as the bull shark (Jason Blackburn, personal communication). There is currently no directed fishery for cownose rays, although they are often taken as bycatch in several fisheries (Smith and Merriner 1987, Trent et al. 1997). In the northern Gulf of Mexico, cownose rays are encountered at temperatures from 15.5 to 33.6 °C, and salinities ranging from 17 to 37 ppt (John Carlson, personal communication), suggesting that they are both eurythermal and euryhaline.

Bioenergetics Model Description

Overview. The cownose ray bioenergetics model followed a cohort of female individuals from birth over their lifetime. Numbers of individuals in the cohort were decremented daily based on a specified size-dependent mortality rate. Body weight of each individual (grams weight wet, g ww) was updated daily based on the revised version of the Wisconsin bioenergetics formulation (Hanson et al. 1997). Size-dependent maturity was used

to determine the age of first reproduction; weight loss associated with birth of a pup was based on observed average weight of pups at birth (Chapter II) and was imposed each May 15th for mature females. The bioenergetics model predicted the daily survival, daily body weight, and annual pup production of female individuals over a maximum age of 25 years. Predictions were summarized as the number of individuals alive, average weight of an individual, and number of pups produced by year (equivalent to age). I used the bioenergetics model to simulate the effects of cooler and warmer water temperature scenarios on cownose ray growth, survival, and reproductive output.

Mortality. Daily probability of dying was determined by fitting a curve between annual mortality rate and body weight. Instantaneous annual natural mortality was assumed to be 0.2 for the smallest individuals and decreased exponentially with weight, approaching 0.1 for the heaviest (oldest) individuals:

$$IMR = \left(0.1 + 0.6658 * EXP^{\frac{-W}{921.49}} \right) \quad (1)$$

where *IMR* = natural annual instantaneous mortality rate and *W* = weight of ray in g ww. Fishing mortality was assumed to be zero as there is currently no directed fishery for this species. An upper mortality rate of 0.2/year was calculated using a general equation between mortality rate and longevity for unexploited or lightly exploited fish stocks (Hoenig 1983) and the observed and theoretical maximum age determined from the vertebral ageing study (Chapter II, Neer and Thompson in press). As there is no directed fishery for the cownose ray, *Z* (total instantaneous mortality) can approximate *M* (natural instantaneous mortality rate). The lower value of 0.1/year was chosen following Brewster-Geisz and Miller (2000) and the assumption that natural mortality decreases as animal weight increase (Roff 1992, Cortés 2004). Annual

mortality rates were converted to daily rates and this probability of dying was compared to a randomly generated number from a uniform distribution each day. If randomly generated number was less than the probability of dying, then the individual died and was removed from the cohort.

Growth. Daily change in body weight was based on a mass balance equation:

$$G_S = ((C_{\max} * p * f(T)) - (M_R + SDA) - (F + U)) * C_F - G_R \quad (2)$$

where G_S = somatic growth ; C_{\max} = maximum specific consumption rate; p = proportion of maximum consumption actually obtained; $f(T)$ = temperature dependence function; T = water temperature in °C; M_R = standard respiration rate; SDA = metabolic costs of specific dynamic action; F = egestion; U = excretion; C_F = caloric conversion factor, and G_R = growth used for reproduction. All rates except growth used for reproduction (G_R) are in the units of grams prey/gram ray/day. These rates were converted to grams ray/grams ray/day based on the ratio of the caloric densities of ray to their prey. Ray caloric density was assumed to be 1415 cal/g ww, determined for the lemon shark (Gruber 1984); 6390 cal/g ww was used to reflect the dominant prey of bivalves (Bradley 1996). Therefore, the conversion factor (C_F) in Equation 2 was set to 4.516. The parameters of all of the rates were specified based on my experimental results or from literature reported results except for p -values, which were determined for each age-class by calibration.

Consumption. Realized consumption was estimated as the proportion of maximum daily ration for an individual (Hanson et al. 1997). Consumption was both temperature and body weight dependent. The consumption function used in the model follows Hanson et al. (1997):

$$C = C_{\max} * p * f(T) \quad (3)$$

$$C_{\max} = CA * W^{CB} \quad (4)$$

where C = specific consumption rate in g prey/g ray/day, C_{\max} = maximum specific consumption rate in g prey/g ray/day, p = proportion of maximum consumption realized, $f(T)$ = temperature dependence function, T = water temperature in °C, CA = intercept of the allometric mass function in g prey/g ray/day, CB = slope of the allometric mass function, and W = wet weight in grams.

Estimates for CA and CB were determined using available information on daily ration of elasmobranchs. Wetherbee and Cortés (2004) reported that feeding rates for elasmobranchs ranged from 0.3 – 4.3% body weight (BW)/day, but rarely surpassed 3% BW/day, and Bradley (1996) estimated the realized daily ration of the Atlantic stingray, *Dasyatis sabina*, to be 2.52% BW/day. Additionally, evidence indicates that consumption rates of adults may be up to an order of magnitude less than those of pups (Van Dykhuizen and Mollet 1992, Enric Cortés unpublished data). Using this information as a target, values of CA and CB were substituted in the C_{\max} equation (Equation 4) for a range of ray weights (1000 – 22,000 g ww) until values of CA and CB were found that produced C_{\max} estimates ranging from ~7% BW/day for small individuals to ~3% BW/day for the largest rays.

The temperature dependence function for consumption used in the model follows Equation 2 (warm-water species) from Hanson et al. (1997):

$$f(T) = V^X * EXP^{X*(1-V)} \quad (5)$$

$$\text{where } V = \frac{CTM - T}{CTM - CTO} \quad (6)$$

$$X = \frac{Z^2 * \left(1 + \left(1 + \frac{40}{Y}\right)^{0.5}\right)^2}{400} \quad (7)$$

$$Z = LN(CQ) * (CTM - CTO) \quad (8)$$

$$Y = LN(CQ) * (CTM - CTO + 2) \quad (9)$$

where CTM = maximum water temperature above which consumption ceases, T = temperature in °C, CTO = optimal temperature for consumption, and CQ = rate at which the function increases over relatively low water temperatures (similar to a Q₁₀ relationship).

Using the values of CA and CB determined above, respiration-related parameters set to values I measured, and a p-value of 0.5, various combinations of values for CTO and CTM were substituted into the consumption equation (Equation 3) until realistic realized consumption rates were obtained. Initial starting values (CTO = 25 °C, CTM = 35 °C) were those determined for the bonnethead shark (John K. Carlson, unpublished data). The target for realized consumption was that the highest realized consumption rate across a range of body weights occurred at around 25 °C, and that respiration rate comprised ~15 -25% of the realized consumption rate (Hanson et al. 1997). The final values used in the model were CTO = 28 °C and CTM = 36 °C (Table 4.1).

Respiration. Respiration, defined as the amount of energy used for routine metabolism, is dependent on water temperature, fish size, and activity level (Hanson et al. 1997). Standard respiration rate is determined as a function of mass, and then increased using a temperature dependent function and a factor representing activity (Hanson et al. 1997):

$$R = RA * W^{RB} * f(T) * ACT \quad (10)$$

Table 4.1. Bioenergetics parameter values used in the cownose ray bioenergetics model.

Parameter	Equation	Units	Value
Consumption (C)	$C_{\max} * p * f(T)$	g prey/g ray/day	
Cmax	$CA * W^{CB}$	g prey/g ray/day	
CA		g prey/g ray/day	0.289
CB		unitless	-0.374
CQ		unitless	2.33
CTO		°C	28.0
CTM		°C	36.0
p		proportion	0.0 - 1.0
Respiration (R)	$RA * W^{RB} * f(T) * ACT$	g prey/g ray/day	
RA		g prey/g ray/day	0.0068
RB		unitless	-0.0919
Q ₁₀		unitless	2.33
TREF		°C	24.0
ACT		unitless	1.9
Reproduction			
G _R		g wet weight	777
Specific Dynamic Action (S)	$SDA * C$	g prey/g ray/day	
SDA		proportion	0.14
Egestion & Excretion (F)	$FA * C$	g prey/g ray/day	
FA		proportion	0.27

where R = specific respiration rate in g prey/ g ray/day, RA = intercept of the allometric mass function in g prey/ g ray/day, W = wet weight in grams, RB = slope of the allometric mass function, $f(T)$ = temperature dependence function, and ACT = activity multiplier.

The values of RA and RB were obtained from oxygen consumption data reported in Chapter III. Standard respiration rate (in mg O₂ kg⁻¹ hr⁻¹) was obtained from 19 acclimatized cownose rays using flow-through respirometry. Animals ranged from 0.4 to 8.25 kg and experiments were conducted at temperatures from 19.0 to 28.8 °C (see Chapter III for details). Respiration rates were converted from oxygen consumption rates using an oxycalorific coefficient of 3.25 cal mg⁻¹ O₂ (Brett and Groves 1979).

The activity multiplier used in the model (1.9) was determined from experimental data for the bonnethead shark (John Carlson, unpublished data). The temperature dependence function was determined using the following equation:

$$f(T) = Q_{10}^{\frac{T_{ind} - TREF}{10}} \quad (11)$$

where $f(T)$ = temperature dependence function, Q_{10} = temperature sensitivity, T_{ind} = temperature experienced by each individual ray in °C, and TREF = reference temperature representing the temperature that corresponds to the values of RA and RB. The value of Q_{10} , the change in respiration rate over a 10-degree change in temperature (Schmidt-Nielsen 1983), used in the model was 2.33 and was experimentally determined for the cownose ray (Chapter III). TREF was set to 24 °C because this was the average temperature at which the oxygen consumption experiments were conducted that formed the basis for estimating the values of RA and RB (Table 4.1).

Specific dynamic action: Specific dynamic action was assumed to be proportional to realized consumption:

$$S = SDA * C \quad (12)$$

where S = proportion of assimilated energy lost to specific dynamic action, SDA = specific dynamic action, and C = specific consumption rate in g prey/g ray/day. The value of SDA used in the model was 0.14, determined for the bull ray, *Myliobatus aquila*, at 20 °C (Du Preez et al. 1988, Table 4.1)).

Egestion and excretion. Egestion and excretion were lumped together and expressed as a proportion of realized consumption:

$$F = FA * C \quad (13)$$

where F = combined egestion and excretion in g prey/g ray/day; FA = proportion of consumption that goes to egestion and excretion; and C = specific consumption rate in g prey/g ray/day. Wetherbee and Gruber (1993) reported that energy lost as non-assimilated food (urine and feces) represented 27% of the total ingested energy for the lemon shark; therefore FA was set to 0.27 in the model (Table 4.1).

Reproduction. The model assumes all individuals are female. The probability of an individual reproducing at a given age was determined based upon a logistic function that related the fraction of the population that was mature to body weight (Chapter II, Neer and Thompson in press). This probability was compared to a randomly generated value from a uniform distribution. If the random number was smaller than the fraction mature, the individual would reproduce at that age. The reproductive event was modeled by the loss of 777 g ww on May 15th, representing the average birth weight of one pup. Cownose rays have one litter/year, with each litter being comprised of a single pup (Chapter II, Neer and Thompson in press).

Temperature. A daily temperature function, starting on May 1st and ending on April 30th, was developed using data provided by the National Marine Fisheries Service – Panama City, Florida Laboratory (John Carlson unpublished data) and from data retrieved from the National Ocean Services Center for Operational Oceanography Products and Services. Data sources selected were from the Panama City, Florida region, where the biological data used to develop and calibrate the model were collected. The daily temperature function generated an average water temperature for each day of the year in the simulations (Figure 4.1).

Individual-level variability. Three sources of individual variability in ray growth were simulated: daily temperature experienced, weight-specific respiration rate, and daily value of p . For each day of the simulation, each ray was assigned a daily water temperature from a normal distribution with the mean equal to the temperature predicted by the temperature function and a standard deviation of 1.5 °C. Minimum and maximum daily water temperature limits were set at plus and minus 2 °C of the daily generated mean temperature. This individual temperature variability was incorporated to account for the fact that all rays are not located in the same place, and therefore would experience similar but not identical daily temperatures. Individual variability in the RA parameter was incorporated by assigning each ray a value of RA drawn from a normal distribution with a mean of 0.0068 and a coefficient of variation (CV) of 5%. Variation in values of RA was a crude way to allow for individual variation in growth efficiency. Rays were assigned individual daily p -values from a normal distribution having a mean of the age-specific p -value determined through the calibration process, and a CV of 5%. Variability in p -values was incorporated to reflect the variability in prey encountered and ingested among individual rays.

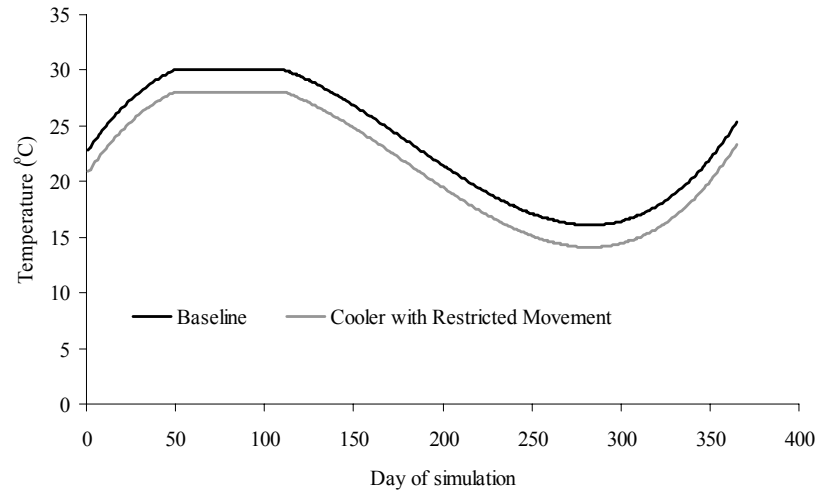
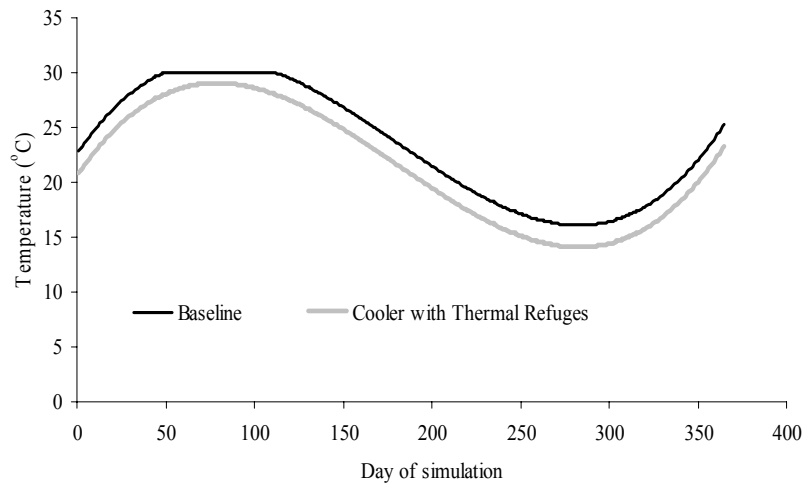
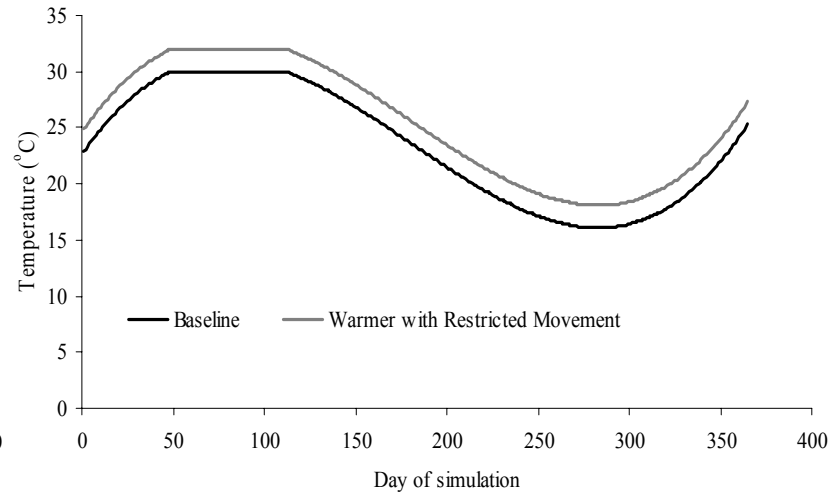
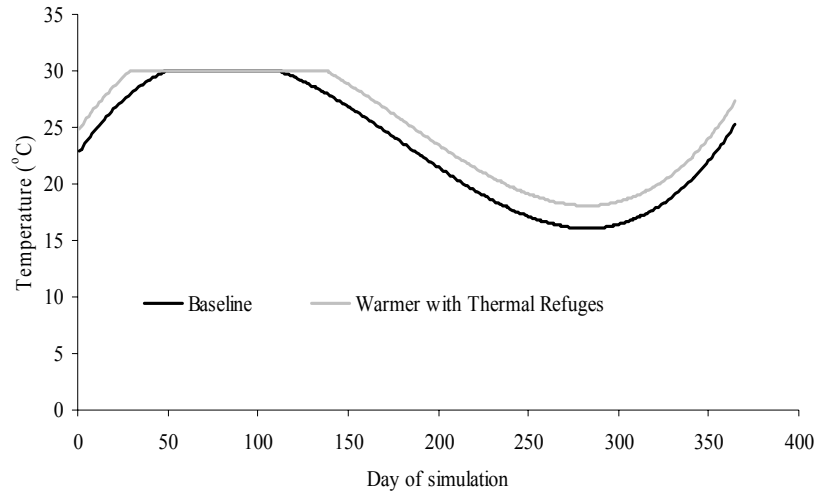


Figure 4.1. Average daily temperature experienced by the rays in the bioenergetics model for the four altered temperature scenarios. Baseline is shown on all graphs. Day 1 represents May 1st.

Initial conditions. All simulations of the bioenergetics model started with 1000 female individuals on May 1. Initial weights (g ww) were generated from a normal distribution with a mean of 777 g ww and a standard deviation of 171 g ww. Minimum (500 g ww) and maximum (1000 g ww) initial weights were imposed to ensure realistic initial sizes based on observed weight-at-birth information (Chapter II, Neer and Thompson in press). If a generated initial weight was less than 500 g ww or greater than 1000 g ww, a new weight was generated from the normal distribution. The model year went from May 1 to April 30.

Calibration of p-values. The value of p , defined as the fraction of C_{\max} actually obtained by a ray each day, was estimated for each year (age) of the 25-year simulation. The model was calibrated by using iterative simulations that adjusted each age's p -value until the model simulated daily growth resulted in a predicted weight at the end of each age that matched observed weights-at-age determined from field data. The observed growth information was obtained from an age and growth study on the cownose ray using vertebral centra (Chapter II, Neer and Thompson in press). I used a bisection algorithm to determine successive values of p , and stopped when predicted mean weight was within 1% of the observed mean weight for each age.

Matrix Projection Model Description

I used an age-structured matrix projection model to analyze the population-level consequences of the cooler and warmer water temperature scenarios. The predictions of the bioenergetics model of growth, survival, and reproductive output under Baseline, cooler, and warmer scenarios were used to estimate the parameters of a matrix projection model. I then analyzed the resulting matrix projection models to obtain estimates of population growth rate, the stable age-distribution, reproductive values by age, and elasticity.

The population dynamics model followed females using a birth-pulse structure with a post-breeding census (Caswell 2001). In an age-structured model, each individual will meet one of two fates each time step (1 year in this case): 1) individuals die during the time interval or 2) survive and enter the next age class. Survival probabilities represent the chance that an individual in age class i survives to age class $i+1$ (Gotelli 2001). The survival probabilities were determined following Caswell (2001) for a post-breeding census:

$$P_i = \frac{l_i}{l_{(i-1)}} \quad (14)$$

$$l_i = \frac{N_i}{N_0} \quad (15)$$

where P_i = age-specific survival probability, l_i = the probability that a new individual is alive at the beginning of age _{i} , N_i = number of individuals alive at the start of each age class, and N_0 = initial number of individuals. The number of individuals alive at the start of each age class (N_i) was obtained from the output of the bioenergetics model.

The fertility coefficients were determined using the equation:

$$f_i = P_i * m_i \quad (16)$$

where f_i = fertility at age, P_i = age-specific survival probability and m_i = age specific reproductive output (Caswell 2001). The age-specific fecundity estimates (number of pups/female individual) predicted by the bioenergetics model were divided by two (to reflect a one to one male-to-female sex ratio, Chapter II, Neer and Thompson in press) to obtain values for m_i .

The matrix (**A**) for a post-breeding census was expressed in the following form:

$$\mathbf{A} = \begin{bmatrix} f_1 & f_2 & f_3 & \dots & f_{k-1} & f_k \\ P_1 & 0 & 0 & \dots & 0 & 0 \\ 0 & P_2 & 0 & \dots & 0 & 0 \\ 0 & 0 & P_3 & \dots & 0 & 0 \\ 0 & 0 & 0 & \dots & P_{k-1} & 0 \end{bmatrix}$$

The population growth rate (λ) was determined from the dominant eigenvalue of the matrix **A**. The intrinsic rate of change of the population (r) was obtained by taking the natural log of the population growth rate. Net reproductive rate, the mean number of offspring by which a newborn will be replaced by the end of its lifetime (R_0), and estimates of generation time were calculated following Caswell (2001). Three different estimates of generation time were computed:

1) time (T) required for the population to increase by a factor of R_0 , given by

$$T = \log \frac{R_0}{\log \lambda} \quad (17)$$

where $R_0 = \sum l_i m_i$

2) mean age (μ_1) of the parents of the offspring produced by a cohort over its lifetime

$$\mu_1 = \frac{\sum l_i m_i * x}{\sum l_i m_i} \quad (18)$$

where x = age class

3) mean age (\bar{A}) of the parents of the offspring produced by a population at the stable age distribution, given by

$$\bar{A} = \frac{\sum e^{-rx} * l_i m_i * x}{\sum e^{-rx} * l_i m_i} \quad (19)$$

The three estimates were calculated due to recent concerns within CITES (Convention of International Trade in Endangered Species) that different definitions of generation time may

produce greatly different estimates, and therefore the selection of the generation time formulae can affect conservation decisions (Enric Cortés, personal communication). In my analysis, all three formulations produced very similar estimates. I therefore only report \bar{A} , which is the most commonly used estimate of generation time in elasmobranch studies (e.g. Cortés 2002, Mollet and Cailliet 2002).

The stable age distribution and reproductive value of the population were obtained from the eigenvectors associated with the dominant eigenvalue of the matrix \mathbf{A} (Ebert 1999, Caswell 2001). The reproductive value (V_x), given by the left eigenvector, represents the relative number of offspring that are yet to be born by individuals in a given age class (Gotelli 2001). As the reproductive value of newborns is always one, reproductive value is measured relative to the first age class (Gotelli 2001). If a population is growing at a constant rate r , the population will eventually converge on a stable age distribution (C_x), where the proportion of individuals in each age class remains constant. These proportions are given by the right eigenvector associated with the dominant eigenvalue of matrix \mathbf{A} .

Elasticity examines the relative impacts of proportional changes in fertility and survival (elements in the projection matrix) on the population growth rate λ (Heppell et al. 2000). An elasticity matrix \mathbf{E} was calculated from the eigenvectors of projection matrix \mathbf{A} (Caswell 2001). Age-specific elasticities were examined to determine the influence on λ of each element of the matrix projection model. Aggregated elasticities were also computed that examined the combined effects of fertility (f_i), juvenile survival (P_i 's of immature individuals), and adult survival (P_i 's of mature individuals) on λ . Fertility elasticity [$e(f)$] was calculated as the sum of elements in the top row of \mathbf{E} , and is defined as an effect of a proportional change in reproductive output on λ for all reproducing age classes (Heppell et al.

2000). Juvenile survival elasticity [$e(P_j)$] is defined as the effect on λ of a proportional change in all annual survival rates for age 1 to the age just prior to maturation, and was calculated as the sum of the subdiagonal elements of \mathbf{E} from column 1 to column $\alpha - 1$, where α represents the first age class that includes reproductive females (Heppell et al. 2000). Adult survival elasticity [$e(P_a)$] is the effect on λ of a proportional change in all annual survival rates for reproductive individuals, and was calculated as sum of the subdiagonal elements of \mathbf{E} from α to k (oldest age class; Heppell et al. 2000). All calculations were completed using PopTools, an add-in to Microsoft Excel, which is available from Greg Hood, CSIRO (<http://www.cse.csiro.au/poptools/>).

Cooler and Warmer Water Temperature Scenarios

Five scenarios were simulated using the bioenergetics and matrix projection models. These scenarios were baseline conditions, and a warmer scenario and a cooler scenario, each under the assumption of thermal refuges or restricted movement. Previous research indicates that many species of teleosts behaviorally thermoregulate, meaning that they seek out temperatures close to their optimal temperature for growth (Neill and Magnuson 1974, Neill 1979) and that this ability to thermoregulate can have an affect on growth (Hill and Magnuson 1990). More recent research indicates that some elasmobranchs may behaviorally thermoregulate as well (e.g., Matern et al. 2000). Thermal refuges in model simulations assumed that cownose rays would be able to find locations having a maximum water temperature of ~ 30 °C, and so when temperatures exceeded 30 °C they moved to locate water that was cooler in temperature than their upper avoidance temperature of 30 °C. Restricted movement in model simulations assumed that cownose rays were unable to move around

enough to find cooler water. Under restricted movement, cownose rays could experience water temperatures warmer than their upper avoidance temperature of 30 °C.

The cooler and warmer scenarios involved changes of 2 °C in the daily water temperature used for baseline conditions. The warmer scenario was selected to crudely mimic warmer than average years or the moderate level changes predicted by global climate warming (Smith 2004). The cooler scenario was conducted to examine the symmetry of response of the rays to temperature variation around the average (baseline) conditions.

Baseline Scenario. The baseline scenario represents present day water temperature conditions (Figure 4.1). The maximum daily temperature allowed to be experienced by a cownose ray was 30 °C, as field data demonstrated that rays left the study area at warmer water temperatures. Catch rates of cownose rays decreased dramatically between 28 °C and 30 °C, and very few rays were captured at temperatures warmer than 30 °C (John Carlson, personal communication). In the simulations, some rays experienced slightly warmer temperatures than 30 °C due to individual variability in temperatures being applied after the truncation of the daily mean at 30 °C.

Scenario 1: Warmer with Thermal Refuges (TR). Water temperature was increased by 2 °C every day over the Baseline scenario (Figure 4.1). To simulate the ability of cownose rays to move around and find waters with cooler temperatures, the maximum daily temperature was truncated at 30 °C after the 2 °C increase was added. Individual variability was then imposed so the warmest water rays could experience was slightly warmer than 30 °C.

Scenario 2: Warmer with Restricted Movement (RM). The same 2 °C increase as in scenario 1 was imposed, but in scenario 2 the increase occurred after the temperature

truncation (Figure 4.1). Thus, the maximum daily temperature allowed in the model was 32 °C, and some individuals experienced slightly warmer temperatures than 32 °C due to individual variability in daily temperatures. The restricted movement scenario was designed to simulate individuals being unable to locate thermal refuges beyond what they found under the Thermal Refuges scenario. The 30 °C refuges under the Thermal Refuges scenario would now be 32 °C, and some rays could experience water temperatures slightly warmer than 32 °C.

Scenario 3: Cooler with Thermal Refuges (TR). Scenario 3 simulated a cooler scenario by decreasing baseline daily temperatures by 2 °C (Figure 4.1). Baseline daily temperatures were first decreased by 2 °C and then any days that had temperatures warmer than 30 °C were set to 30 °C. No minimum temperature truncation was necessary, as the lowest temperature observed in the model was warmer than the lowest temperature at which rays are captured (Neer unpublished data).

Scenario 4: Cooler with Restricted Movement (RM). Scenario 4 also decreased the daily temperature by 2 °C like in scenario 3, but in scenario 4, the decrease was imposed after the temperature truncation (Figure 4.1). Individuals essentially can be thought of finding what were 30 °C refuges under the Cooler with Thermal Refuges scenario, which are now 28 °C. Thus, in this scenario, the daily maximum temperature was 28 °C, with individual variability resulting in some rays experiencing slightly warmer temperatures than 28 °C water.

Simulations

Bioenergetics model. For each of the five scenarios, two alternative simulations were performed: Temperature Effect and Consumption Effect. The Temperature Effect simulations examined the effect of a daily temperature change on the predicted growth of individuals,

given that the p-values (fraction of C_{\max} actually obtained) were held constant. The age-specific p-values determined from the Baseline simulation were used unchanged in Temperature Effect simulations. This assumed that the cownose rays would not change their foraging in response to altered water temperatures and that prey dynamics remained the same as Baseline. For the Temperature Effect simulations, I compared predicted weight-at-age, survival by age, and reproduction (first age of reproduction and number of pups) by age between the Baseline scenario and the four altered temperature scenarios.

The Consumption Effect simulations examined how the age-specific p-values would have to change under the altered temperature scenarios in order for the rays to maintain the Baseline (i.e., field-determined) weights-at-age. I allowed the age-specific p-values to be re-estimated for each of the four altered temperature scenarios. The new estimates of the p-values for each temperature scenario were then compared to the Baseline values, and differences reported as the percent change in p-values by age. Additionally, the change in daily consumption required, expressed as age-specific % BW/day ($100 * \text{grams ray/grams ray/day}$), was also compared to Baseline estimates. Because p-values were allowed to change, predicted weights-at-age were virtually identical to Baseline values. Thus, predicted survival and reproduction, which were size-based in the model, were also unchanged from their Baseline values.

Three replicates of each scenario were run to examine the variability of the results due to the stochastic sources of variability incorporated into the model. I computed the percent difference in predicted weights-at-age among the three replicates by first computing the mean of the replicates for each age, then computing the percent change of each of the replicates to that mean value. The predictions of average weight-at-age produced by the three replicate

simulations under Baseline conditions varied by 0.1 to 1.1%, with an overall average difference over all ages of 0.34%. Similar consistency among replicate simulations was also obtained for the four temperature scenarios. Overall average percent differences in weight-at-age were 0.74% for the Warmer with Thermal Refuge scenario, 1.04% for the Warmer with Restricted Movement scenario, 0.74% for the Cooler with Thermal Refuges scenario, and 0.72% for the Cooler with Restricted Movement scenario. Therefore, I only present the results of one of the replicate simulations for each scenario below.

Matrix projection model. The matrix projection model was used to determine the equilibrium characteristics of the cownose ray population for the Baseline scenario, and for the four altered temperature scenarios under the Temperature Effect simulations. Because p-values were fixed at Baseline values in the Temperature Effect simulations, the bioenergetics model predicted changes in weight, and therefore changes in survival and reproductive rate, under the altered temperature scenarios. The matrix projection model extrapolated these changes in survival and reproduction to the population level. The Consumption Effect simulations were not analyzed with the matrix projection model because changed p-values resulted in Baseline weights-at-age, which meant that survival and reproduction also were the same as Baseline. I compared estimated values of population growth rate, stable age distribution, reproductive values, and elasticities to survival and to fertilities among the Baseline and the Temperature Effect version of the cooler and warmer scenarios.

Results

Bioenergetics Model

Baseline calibration. Baseline simulation results fit the observed weight-at-age data very well because the model was calibrated to these data. Model-predicted weights-at-age under Baseline conditions closely matched the Gompertz growth curve derived from observed size-at-age data (Figure 4.2). Individual variability in weight-at-age was also well captured by the Baseline model simulation (Figure 4.3). One would expect somewhat greater variability in the simulated weights-at-age compared to the observed weights-at-age due to the much larger sample size possible with the simulation model.

Estimated p-values by age under Baseline conditions increased with age and varied from 0.414 for age 1 to 0.828 for age 25. Age-specific survival from one age class to the next ranged from 74 to 95%, with an average survival over all age classes of 90%. Predicted age at first reproduction was 4 years, and pup production (averaged over all age classes) was 0.75 pups/female.

Growth responses: Scenario 1. Temperature Effect: Model-predicted growth under the Warmer with Thermal Refuges (TR) scenario produced a smaller average weight with age when compared to the Baseline scenario (Figure 4.4). Age-specific average weights were between 4.8 and 11.2% smaller under the Warmer with TR scenario compared to the Baseline scenario. The overall average decrease in weight-at-age (averaged over all ages) was 9.6%.

Consumption Effect: Age-specific p-values increased under the Warmer with TR scenario compared to Baseline values (Table 4.2). The new p-values ranged from 1.4 to 3.8

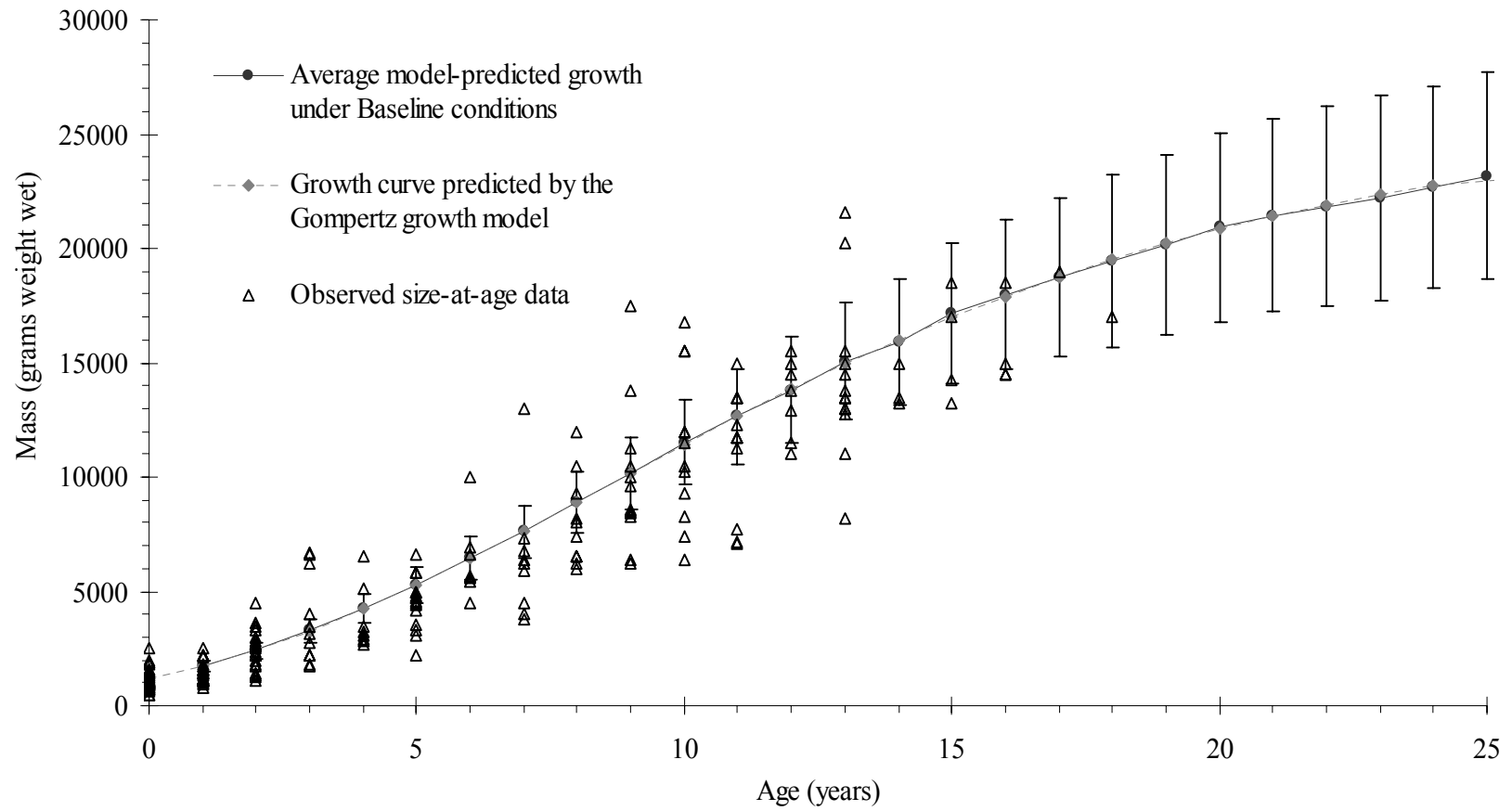


Figure 4.2. Comparison of model-predicted average weights-at-age with the Gompertz growth curve determined from cownose ray weight-at-age field data. Error bars represent plus or minus one standard deviation from the mean of the model-predicted data.

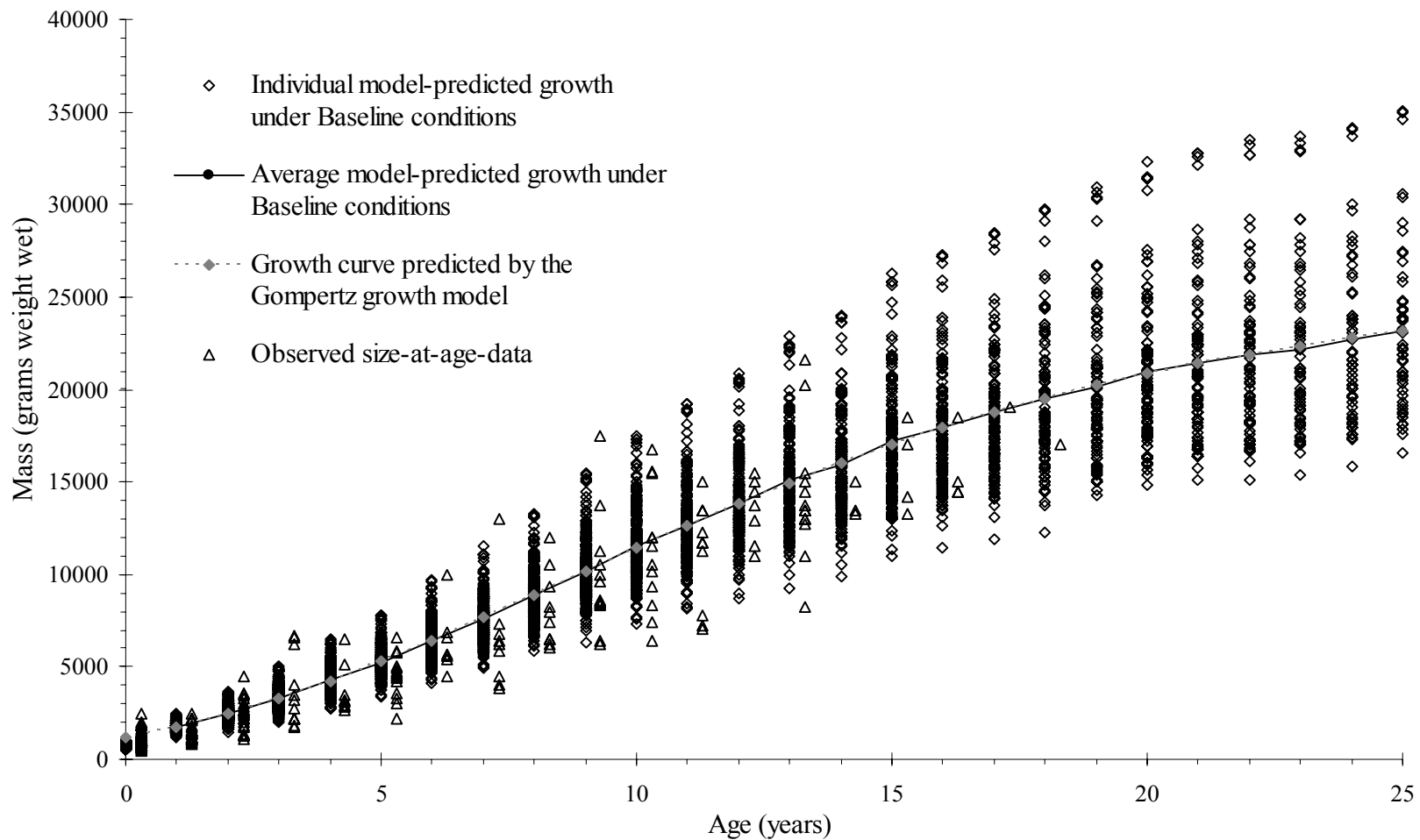


Figure 4.3. Comparison of model-predicted individual weight-at-age data with the observed cownose ray weight-at-age field data. The model-predicted average weights-at-age and the Gompertz growth curve are also shown.

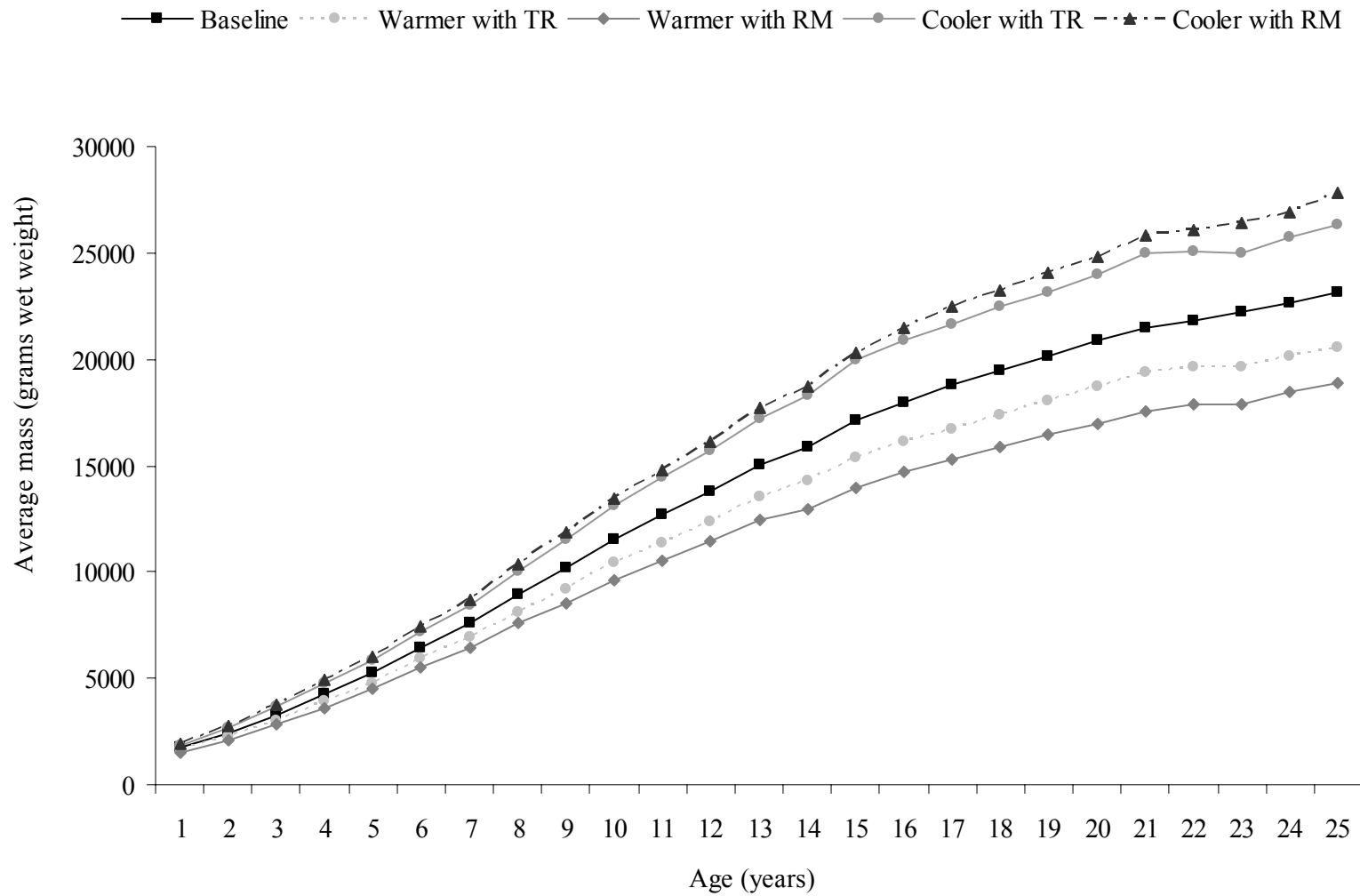


Figure 4.4. Average weight of all individuals alive on Day 365 of each year of the simulation.

Table 4.2. Percent change in age-specific p-values in relation to the Baseline scenario.

Age	Scenario			
	Warmer with TR	Warmer with RM	Cooler with TR	Cooler with RM
1	1.4	4.7	-2.9	-3.3
2	2.2	4.4	-2.7	-4.0
3	2.4	4.1	-3.3	-4.0
4	2.3	4.6	-3.0	-4.5
5	3.2	5.0	-2.9	-3.6
6	2.7	4.7	-3.4	-4.7
7	3.2	5.8	-2.6	-3.9
8	2.5	4.9	-3.7	-4.3
9	3.0	4.7	-3.5	-4.7
10	2.3	4.6	-4.5	-5.1
11	3.4	5.6	-3.3	-4.4
12	3.3	5.4	-3.5	-4.4
13	2.6	4.8	-4.8	-5.3
14	3.7	5.8	-3.7	-4.7
15	2.1	5.1	-4.6	-5.6
16	3.0	5.1	-4.0	-5.0
17	3.5	5.0	-4.0	-5.0
18	3.0	6.0	-4.0	-4.5
19	3.0	5.9	-4.2	-4.9
20	3.0	4.9	-3.9	-4.4
21	2.0	4.8	-4.8	-4.8
22	9.0	5.8	-3.8	-3.8
23	3.4	6.7	-2.9	-3.8
24	2.6	5.5	-3.6	-4.0
25	3.8	5.7	-4.2	-4.2
MEAN	2.8	5.2	-3.7	-4.4

percent greater than the Baseline values, with a mean increase over all ages of 2.8%. Age-specific daily consumption values also increased compared to Baseline values (Table 4.3). The higher p-values translated into cownose rays having to consume ~12.0% more BW/day in order to maintain their weights-at-age at Baseline values (Table 4.3). The age-specific increases in daily consumption rates ranged from 10.4 to 13.0% BW/day.

Growth responses: Scenario 2. Temperature Effect: The Warmer with Restricted Movement (RM) scenario generated the greatest reduction in cownose ray growth and the smallest weights at age of any of the scenarios examined (Figure 4.4). The average weights-at-age predicted under the Warmer with RM scenario ranged from 11.5 to 19.4% smaller compared to Baseline values, with an overall average reduction in weight-at-age of 16.8%.

Consumption Effect: Under the Warmer with Restricted Movement (RM) scenario, the new calculated age-specific p-values were greater than Baseline values (Table 4.2). P-values by age increased by 4.1 to 6.7% over Baseline values, with an overall average increase of 5.2%. Under the Warmer with RM scenario, cownose rays would have to consume about 11.7% more of their body weight than under Baseline conditions every day for their lifetime to achieve the same weights-at-age as under Baseline conditions (Table 4.3). Age-specific increases in consumption ranged from 10.0 to 12.9% BW/day.

Growth responses: Scenario 3. Temperature Effect: When the age-specific p-values determined from the Baseline scenario were used with the Cooler with Thermal Refuges (TR) scenario, the model predicted faster growth compared to the Baseline scenario (Figure 4.4). Mean weights-at-age increased

Table 4.3. Percent change in age-specific daily consumption (%BW/day in g ray/g ray/day) in relation to the Baseline scenario.

Age	Scenario			
	Warmer with TR	Warmer with RM	Cooler with TR	Cooler with RM
1	10.8	11.4	-12.7	-13.6
2	12.0	10.5	-12.3	-13.8
3	11.6	10.9	-12.7	-13.5
4	11.2	10.0	-12.7	-14.3
5	11.5	11.1	-12.7	-13.5
6	11.2	10.0	-12.9	-14.5
7	11.8	11.4	-12.7	-13.9
8	12.0	11.6	-12.9	-13.7
9	12.7	11.9	-12.3	-14.0
10	11.5	11.1	-13.7	-14.5
11	11.7	11.3	-12.6	-13.9
12	12.4	12.4	-12.8	-13.7
13	11.6	11.6	-13.4	-14.3
14	12.7	13.2	-11.8	-13.6
15	11.8	11.4	-12.7	-14.1
16	12.4	12.9	-12.0	-13.4
17	13.0	12.5	-12.5	-13.4
18	12.6	12.6	-12.6	-13.0
19	12.7	12.2	-12.7	-13.1
20	12.7	12.7	-12.3	-12.7
21	11.3	11.7	-13.6	-13.6
22	12.3	11.8	-12.7	-13.2
23	12.9	12.4	-11.9	-12.9
24	12.4	12.9	-12.0	-12.4
25	10.4	10.4	-13.7	-14.2
MEAN	12.0	11.7	-12.7	-13.6

between 6.9 and 16.4% over the Baseline scenario, with an average increase over all ages of 13.4%.

Consumption Effect: Age-specific p-values re-estimated under the Cooler scenario with Thermal Refuges (TR) were smaller than those estimated under the Baseline scenario (Table 4.2). Percent reductions in p-values ranged from 2.6 to 4.8%, with an overall average decrease of 3.7%. Smaller p-values translated into lower daily consumption rates being needed to maintain Baseline weights, with rays needing (on average) 12.7% less energy per day, with age-specific decreases between 13.0 and 14.5% BW/day (Table 4.3).

Growth responses: Scenario 4. Temperature Effect: The Cooler with Restricted Movement (RM) scenario produced similar weights-at-age as the Cooler with Thermal Refuges (TR) scenario, with predicted mean weights-at-age being heavier than Baseline values (Figure 4.4). Percent increase in mean weights-at-age ranged from 10.4 to 20.2%, with an overall average increase of 17.2%.

Consumption Effect: Age-specific p-value re-estimated under the Cooler with Restricted Movement (RM) scenario were less than those estimated under Baseline conditions (Table 4.2). The decrease in p-values from Baseline ranged from 3.3 to 5.3%, with a mean decrease of 4.4%. Under cooler conditions and restricted movement, cownose rays could maintain their Baseline weights at age with approximately 13.6% less energy (range of 13.0 to 14.5%) consumed each day (Table 4.3).

Reproduction responses under the Temperature Effect simulations. Changes in reproductive output by age among the temperature scenarios (Table 4.4) were caused by growth differences affecting the percent mature by age (Table 4.5). The slowest growth was predicted for the Warmer with Restricted Movement scenario (Figure 4.4), which resulted in

Table 4.4. Reproductive output by age (m_i ; number of female pups/female) for the Baseline, cooler, and warmer scenarios under the Temperature Effect simulations.

Age	Baseline	Warmer with TR	Warmer with RM	Cooler with TR	Cooler with RM
0	0.000	0.000	0.000	0.000	0.000
1	0.000	0.000	0.000	0.000	0.000
2	0.000	0.000	0.000	0.000	0.000
3	0.000	0.000	0.000	0.000	0.000
4	0.004	0.002	0.000	0.003	0.010
5	0.024	0.011	0.009	0.063	0.080
6	0.141	0.099	0.055	0.214	0.245
7	0.288	0.235	0.169	0.390	0.400
8	0.435	0.372	0.330	0.466	0.467
9	0.474	0.440	0.423	0.485	0.489
10	0.495	0.480	0.472	0.497	0.492
11	0.496	0.495	0.487	0.498	0.496
12	0.496	0.500	0.492	0.496	0.496
13	0.500	0.500	0.497	0.498	0.498
14	0.500	0.500	0.497	0.495	0.500
15	0.500	0.496	0.500	0.497	0.500
16	0.500	0.500	0.496	0.500	0.494
17	0.496	0.500	0.496	0.500	0.496
18	0.500	0.500	0.500	0.500	0.500
19	0.490	0.500	0.495	0.496	0.496
20	0.500	0.500	0.500	0.495	0.495
21	0.500	0.500	0.500	0.500	0.500
22	0.500	0.500	0.500	0.495	0.495
23	0.486	0.491	0.500	0.500	0.500
24	0.492	0.500	0.491	0.493	0.500
25	0.500	0.500	0.490	0.500	0.493

Table 4.5. Percent of the population reproducing by age for the Baseline, cooler, and warmer scenarios under the Temperature Effect simulations.

Age	Baseline	Warmer with TR	Warmer with RM	Cooler with TR	Cooler with RM
0	0.0	0.0	0.0	0.0	0.0
1	0.0	0.0	0.0	0.0	0.0
2	0.0	0.0	0.0	0.0	0.0
3	0.0	0.0	0.0	0.0	0.0
4	0.8	0.4	0.0	0.5	1.9
5	4.7	2.3	1.7	12.7	15.9
6	28.1	19.8	11.0	42.7	49.0
7	57.7	47.0	33.8	78.0	80.0
8	87.0	74.4	66.1	93.3	93.3
9	94.7	88.0	84.6	96.9	97.7
10	98.9	96.0	94.4	99.3	98.4
11	99.2	99.1	97.5	99.6	99.3
12	99.1	100.0	98.3	99.2	99.2
13	100.0	100.0	99.4	99.6	99.5
14	100.0	100.0	99.3	99.0	100.0
15	100.0	99.3	100.0	99.5	100.0
16	100.0	100.0	99.2	100.0	98.7
17	99.2	100.0	99.1	100.0	99.3
18	100.0	100.0	100.0	100.0	100.0
19	98.0	100.0	99.0	99.2	99.2
20	100.0	100.0	100.0	99.1	99.1
21	100.0	100.0	100.0	100.0	100.0
22	100.0	100.0	100.0	98.9	98.9
23	97.2	98.3	100.0	100.0	100.0
24	98.4	100.0	98.1	98.6	100.0
25	100.0	100.0	98.0	100.0	98.5

the most delayed maturity by age and the lowest reproductive output by age. In contrast, the fastest growth was predicted for the Cooler with Restricted Movement scenario (Figure 4.4), which resulted in the earliest maturity by age and highest reproductive output by age. Baseline and the other two temperature scenarios generated reproductive output and maturity by age intermediate to these two extreme scenarios. Age at first reproduction was 5 years and approximately 100% maturity was not reached until age 13 – 14 for the Warmer with Restricted Movement scenario, compared to an age of first reproduction of 4 years and approximately 100% maturity being reached at ages 11 -12 for the Cooler with Restricted Movement scenario. Percent mature for the Warmer with Restricted Movement and Cooler with Restricted Movement were 11.0 versus 49.0% at age-6 and 33.8 versus 80.0% at age-7. At least 98% maturity was predicted for all scenarios for individuals age-12 and older (Table 4.5).

Survivorship responses under the Temperature Effect simulations. The number of individuals surviving to each age under the Temperature Effect simulations was higher than Baseline under the cooler scenarios and lower than Baseline under the warmer scenarios (Figure 4.5). The largest differences in survival were predicted for the intermediate age classes. The Cooler temperature scenarios predicted greater numbers surviving to each age, especially for ages 2 through 13, when compared to the Baseline predictions. Fewer individuals survived to each age class in the Warmer temperature scenarios compared to Baseline, with much lower survivorship between ages 2 through 16. Compared to Baseline, an average of 9.7% fewer individuals survived per year under the Warmer with Thermal Refuges scenario and an average of 12.8% fewer individuals survived per year under the Warmer with Restricted Movement scenario. For the cooler temperature

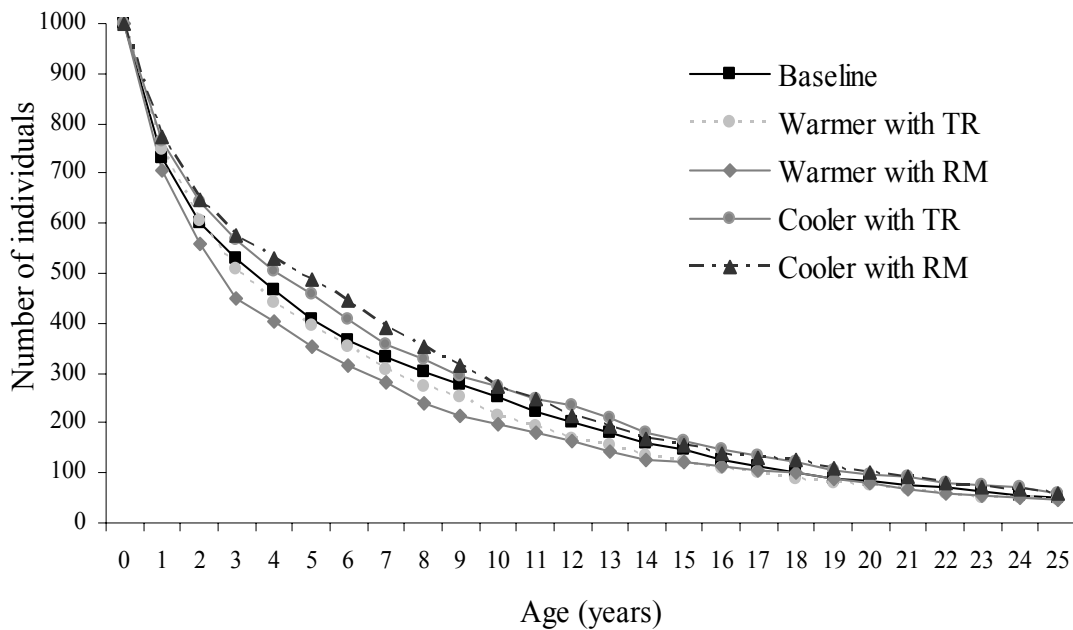


Figure 4.5. Predicted survivorship curves for the Baseline scenario and four alternative temperature scenarios for the Temperature Effect simulations.

scenarios, 13.3% more individuals survived per year under the Thermal Refuges scenario and 13.4% more individuals survived per year under the Restricted Movement scenario. Overall survivorship from birth to age-25 was 5.0% under Baseline, 4.6% for the Warmer with Restricted Movement, 4.5% for the Warmer with Thermal Refuges, 5.9% for the Cooler with Restricted Movement, and 6.0% for the Cooler with Thermal Refuges scenarios.

Matrix Projection Model

The finite rate of population change (λ) for the Baseline simulation indicated that the simulated cownose ray population would increase by 2.7% per year (Table 4.6). The net reproductive rate (R_0) was determined to be 1.411, indicating that each newborn female can expect to be replaced by 1.411 females over her lifetime. Generation time, \bar{A} (mean age of

Table 4.6. Demographic parameters calculated from the matrix projection model configured with bioenergetics outputs under the Baseline and four Temperature Effect simulations. λ = population growth rate; r = intrinsic rate of change; R_0 = net reproductive rate; \bar{A} = mean age of the parents of the offspring produced by a population at the stable age distribution.

Scenario	λ	r	R_0	\bar{A}
Baseline	1.027	0.027	1.411	12.386
Warmer with Thermal Refuges	1.012	0.012	1.177	12.985
Warmer with Restricted Movement	1.005	0.005	1.070	13.770
Cooler with Thermal Refuges	1.044	0.043	1.696	11.772
Cooler with Restricted Movement	1.047	0.046	1.731	11.403

the parents of the offspring produced by a population at the stable age distribution) was estimated as 12.4 years (Table 4.6).

The slowed growth of individuals, and associated changes in reproduction and survival rates, under warmer temperatures resulted in slowed population growth rate, while the faster individual growth under cooler temperatures resulted in faster population growth rates (Table 4.6). Intrinsic annual population growth rates (r) were 0.012 for the Warmer with Thermal Refuges scenario, 0.005 for the Warmer with Restricted Movement scenario, 0.043 for the Cooler with Thermal Refuges scenario, and 0.046 for the Cooler with Restricted Movement scenario.

Changes in population growth rate were reflected in the estimated generation times and the net reproductive rates (Table 4.6). The shortest generation time (11.4 years) and highest net reproductive rate (1.73 females/female over her lifetime) was predicted for the fastest-population-growth Cooler with Restricted Movement scenario, while the longest generation time (13.8 years) and lowest net reproductive rate (1.07 females/female over her lifetime) was predicted for the slowest-population-growth Warmer with Restricted Movement scenario.

Stable age distributions were very similar among the Baseline and all four altered temperature scenarios (Figure 4.6). The Cooler temperature scenarios consistently had slightly greater proportions in the younger age classes than the Baseline and warmer scenarios. The faster individual growth under the cooler temperature scenarios, coupled with mortality rate that decreased with increasing body weight, resulted in higher survivorship and a greater proportion of the population in the younger age classes under the cooler temperatures.

Reproductive values by age were more responsive to the temperature scenarios than were the stable age distributions (Figure 4.7). Peak reproductive value was at age 7 for the Baseline and the cooler scenarios, while peak reproductive value was at age 8 for Warmer with Thermal Refuges scenario and at age 9 for the Warmer with Restricted Movement scenario. The value of the peak reproductive age class ranged from 2.7 for age 7 in the Cooler with Restricted Movement scenario to 3.8 for age 9 in the Warmer with Restricted Movement scenario; the peak reproductive value for the Baseline scenario was 3.2 at age 7. The Baseline scenario had four ages (6 through 9) where the reproductive value was relatively high (greater than 3.0). The Warmer with Thermal Refuges scenario had six ages (7 through

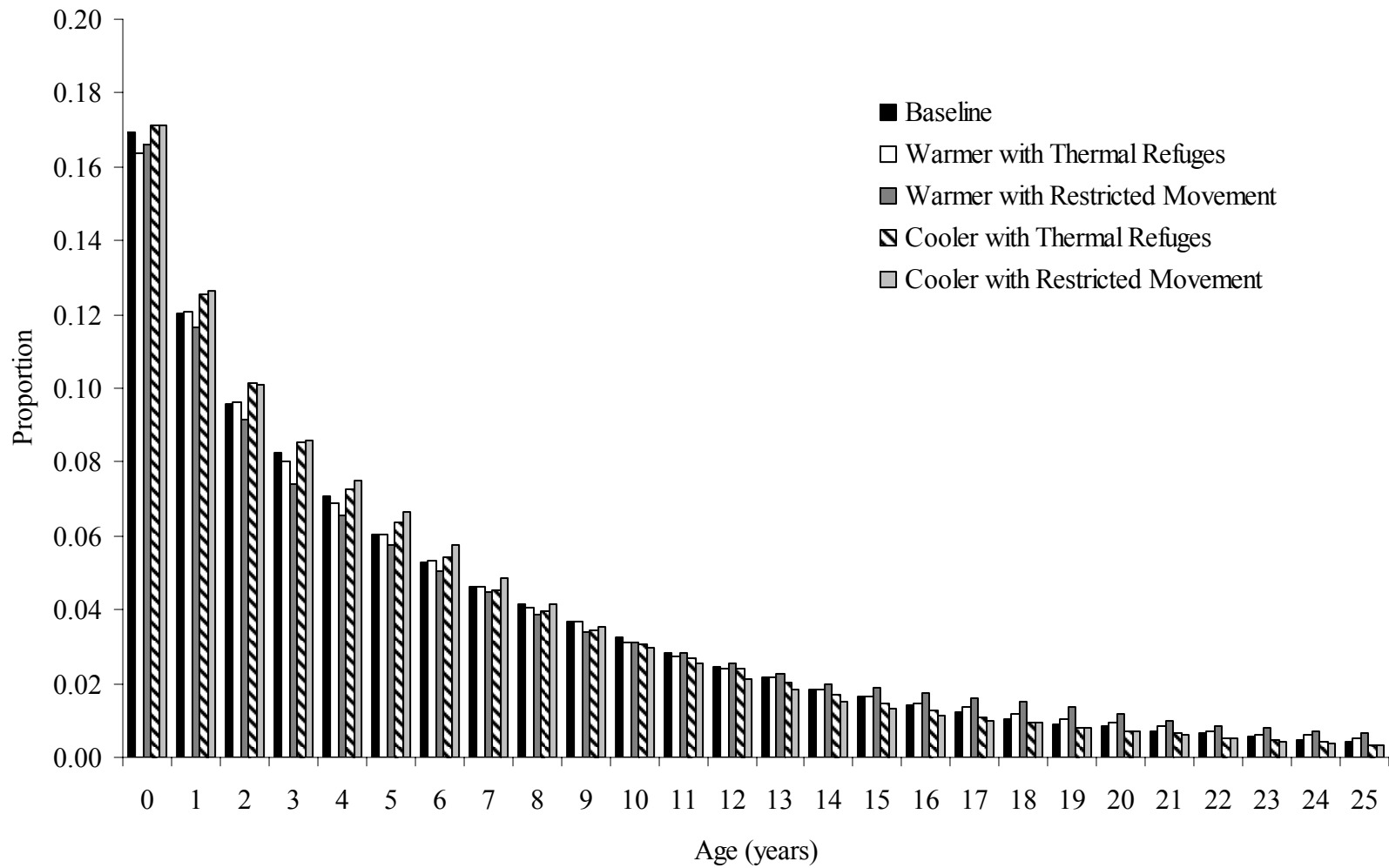


Figure 4.6. Predicted stable age distributions for the Baseline and four temperature scenarios.

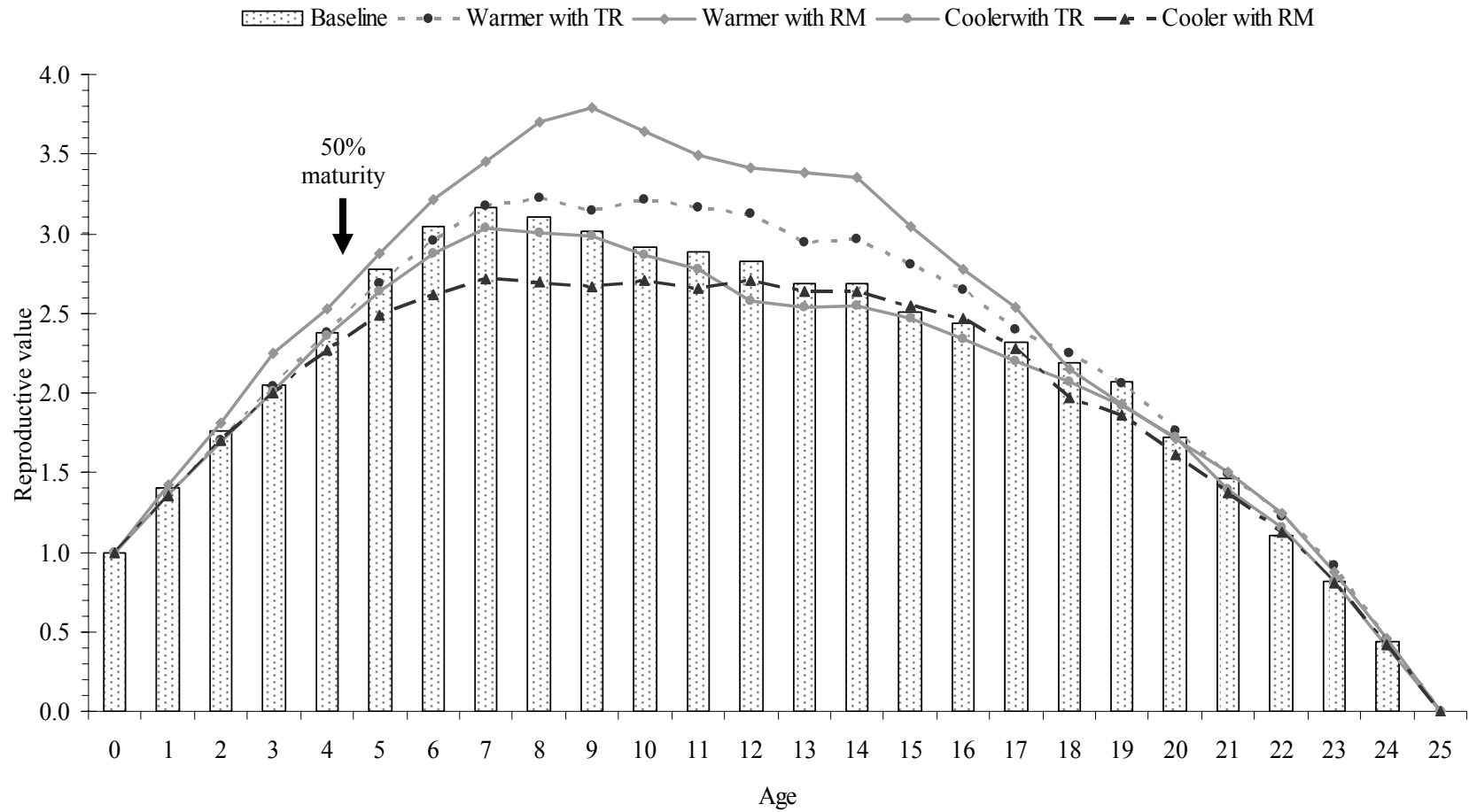


Figure 4.7. Predicted reproductive values for the Baseline and four alternative temperature scenarios. Fifty percent maturity, determined from field data, is also shown.

12) and the Warmer with Restricted Movement scenario had ten ages (6 through 15) with reproductive values that were relatively high. Fewer ages with reproductive values greater than 3.0 were predicted for the cooler scenarios (7 and 8 for the Thermal Refuges scenario; no ages for the Restricted Movement scenario).

Elasticities to survival varied among ages and scenarios (Figure 4.8). As expected, all pre-reproductive age classes within each scenario had equal elasticity to survival (Heppell et al. 2000). Elasticity to survival was greatest for the pre-reproductive ages, then declined slowly by age class soon after reproduction commenced (Figure 4.8). Elasticity to survival was greatest for the cooler scenarios, intermediate for Baseline, and lowest for warmer scenarios. This pattern reversed once the majority of the population was reproducing, with the warmer scenarios having the highest elasticities to survival throughout the remainder of the age classes, while the cooler scenarios had the lowest elasticities with the older ages.

Differences in elasticity to fertility among scenarios were predicted primarily during the first reproductive age classes (Figure 4.8). As expected, the sum of the elasticities to fertility equaled the elasticity of survival to the first age class (P_1) and elasticities to fertility were smaller than the elasticities to survival (Heppell et al. 2000). The values of elasticities to fertility were greatest for the cooler scenarios, intermediate for Baseline, and least for the warmer scenarios for ages 4 through 10. For younger and older ages, elasticities to fertilities became very similar for all scenarios.

When examined by life stage, elasticity to adult survival [$e(P_a)$] was highest, elasticity to juvenile survival [$e(P_j)$] was intermediate, and elasticity to fertility [$e(f)$] was lowest across all scenarios (Figure 4.9). Life stage aggregated elasticities were very similar among

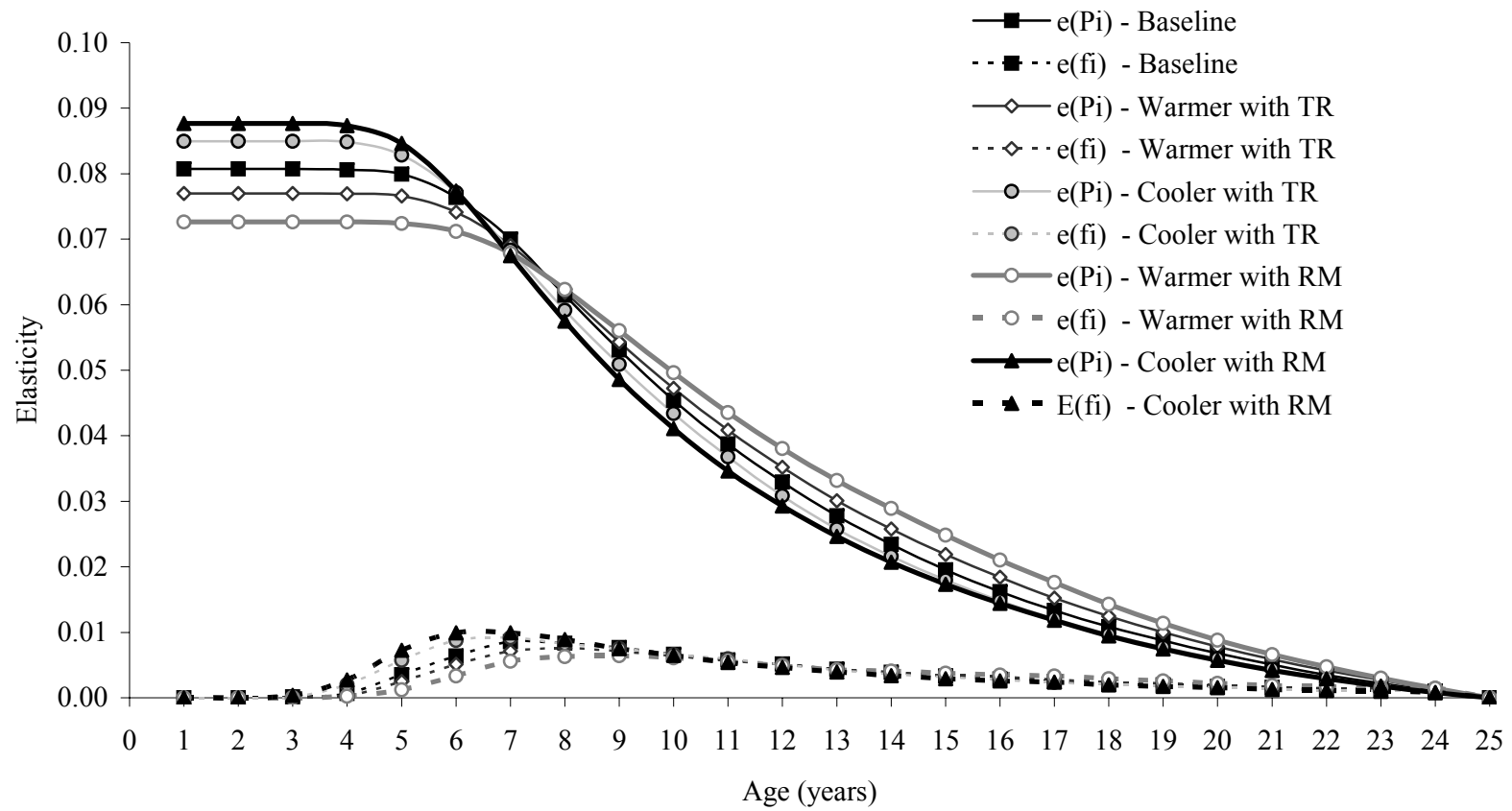


Figure 4.8. The elasticity of age-specific survival ($e(P_i)$), and elasticity of age-specific fertility ($e(f_i)$) for the Baseline and four alternative temperature scenarios.

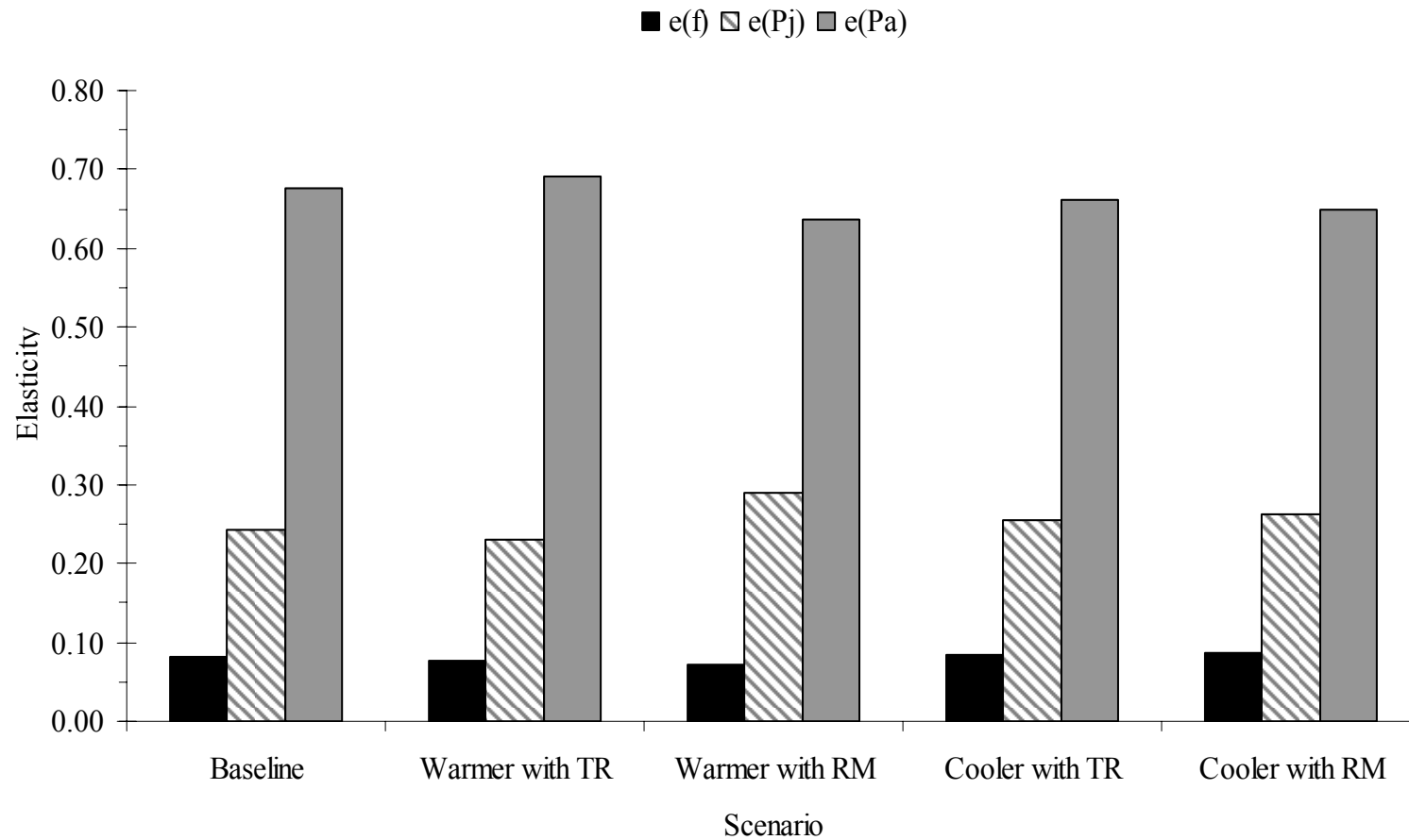


Figure 4.9. The elasticity of λ to fertility ($e(f)$), juvenile survival ($e(P_j)$) and adult survival ($e(P_a)$) examined by life stage for each scenario.

scenarios, with $e(P_a)$ ranging from 0.637 to 0.692, $e(P_j)$ ranging from 0.231 to 0.290, and $e(f)$ ranging from 0.073 to 0.088.

Discussion

Ecological Implications of Altered Temperatures

Realized consumption must vary under the different temperature scenarios and movement assumptions for simulated average weights-at-age to match the growth pattern predicted by the Baseline scenario. Rays must consume approximately 11% more energy per day under the warmer scenarios to compensate for the increased metabolic costs associated with inhabiting warmer water. This would imply that rays would have to alter their foraging behavior to increase prey consumption or change their diet to consume more energetically valuable prey. As the caloric content of their bivalve prey is already very high when compared to the energy density of themselves, rays would most likely have to change their foraging behavior. Increased prey demands could be met if rays could forage for a longer portion of the day or in areas of higher prey densities, and provided the prey resources themselves would be unaffected by the temperature changes and the added predation mortality. A similar magnitude decrease in realized consumption (11 – 13% BW less per day) would be necessary under the cooler scenarios for the rays to maintain the same life time growth trajectory as predicted by the Baseline scenario. More information on ray foraging behavior and the population dynamics of their prey would enable further investigation into how interannual variation and anomalous years of water temperatures would affect cownose ray growth.

A symmetrical response in growth rate under the Temperature Effect simulations was predicted for plus 2 °C and minus 2 °C changes in temperature, indicating that the influence of

temperature on cownose ray growth within this range is predictable from temperature alone. The increased metabolic costs incurred when occupying warmer waters forces the rays to use more of the consumed energy for maintenance than for somatic growth, leading to lower growth rates over their life times. Cooler waters allow for an increase in energy available for growth due to lower metabolic costs. The predicted changes in weight-at-age are consistent with cownose ray growth rate being somewhat indeterminate. This flexibility in utilizing surplus energy for somatic growth, whether obtained from increased feeding rate or changes in resource partitioning, has been observed for several other species of elasmobranchs (Cortés and Gruber 1994, Mollet et al 2002, Wetherbee and Cortés 2004).

The ability for rays to behaviorally thermoregulate to avoid warmer water affected ray growth. While both warmer scenarios predicted a decrease in average weight-at-age, the ability to always find thermal refuges (i.e. behaviorally thermoregulate) resulted in a smaller decrease in average weight-at-age from Baseline (9.6% over all ages) than the decrease predicted under the Restricted Movement assumption (16.8% over all ages). In contrast, under the cooler temperature scenario, both the Restricted Movement and Thermal Refuges assumptions predicted more similar growth rate increases (17.2% and 13.4% over all ages). My results demonstrate that the sensitivity of cownose ray growth to long-term exposure to moderate increases in water temperature, and the magnitude of the effect, depends on the behavioral response of the rays and how well they can locate water with cooler temperatures.

The movement patterns of cownose rays observed in the field are likely related to variation in water temperatures. While warmer temperatures may provide a short term advantage to certain behaviors such as foraging (Matern et al. 2000), my results show that long term exposure to warmer temperatures would be detrimental to cownose ray growth

when viewed over their life time. Matern et al (2000) proposed that bat rays (*Myliobatis californica*) behaviorally thermoregulate to maximize their feeding efficiency. They suggested that bat rays feed in the warmer, shallow portions of Tomales Bay, CA during the day and then move to cooler waters at night. The warmer temperatures enable the bat rays to capitalize on their increased metabolic rate to acquire more prey. The move to cooler waters reduces their metabolic costs and decreases gastric evacuation rate while they maintain their assimilation efficiency. While this behavior was described for bat rays based on a daily time scale, it is possible that cownose rays are following the same general pattern but on a longer time scale. Cownose rays enter the bays and estuaries in the northern Gulf of Mexico once water temperatures become tolerable (~14-16 °C, J. Carlson personal communication). Rays occupy and utilize these habitats and prey resources as long as general metabolic costs are not too high. At some temperature, however, the metabolic costs of inhabiting those areas outweigh the benefits, and the rays move to locate conditions that are more suitable. This general pattern of abundance and distribution in relation to temperature has been reported for many species of elasmobranchs (Hopkins and Cech 2003, Simpfendorfer and Heupel 2004).

Changes in growth rate in response to warmer and cooler temperatures and alternative assumptions about movement behaviors affect individual survival and reproductive output, and in turn can cascade up to the population level. Both mortality rate and reproduction rate were weight-dependent in the bioenergetics model. The faster individual growth rates predicted for the cooler scenarios allowed individuals to attain a larger size more quickly, which with weight-dependent mortality, lead to higher survival. This was especially noticeable in the younger age classes, which typically have more rapid somatic growth rates than the older, reproductive age classes. Additionally, faster growing individuals reached

reproductive size in a shorter time than slower growing individuals. The warmer scenarios displayed decreased survivorship among individuals, as slower growth subjected the individual rays to higher probabilities of dying for longer periods of time and individuals would take longer to reach reproductive size.

Differences in individual growth rates predicted by the bioenergetics model affected the population dynamics of cownose ray. The matrix projection model predicted that under equilibrium conditions the simulated population of cownose rays would increase at 2.7% per year. The faster growth rate predicted for the cooler scenarios under the Temperature Effect assumption would lead to shorter generation times, which with an increased net reproductive rate, translated into a faster rate of annual population increase (4.4% and 4.7% versus 2.7% under Baseline). Warmer water temperatures were predicted to decrease the population growth rate and net reproductive rate, and lengthen the generation time of the population. Under the most extreme scenario, Warmer with Restricted Movement, the population would go from increasing at 2.7% per year under Baseline conditions to close to steady state conditions (increase at only 0.5%/year). This implies that any additional sources of mortality would likely cause the population to decline. The differences in long-term population growth rates predicted under the cooler and warmer scenarios, while relatively small in magnitude, could become important to population sustainability under changed environmental conditions and additional anthropogenic stresses. The “K-strategy” life history of cownose rays results in a population with relatively low resistance and resilience, making even small changes in population growth rate difficult to reverse or compensate for via density-dependent responses (Heppell et al. 1999, Cortés 2002, Rose et al. 2001). The differences in demographic

parameters predicted here demonstrate that changes in growth rates at the individual level can be directly linked to population-level metrics.

The pattern of reproductive values with age further support the differences between the slower growing individuals under the warmer scenarios and the faster growing individuals under the cooler scenarios. Reproductive values depend on both age-specific survivorship and the intrinsic rate of change of the population (r). Reproductive values were reported relative to the value of one assigned to the youngest age class. The Warmer with Restricted Movement scenario predicted the lowest r (Table 4.6) and the lowest survival for the largest number of age classes (~ages 2 – 16; Figure 4.5). Consistent with the slow growth of individuals and lower survival, the Warmer with Restricted Movement scenario also had the greatest age-specific reproductive values over the greatest number of age classes (Figure 4.7). Because slower growing individuals begin reproducing at an older age, it takes longer for the reproductive value to peak. However, once the peak is reached, the potential relative number of offspring yet to be born is large. Additionally, that potential remains high over a greater number of age classes. Reproductive values were lowest for the fastest growing individuals (Cooler with Restricted Movement scenario). The earlier onset of reproduction in effect spreads the reproductive potential out among more age classes, thereby decreasing the actual age-specific reproductive values.

Population growth rates of cownose rays are more sensitive to variation in age-specific survival rates than to age-specific fertility rates (Figure 4.8). The importance of survival has also been documented for other long-lived species (Heppell et al. 1999). In my analysis, elasticity to fertility was low, which indicated that the population growth rate was relatively insensitive to variation in fertility rates. Frisk et al. (2002) examined the demographics of

three species of skates and suggested that for species with low fecundity, a trade off between somatic growth and reproductive output could cause population growth rate to be insensitive to fertility. Given that cownose rays have very low fecundity (one pup/litter and one litter/year) and that changes in the observed fecundity pattern are unlikely due to biological constraints, such as space available for a female to carry young, my finding that population growth rate was insensitive to fertility appears consistent with previous analyses.

The elasticity patterns generated when age classes were grouped into life stages indicate that elasticity to adult survival had the greatest effect on population growth rate. Evidence from other analyses at the elasmobranch level appears contradictory about whether the survival rates of juvenile or mature adults is most important to determining population growth rate. Frisk et al. (2002) reported that adult survival was the dominant life trait for the barndoor skate, *Dipturus laevis*, and Mollet and Cailliet (2002) reported similar results for the pelagic stingray, *Dasyatis violacea*. However, juvenile survival has been reported as having the greatest impact on population growth rate for sharks in a variety of studies (Heppell et al. 1999, Brewster-Geisz and Miller 2000, Cortés 2002). This shift between the importance of juvenile survival for sharks versus adult survival for batoids may be explained by differences in the basic life history characteristics of the two groups. Based on my review of the literature, it appears that rays reproduce at an earlier age in relation to their longevity than many sharks, resulting in rays having a relatively shorter juvenile stage and a relatively longer adult stage (Martin and Cailliet 1988a, Martin and Cailliet 1988b, Cortés 2000, Neer and Cailliet 2001, Frisk et al. 2002, Mollet et al. 2002, Wade Smith - Moss Landing Marine Laboratories, unpublished data). If rays generally had relatively longer adult stages than sharks, then this would act to amplify the importance of their adult survival rates to

population growth rate because individual age elasticities are summed to obtain single values for juveniles and for adults.

Previous demographic analyses of elasmobranchs have been conducted using life table and age-structured matrix projection approaches (Sminkey and Musick 1996, Simpfendorfer 1999, Cortés 2002, Frisk et al. 2002) or stage-based modeling (Cortés 1999, Brewster-Geisz and Miller 2000, Frisk et al. 2002, Mollet and Cailliet 2002). Stage-based models are often employed when age-specific data are lacking, thereby requiring the estimation of fewer parameters (Brewster-Geisz and Miller 2000, Gotelli 2001). In the majority of these age- and stage-based studies, well-defined estimates of age-specific survivorship and fecundity (age-structured models) or transition probabilities (stage-based approaches) were lacking. In the case of the age-structured models, the representation of reproduction in the model is usually a step function at the age of first reproduction (e.g., Frisk et al. 2002, Mollet and Cailliet 2002), ignoring differences in maturity among individuals of the same age. Additionally, natural mortality is often assumed to be equal for all age classes, when in reality mortality rate is often size-dependent (Sminkey and Musick 1996, Cortés 1998, Simpfendorfer 1999, Frisk et al. 2002). My analysis attempted to address these issues by utilizing size-based functions of mortality and reproduction within the bioenergetics model to predict age-specific estimates of survival and fecundity, which were then used as the basis of the age-structured matrix projection model.

Model Caveats

Additional measurements and laboratory experiments designed to estimate specific components of the bioenergetics model would allow for increased accuracy and precision in model predictions. Values of parameters related to specific dynamic action, egestion,

excretion, and the multiplier representing the metabolic cost of activity used in the model were all obtained from the literature. While the estimate of specific dynamic action was experimentally determined for another batoid, all the other parameter values were based on experiments with sharks. Error can be introduced by utilizing parameter estimates from different taxa, and this error could bias simulated growth results (Bartell et al. 1986).

Therefore, experiments to obtain species-specific information for these parameters would aid in refining the bioenergetics and matrix projection models.

Of particular importance would be accurate estimates of maximum consumption rates and the dependence of consumption on water temperature. The parameters used to model maximum consumption rates were derived using semi-quantitative information from other elasmobranchs. Experimental determination of maximum consumption for the cownose ray for a range of sizes and over a variety of temperatures would likely improve model performance and restrict some of the flexibility now in the model calibration of p-values.

The assumption of a closed population, while common for demographic analysis, may not hold true for highly migratory species like cownose rays (Schwartz, 1990, Brewster-Geisz and Miller 2000). Cownose rays are known to undertake long distance migrations (Schwartz, 1990); however, the details of these migrations within the Gulf of Mexico are currently unknown. The metabolic costs of migration were not explicitly incorporated into the bioenergetics model. Should these costs be significantly different, (most likely greater) than the metabolic cost of normal activity as presently represented in the bioenergetics model, the results presented here could change. Additional information on the metabolic costs of activity in general, and migration in particular, would be useful.

The current bioenergetics and matrix projection models do not account for changes in growth, survival, and reproduction associated with density-dependent compensation. Despite the documentation of density-dependent regulation for a variety of teleost species (for review see Rose et al. 2001), very little empirical evidence exists for elasmobranchs (Carlson and Baremore 2003). Shifts in age at maturity and juvenile survivorship are the most likely mechanism for compensation in sharks, as most species have a limited capacity for increased fecundity due to physical constraints (Cortés 2002). Sminkey and Musick (1995) observed a slight increase in growth rate of juvenile sandbar sharks in the Chesapeake Bay after population depletion due to fishing, but they were not able to determine if age at maturity had also been reduced. Carlson and Baremore (2003) suggested that an observed decrease in age at maturity and increased growth rate for the Atlantic sharpnose shark, *Rhizoprionodon terraenovae*, compared to previous studies lead support to the compensatory hypothesis; however, they were unable to determine whether their results were due to differences in methodology, anthropogenic influences, or variation in other natural factors. Whether and how density dependent compensation may occur in the cownose ray has yet to be determined.

Conservation Implications

The management implications of the elasticity analyses and reproductive values by age obtained from the cownose ray model were complicated. Elasticities indicated that adult survival had the greatest effect on population growth rate (Figure 4.9). From a management perspective, this would indicate that conservation measures should focus on preserving the adult life stage. However, reproductive values by age indicated that intermediate ages were important contributors to reproductive output (Figure 4.7), implying that conservation efforts should be directed towards ensuring the health of individuals between about 5 and 15 years

old. How potential harvesting might be managed is not clear, although targeting older age classes or an analogy to a slot limit (only harvest young and old individuals) should be investigated further.

Changes in species distribution may occur under altered temperatures. Temperature has been cited as one of the driving environmental factors that controls the distribution of marine elasmobranchs (Simpfendorfer and Heupel 2004). Climate change models predict that climate zones and habitats will generally shift northward in the face of increased warming (Smith 2004). As cownose rays are sensitive to increases in temperature, they will likely shift their distribution northward to avoid warmer waters. This shift may permanently alter their distributional and migration patterns, with the population currently occupying the Gulf of Mexico perhaps moving to join the Atlantic Ocean population. Further modeling should focus on potential shifts in the geographic distribution of cownose rays, and how these shifts may affect individual and population growth rates.

Conclusions

The use of the age-specific survivorship and fecundity information derived from an individual-based bioenergetics model as inputs to an age-structured matrix model is a powerful approach to demographic analysis for the many species with limited data. My analysis demonstrated how such a coupled modeling approach could be used to predict the effects of changes in environmental conditions on individuals and how these changes in individuals can express themselves at the population level.

My results showed the sensitivity of individual and population growth rates of cownose rays to changes in water temperature. Relatively small changes in temperature caused changes in survival and reproductive output at the individual level, which were then

translated into effects at the population level. The life history of the cownose ray makes them extremely susceptible to changes in mortality. Changes in water temperatures in their habitats, either due to natural variation or climate change, should be closely monitored.

Literature Cited

- Adams, S.M. and J.E. Breck. 1990. Bioenergetics. Pages 389-415 in C.B. Schreck and P.B. Moyle, editors. Methods for fish biology. American Fisheries Society, Bethesda, Maryland.
- Bartell, S.M., J.E. Breck, R.H. Gardner, and A.L. Brenkert. 1986. Individual parameter perturbation and error analysis of fish bioenergetics models. Canadian Journal of Fisheries and Aquatic Science 43:160-168.
- Bigelow, H.B. and W.C. Schroeder. 1953. Fishes of the Western North Atlantic. Part I, Lancets, cyclostomes and sharks. Memoir of the Sears Foundation for Marine Research.
- Borgmann, U. and D.M. Whittle. 1992. Bioenergetics and PCB, DDE, and mercury dynamics in Lake Ontario lake trout (*Salvelinus namaycush*): a model based on surveillance data. Canadian Journal of Fisheries and Aquatic Sciences 49:1086-1096.
- Bradley, J.L. 1996. Prey energy content and selection, habitat use and daily ration of the Atlantic stingray, *Dasyatis sabina*. Masters thesis. Department of Biological Sciences. Melbourne, Florida Institute of Technology. 51 pages.
- Brandt, S.B. and K.J. Hartman. 1993. Innovative approaches with bioenergetics models: future applications to fish ecology and management. Transactions of the American Fisheries Society 122:731-735.
- Brett, J.R. and T.D.D. Groves 1979. Physiological energetics. Pages 279-352 in W.S. Hoar and D.J. Randall, editors. Fish Physiology Vol. VII. Academic Press, New York
- Brewster-Geisz, K.K. and T.J. Miller 2000. Management of the sandbar shark, *Carcharhinus plumbeus*: implications of a stage-based model. Fishery Bulletin 98(2): 236-249.
- Carlson, J. K. and I. E. Baremore. 2003. Changes in biological parameters of Atlantic sharpnose shark *Rhizoprionodon terraenovae* in the Gulf of Mexico: evidence for density-dependent growth and maturity? Marine and Freshwater Research 54:227-234.
- Carlson, J.K., K. J. Goldman, and C.G. Lowe. 2004. Metabolism, energetic demand, and endothermy. Pages 201- 222 in Carrier, J.C., J.A. Musick, and M.R. Heithaus, editors. Biology of sharks and their relatives. CRC Press, Boca Raton, Florida.

- Castro, J. I. 1993. The shark nursery of Bulls Bay, South Carolina, with a review of the shark nurseries of the southeastern coast of the United States. *Environmental Biology of Fishes* 38: 37-48.
- Caswell, H. 2001. *Matrix population models: construction, analysis, and interpretation*. 2nd Edition. Sinauer Associates, Inc., Sunderland, Massachusetts.
- Compagno, L. J. V. 1990. Alternative life history styles of cartilaginous fishes in time and space. *Environmental Biology of Fishes* 28:33-75.
- Cortés, E. 1998. Demographic analysis as an aid in shark stock assessment and management. *Fisheries Research* 39(2): 199-208.
- Cortés, E. 1999. A stochastic stage-based population model of the sandbar shark in the western north Atlantic. Pages 115-136 *in* J. A. Musick, editor. *Life in the slow lane: ecology and conservation of long-lived marine animals*. American Fisheries Society Symposium 23, Bethesda, Maryland.
- Cortés, E. 2000. Life history patterns and correlations in sharks. *Reviews in Fisheries Science* 8(4):299-344.
- Cortés, E. 2002. Incorporating uncertainty into demographic modeling: application to shark populations and their conservation. *Conservation Biology* 16(4): 1048-1062.
- Cortés, E. 2004. Life history patterns, demography, and population dynamics. Pages 449-469 *in* Carrier, J.C., J.A. Musick, and M.R. Heithaus, editors. *Biology of sharks and their relatives*. CRC Press, Boca Raton, Florida.
- Cortés, E. and S.H. Gruber. 1994. Effect of ration size on growth and gross conversion efficiency of young lemon sharks, *Negaprion brevirostris*. *Journal of Fish Biology* 44:331-341.
- Du Preez, H.H., A. McLachlan, and J.F.K. Marais. 1988. Oxygen consumption of two nearshore marine elasmobranchs, *Rhinobatos annulatus* (Muller & Henle, 1841) and *Myliobatus aquila* (Linnaeus, 1758). *Comparative Biochemistry and Physiology* 89A(2): 283-294.
- Du Preez, H.H., A. McLachlan, J.F.K. Marais, and A.C. Cockcroft. 1990. Bioenergetics of fishes in a high-energy surf-zone. *Marine Biology* 106: 1-12.
- Ebert, T.A. 1999. *Plant and Animal Populations: Methods in Demography*. Academic Press, San Diego, California.

- Ezcurra, J.M. 2001. The mass-specific routine metabolic rate of captive pelagic stingrays, *Dasyatis violacea*, with comments on energetics. Masters thesis. Moss Landing Marine Laboratories. Stanislaus, California State University, Stanislaus. 51 pages.
- Frisk, M.G., T.J. Miller, and M.J. Fogarty. 2002. The population dynamics of little skate *Leucoraja erinacea*, winter skate *Leucoraja ocellata*, and barndoor skate *Dipturus laevis*: predicting exploitation limits using matrix analyses. ICES Journal of Marine Science 59: 576-586.
- Gotelli, N.J. 2001. A primer of ecology. 3rd Edition. Sinauer Associates, Sunderland, Massachusetts.
- Gruber, S.H. 1984. Bioenergetics of the captive and free-ranging lemon shark (*Negaprion brevirostris*). American Association of Zoological Parks and Aquariums 60:340-373.
- Hanson, P.C., T.B. Johnson, D.E. Schindler, and J.F. Kitchell. 1997. Fish Bioenergetics 3.0. University of Wisconsin-Madison Center for Limnology. Wisconsin Sea Grant Institute.
- Hartman, K.J. and F.J. Margraf. 1992. Effects of prey and predator abundances on prey consumption and growth of walleye in western Lake Erie. Transactions of the American Fisheries Society 121:245-260.
- He, K., J.F. Kitchell, S.R. Carpenter, J.R. Hodgson, D.E. Schindler, and K.L. Cottingham. 1993. Food web structure and long-term phosphorus recycling: a simulation model evaluation. Transactions of the American Fisheries Society 122:773-783.
- Heppell, S.S., L.B. Crowder, and T.R. Menzel. 1999. Life table analysis of long-lived marine species with implications for conservation and management. Pages 137-146 in J. A. Musick, editor. Life in the slow lane: ecology and conservation of long-lived marine animals. American Fisheries Society Symposium 23, Bethesda, Maryland.
- Heppell, S. S., H. Caswell, and L.B. Crowder. 2000. Life histories and elasticity patterns: perturbation analysis for species with minimal demographic data. Ecology 81(3): 654-665.
- Hill, D.K. and J.J. Magnuson. 1990. Potential effects of global climate warming on the growth and prey consumption of Great Lakes Fish. Transactions of the American Fisheries Society 119:265-275.
- Hoenig, J.M. 1983. Empirical use of longevity data to estimate mortality rates. Fishery Bulletin 82(1):898-903.
- Hoenig, J.M. and S.H. Gruber. 1990. Life-history patterns in the elasmobranch: implications for fisheries management. Pages 1-16 in H.L. Pratt, S.H. Gruber, and T. Taniuchi, editors. Elasmobranchs as living resources: Advances in the biology, ecology, systematics, and

the status of the fisheries. U.S. Department of Commerce. NOAA Technical Report NMFS 90.

- Holden, M.J. 1974. Problems in the rational exploitation of elasmobranch populations and some suggested solutions. Pages 117-137 *in* Sea fisheries research. F.R. Harden-Jones, editor. John Wiley and Sons, New York.
- Hopkins, T.E. and J. J.J. Cech. 2003. The influence of environmental variables on the distribution and abundance of three elasmobranchs in Tomales Bay, California. *Environmental Biology of Fishes* 66:279-291.
- Kennedy, V.S., R.R. Twilley, J.A. Kleypas, J.H. Cowan, Jr., and S.R. Hare. 2002. Coastal and marine ecosystems and climate change: Potential effects on U.S. resources. A report prepared for the Pew Center on Global Climate Change. 64 pages.
- Kingsland, S.E. 1985. *Modeling nature: episodes in the history of population ecology*. Chicago University Press, Chicago, Illinois.
- Lowe, C.G. 2002. Bioenergetics of free-ranging juvenile scalloped hammerhead sharks (*Sphyrna lewini*) in Kane'ohe Bay, O'ahu, Hawai'i. *Journal of Experimental Marine Biology and Ecology* 278:141-156.
- Lowe, C.G. and K.J. Goldman. 2001. Thermal and bioenergetics of elasmobranchs: bridging the gap. Pages 251-266 *in* Tricas, T.C. and S.H. Gruber, editors. *The behavior and sensory biology of elasmobranch fishes: an anthology in memory of Donald Richard Nelson*. *Environmental Biology of Fishes* 60:251-266.
- Matern, S. A., J.J. Cech, and T.E. Hopkins. 2000. Diel movements of bat rays, *Myliobatis californica*, in Tomales Bay, California: evidence for behavioral thermoregulation?" *Environmental Biology of Fishes* 58:173-182.
- Martin, L.K. and G.M. Cailliet 1988a. Age and growth determination of the bat ray, *Myliobatis californica* Gill, in central California. *Copeia* 1988(3):762-773.
- Martin, L.K. and G.M. Cailliet 1988b. Aspects of the reproduction of the bat ray, *Myliobatis californica*, in central California. *Copeia* 1988(3):754-762.
- McEachran, J.D. & C. Capapé. 1984. Rhinopteridae. Page 208 *in* Whitehead, P.J.P., M.-L. Bauchot, J.-C. Hureau, J. Nielsen, & E. Tortonese, editors. *Fishes of the North-eastern Atlantic and Mediterranean*. Volume 1. UNESCO.
- McEachran, J.D. & J.D. Fechhelm. 1998. *Fishes of the Gulf of Mexico*. Volume 1. University of Texas Press.

- Medved, R. J., C. E. Stillwell, and J.G. Casey. 1988. The rate of food consumption of young sandbar sharks (*Carcharhinus plumbeus*) in Chincoteague Bay, Virginia. *Copeia* 1988(4): 956-963.
- Mollet, H.F. and G.M. Cailliet. 2002. Comparative population demography of elasmobranchs using life history tables, Leslie matrices and stage-based matrix models. *Marine and Freshwater Research* 53: 503-516.
- Mollet, H.F., J.M. Ezcurra, and J.B. O'Sullivan. 2002. Captive biology of the pelagic stingray, *Dasyatis violacea* (Bonaparte, 1932). *Marine and Freshwater Research* 53:531-541.
- Neer, J.A. and B.A. Thompson. In press. Life history of the cownose ray, *Rhinoptera bonasus*, in the northern Gulf of Mexico, with comments on geographic variability in life history traits. *Environmental Biology of Fishes*.
- Neer, J.A. and G.M. Cailliet 2001. Aspects of the life history of the Pacific electric ray, *Torpedo californica* (Ayres). *Copeia* 2001(3):842-847.
- Neill, W.H. 1979. Mechanisms of fish distribution in heterothermal environments. *American Zoologist* 19:305-317.
- Neill, W.H. and J.J. Magnuson. 1974. Distributional ecology and behavioral thermoregulation of fishes in relation to heated effluent from a power plant at Lake Monona, Wisconsin. *Transactions of the American Fisheries Society* 103:663-710.
- Ney, J.J. 1990. Trophic economics in fisheries: assessment of demand-supply relationships between predators and prey. *Reviews in Aquatic Sciences* 2:55-81.
- Ney, J.J. 1993. Bioenergetics modeling today: growing pains on the cutting edge. *Transactions of the American Fisheries Society* 122:736-748.
- Parsons, G. 1987. Life history and bioenergetics of the bonnethead shark *Sphyrna tiburo* (Linnaeus): a comparison of two populations. Ph.D. dissertation. Department of Marine Science, University of South Florida 157 pages.
- Rand, P.S., D.J. Stewart, P.W., P.W. Seelbach, M. Jones, and L.R. Wedge. 1993. Modeling steelhead population energetics in Lakes Michigan and Ontario. *Transactions of the American Fisheries Society* 122:756-772.
- Roff, D.A. 1992. The evolution of life histories: theory and analysis. Chapman and Hall, New York.
- Rose, K.A., J.H. Cowan, K.O. Winemiller, R.A. Meyers, and R. Hilborn. 2001. Compensatory density dependence in fish populations: importance, controversy, understanding and prognosis. *Fish and Fisheries* 2:293-327.

- Russell, R.W. 1999. Comparative demography and life history tactics of seabirds: implications for conservation and marine monitoring. Pages 51-76 in J. A. Musick, editor. Life in the slow lane: ecology and conservation of long-lived marine animals. American Fisheries Society Symposium 23, Bethesda, Maryland.
- Schindler, D.E., J.F. Kitchell, K. He, S.R. Carpenter, J.R. Hodgson, and K.L. Cottingham. 1993. Food web structure and phosphorus cycling in lakes. Transactions of the American Fisheries Society 122:756-772.
- Schindler, D.E., T.E. Essington, J.F. Kitchell, C. Boggs, and R. Hilborn. 2002. Sharks and tunas: Fisheries impacts on predators with contrasting life histories. Ecological Applications 12(3):735-748.
- Schmid, T.H. and F.L. Murru. 1994. Bioenergetics of the bull shark, *Carcharhinus leucas*, maintained in captivity. Zoo Biology 13:177-185.
- Schmidt-Nielsen, K. 1983. Animal Physiology: adaptation and environment. Cambridge University Press, Cambridge, United Kingdom.
- Schwartz, F.J. 1990. Mass migratory congregations and movements of several species of cownose rays, Genus *Rhinoptera*: a world-wide review. Journal of the Elisha Mitchell Scientific Society 106:10-13.
- Simpfendorfer, C.A. 1999. Demographic analysis of the dusky shark fishery in southwestern Australia. Pages 149-160 in J.A. Musick, editor. Life in the slow lane: ecology and conservation of long-lived marine animals. American Fisheries Society Symposium 23, Bethesda, Maryland.
- Simpfendorfer, C.A. and M.R. Heupel. 2004. Assessing habitat use and movement. Pages 553-572 in Carrier, J.C., J.A. Musick, and M.R. Heithaus, editors. Biology of sharks and their relatives. CRC Press, Boca Raton, Florida.
- Sminkey, T.R. and J.A. Musick. 1995. Age and growth of the sandbar shark, *Carcharhinus plumbeus*, before and after population depletion. Copeia 1995(4):871-883.
- Sminkey, T.R. and J.A. Musick. 1996. Demographic analysis of the sandbar shark, *Carcharhinus plumbeus*, in the western North Atlantic. Fishery Bulletin 94(2):341-347.
- Smith, J.B. 2004. A synthesis of potential climate change impacts on the U.S. A report prepared for the Pew Center on Global Climate Change. 56 pages.
- Smith, J.W. & J.V. Merriner. 1985. Food habits and feeding behavior of the cownose ray, *Rhinoptera bonasus*, in lower Chesapeake Bay. Estuaries 8(3):305-310.

- Smith, J.W. and J.V. Merriner 1987. Age and growth, movements and distribution of the cownose ray, *Rhinoptera bonasus*, in Chesapeake Bay. *Estuaries* 10(2): 153-164.
- Sundstrom, L.F. and S.H. Gruber. 1998. Using speed-sensing transmitters to construct a bioenergetics model for subadult lemon sharks, *Negaprion brevirostris* (Poey), in the field. *Hydrobiologia* 371/372:241-247.
- Trent, L., D.E. Parshley, and J.K. Carlson. 1997. Catch and bycatch in the shark drift gillnet fishery off Georgia and east Florida. *Marine Fisheries Review* 59(1):19-28.
- Van Dykhuizen, G. and H.F. Mollet. 1992. Growth, age estimation and feeding of captive sevengill sharks, *Notorynchus cepedianus*, at the Monterey Bay Aquarium. *Australian Journal of Marine and Freshwater Research* 43:297-318.
- Wetherbee, B.M. and S.H. Gruber. 1993. Absorption efficiency of the lemon shark *Negaprion brevirostris* at varying rates of energy intake. *Copeia* 1993(2):416-425.
- Wetherbee, B.M. and E. Cortés. 2004. Food consumption and feeding habits. Pages 225-246 *in* Carrier, J.C., J.A. Musick, and M.R. Heithaus, editors. *Biology of sharks and their relatives*. CRC Press, Boca Raton, Florida.

CHAPTER V.

SUMMARY

The overall goals of this research were to collect data on basic life history information on the cownose ray, *Rhinoptera bonasus*, and to use an individual-based bioenergetics model coupled to a matrix projection model to examine how warmer and cooler water temperatures would affect cownose ray growth and long-term population dynamics. I selected bioenergetics and matrix projection models because bioenergetics models provide a link between the individual and the environment (Adams and Breck 1990, Brandt and Hartman 1993), while matrix projection models provide a link between the individual and the population (Caswell 2001). The usefulness of these models is dependent, in part, on the quality and availability of data for the species of interest (Bartell et al. 1986). As information on the cownose ray in the Gulf of Mexico was lacking, I conducted basic life history research, as well as ecophysiological experiments, in order to estimate parameters and provide calibration data for the bioenergetics model.

I performed a field study that examined the age and growth, and several reproductive components, of the cownose ray (Chapter II). I used vertebral sections for age estimation. Age estimates ranged from 0⁺ to 18⁺ years old for females (n = 121) and from 0⁺ to 16⁺ for males (n = 106). Annual band deposition was carefully verified through marginal increment ratio analysis. I fitted four growth models to the resulting size-at-age data. Log-likelihood tests indicated that a combined sexes Gompertz model provided the best fit to the observed data. Using the parameters generated by the Gompertz model ($DW_{\infty} = 1100.2$ mm, $K = 0.1332/\text{year}$ and $t_0 = -0.2573$ years), I predicted average size-at-age and obtained an estimate of theoretical longevity (26 years). I then converted average size-at-age to average weight-at-

age using a size-weight relationship generated from the field data. The weight-at-age data were used as the basis for the calibration of the bioenergetics model. I also used the observed weight-at-age data as a guide to include individual level variability in initial weights and in growth rates in the bioenergetics model.

The reproductive component of the field study (Chapter II) also yielded valuable information on maturity at age and fecundity of cownose rays, which I used to estimate parameters of the bioenergetics model. I determined disk width at 50% maturity (DW_{50}) for cownose rays using a logistic function applied to binominal maturity data. Male cownose rays had a DW_{50} of 642 mm (~4.6 kg) at maturity, while females reached maturity at a DW_{50} of 653 mm (~4.9 kg). This information was used to derive a relationship between the probability of being mature as a function of ray body weight. I also used the field data to estimate weight-at-birth, fecundity (1 pup/litter), and gestation (1 litter/year), which were then inputted into the bioenergetics model.

I compared my measured life history traits for the cownose rays inhabiting the Gulf of Mexico to those reported by others for the western Atlantic Ocean. Cownose rays in the Gulf of Mexico had lower estimates of DW_{∞} and K , and a higher theoretical longevity than their conspecifics in the western Atlantic Ocean. Additionally, cownose rays in the Gulf of Mexico also attain maturity at a smaller size and at earlier age than their counterparts in the western Atlantic Ocean. Variability in life history traits for geographically separated populations of the same species has been documented for several other species of elasmobranchs (Carlson et al. 2003, Driggers et al. 2004), but has not previously been documented in a batoid (rays and skates).

Metabolism is one of the major components of an organism's daily energy budget, and although highly variable, may account for its largest portion (Lowe 2001). Species-specific metabolic information is vital for constructing accurate energy budgets and for developing bioenergetics models (Carlson et al. 1999). I conducted respirometry experiments to obtain estimates of standard metabolic rate for the cownose ray (Chapter III). I determined standard oxygen consumption rate (MO_2) for 19 seasonally acclimatized cownose rays ranging in weight from 0.4 to 8.25 kg. Estimates of mass-dependent MO_2 ranged from 55.88 mg O_2 kg^{-1} hr^{-1} for an 8.25 kg ray to 332.75 mg O_2 kg^{-1} hr^{-1} for a 2.2 kg animal at 22-25 °C. Rates of oxygen consumption determined for the cownose ray were similar to those reported for other batoids (Du Preez et al. 1988, Hopkins and Cech 1994, Ezcurra, 2001), and provided me with estimates of respiration rate-related parameters for use in the bioenergetics model.

The experiments verified that metabolic rate was both mass and temperature dependent in the cownose ray. Multiple regression analysis examined the effect of temperature, salinity, and mass on standard mass-independent MO_2 . I found that temperature ($p < 0.01$) and mass ($p < 0.0001$) had significant effects on oxygen consumption, whereas salinity did not ($p > 0.05$). Q_{10} , a measure of the rate of change over 10 °C, was calculated as 2.33 (19 – 28 °C). My estimated value was within the estimates determined for two other batoid species: $Q_{10} = 1.87$ for the bull ray (*Myliobatos aquila*) reported by Du Preez et al. (1988) and a $Q_{10} = 3.00$ for the bat ray (*Myliobatis californica*) reported by Hopkins and Cech (1994). I used this information to determine the temperature-related parameters for respiration in the bioenergetics model.

Changes in the average water temperatures affected the individual growth of cownose rays (Chapter IV). A symmetrical response in growth rate under the Temperature Effect

simulations was predicted for plus 2° C and minus 2° C changes in temperature, indicating that the influence of temperature on cownose ray growth within this range is predictable from temperature alone. The increased metabolic costs incurred when occupying warmer waters forced the rays to use more of the consumed energy for maintenance than for somatic growth, and lead to slower growth rates over their life times. Age-specific average weights-at-age decreased between 4.8 – 19.4%, with average decreases of 9.6 and 16.8% for the two warmer scenarios when compared to Baseline conditions. Cooler waters allowed for an increase in energy available for growth due to lower metabolic costs. The model predicted heavier weights-at-age for the cooler scenarios compared to Baseline condition (13.4 and 17.2% averaged over all ages), with age-specific average weights increased between 6.9 and 20.2%. The predicted changes in weight-at-age are consistent with cownose ray growth rate being somewhat indeterminate.

Realized consumption must vary under the different temperature scenarios and ray movement assumptions for simulated average weights-at-age to match the growth pattern predicted by the Baseline scenario. Rays must consume approximately 11% more energy per day under the warmer scenarios to maintain Baseline weight-at-age values. Realized consumption could be reduced by 11 – 13% BW per day under the cooler scenarios for the rays to maintain the same life time growth trajectory as predicted by the Baseline scenario. More information on ray foraging behavior and the population dynamics of their prey would enable further investigation into how interannual variation and anomalous years of water temperatures would affect cownose ray growth.

The ability for rays to behaviorally thermoregulate to avoid warmer water affected simulated ray growth rates and predicted weights-at-age. While both warmer scenarios

predicted a decrease in average weight-at-age, the ability to continue to find thermal refuges (e.g. behaviorally thermoregulate) resulted in a smaller decrease in average weight-at-age from Baseline (9.6% over all ages) than the decrease predicted under the Restricted Movement assumption (16.8% over all ages). In contrast, under the cooler temperature scenario, both the Restricted Movement and Thermal Refuges assumptions predicted similar growth rate increases (17.2% and 13.4% over all ages). My results demonstrate that the sensitivity of cownose ray growth to long-term exposure of moderate increases in water temperature, and the magnitude of the effect, depends on the behavioral response of the rays and whether they can locate water with cooler temperatures.

Changes in growth rate in response to warmer and cooler temperatures and alternative assumptions about movement behavior affected individual survival and reproductive output. The faster individual growth rates predicted for the cooler scenarios allowed individuals to grow more quickly, which with weight-dependent mortality, lead to higher survival. Additionally, faster growing individuals reached reproductive size in a shorter time than slower growing individuals. The warmer scenarios displayed decreased survivorship among individuals, as slower growth subjected the individual rays to higher probabilities of dying for longer periods of time, and individuals took longer to reach reproductive size.

Differences in age-specific survival and reproductive output arising from changes in individual growth rates were extrapolated to the population level (Chapter IV). The matrix projection model predicted that under equilibrium conditions the simulated population of cownose rays would increase at 2.7% per year, with a net reproductive rate (R_0) of 1.4, and generation time (\bar{A}) of 12.4 years. The slower growth rate predicted for the cooler scenarios under the Temperature Effect assumption would lead to shorter generation times, which with

an increased net reproductive rate, translated into a faster rate of annual population increase (4.4% and 4.7% versus 2.7% under Baseline). Warmer water temperatures were predicted to decrease the population growth rate and net reproductive rate, and lengthen the generation time of the population. Under the most extreme scenario, Warmer with Restricted Movement, the population would go from increasing at 2.7% per year under Baseline conditions to close to steady state conditions (increase at only 0.5%/year). The differences in long-term population growth rates predicted under the cooler and warmer scenarios, while relatively small in magnitude, could become important to population sustainability under changed environmental conditions and additional anthropogenic stresses. Predicted stable age distributions were similar for warmer and cooler temperature scenarios, while reproductive values were more responsive to alternations in temperature. Consistent with the slow growth of individuals and lower survival, the Warmer with Restricted Movement scenario had the greatest age-specific reproductive values over the greatest number of age classes. The differences in demographic parameters predicted here demonstrate that changes in growth rates at the individual level can be directly linked to population-level metrics.

Elasticity analysis of the matrix projection models under Baseline and the warmer and cooler scenarios showed that population growth rates of cownose rays were more sensitive to variation in survival rates than to fertility rates. Age-specific elasticities were relatively higher for survival compared to fertility, and were higher for young ages than older ages. Life-stage aggregated elasticities were also higher for survival than for fertility, but were higher for adults than for juveniles. Elasticities were generally similar among temperature scenarios. These results based on elasticities appear to contradict previous analyses that showed that juvenile survival was most important to the growth rate of sharks. This

difference may be related to differences in the relative durations of juvenile versus mature life stages between sharks and batoids. Management implications of my results are complicated by the high elasticities of adult survival but the high reproductive values of intermediate aged individuals.

Additional measurements and laboratory experiments designed to estimate specific components of the bioenergetics model would allow for increased accuracy and precision in model predictions of age-specific survival and reproduction. Values of parameters related to specific dynamic action, egestion, excretion, and the multiplier representing the metabolic cost of activity used in the model were all obtained from the literature. Of particular importance would be accurate estimates of maximum consumption rates and the dependence of consumption on water temperature. The parameters used to model maximum consumption rates were derived using semi-quantitative information from other elasmobranchs. Therefore, experiments to obtain species-specific information for these parameters would aid in refining the bioenergetics and matrix projection models.

In summary, I performed laboratory experiments and collected field data to provide basic life history information on cownose rays, and used this information to configure individual-based bioenergetics and matrix projection models, which were then used to examine the effect of warmer and cooler temperatures on cownose ray growth and population dynamics. The combination of coordinated laboratory experiments, field data collection, and individual-based bioenergetics modeling coupled to matrix projection models provides a powerful approach to demographic analysis of the many species with limited data. My analysis demonstrated how such a coupled modeling approach could be used to predict the

effects of changes in environmental conditions on individuals and how these changes in individuals can express themselves at the population level.

Literature Cited

- Adams, S.M. and J.E. Breck. 1990. Bioenergetics. Pages 389-415 in C.B. Schreck and P.B. Moyle, editors. Methods for fish biology. American Fisheries Society, Bethesda, Maryland.
- Bartell, S.M., J.E. Breck, R.H. Gardner, and A.L. Brenkert. 1986. Individual parameter perturbation and error analysis of fish bioenergetics models. Canadian Journal of Fisheries and Aquatic Science 43:160-168.
- Brandt, S.B. and K.J. Hartman. 1993. Innovative approaches with bioenergetics models: future applications to fish ecology and management. Transactions of the American Fisheries Society 122:731-735.
- Carlson, J.K., C.L. Palmer, and G.R. Parsons. 1999. Oxygen consumption rate and swimming efficiency of the blacknose shark, *Carcharhinus acronotus*. Copeia 1999(1): 34-39.
- Carlson, J.K., E. Cortés, and D. Bethea. 2003. Life history and population dynamics of the finetooth shark, *Carcharhinus isodon*, in the northeastern Gulf of Mexico. Fishery Bulletin 101:281-292.
- Caswell, H. 2001. Matrix population models: construction, analysis, and interpretation. 2nd Edition. Sinauer Associates, Inc., Sunderland, Massachusetts.
- Driggers, W.B. III, J.K. Carlson, D. Oakley, G. Ulrich, B. Cullum, and J.M. Dean. 2004. Age and growth of the blacknose shark, *Carcharhinus acronotus*, in the western North Atlantic Ocean with comments on regional variation in growth rates. Environmental Biology of Fishes 71(2):171-178.
- Du Preez, H. H., A. McLachlan, and J.F.K. Marais. 1988. Oxygen consumption of two nearshore marine elasmobranchs, *Rhinobatos annulatus* (Muller & Henle, 1841) and *Myliobatus aquila* (Linnaeus, 1758). Comparative Biochemistry and Physiology 89A(2): 283-294.
- Ezcurra, J.M. 2001. The mass-specific routine metabolic rate of captive pelagic stingrays, *Dasyatis violacea*, with comments on energetics. Masters thesis. Moss Landing Marine Laboratories. Stanislaus, California State University, Stanislaus. 51 pages.

Hopkins, T.E. and J.J. Cech, Jr. 1994. Effect of temperature on oxygen consumption of the bat ray, *Myliobatis californica* (Chondrichthyes, Myliobatidae). *Copeia* 1994(2): 529-532.

Lowe, C.G. 2001. Metabolic rates of juvenile scalloped hammerhead sharks (*Sphyrna lewini*). *Marine Biology* 139: 447-453.

APPENDIX

LETTER OF PERMISSION FROM ENVIRONMENTAL BIOLOGY OF FISHES

Springer | P.O. Box 17 | 3300 AA Dordrecht | The Netherlands



Ms. Julie A. Neer
NOAA Fisheries
3500 Delwood Beach Road
Panama City, FL 32408
USA

Van Godewijkstraat 30
3311 GX Dordrecht
The Netherlands
tel +31 (0) 78 65 76-000
fax +31 (0) 78 65 76-254
www.springeronline.com

02/03/2005

Re: Environmental Biology of Fishes MS-3775-04 in press, (Neer)

Dear Ms. Neer,

With reference to your request (copy herewith) to reprint material on which Springer Science and Business Media control the copyright, our permission is granted, free of charge, for the use indicated in your enquiry.

This permission

- allows you non-exclusive reproduction rights throughout the World.
- excludes use in an electronic form. Should you have a specific project in mind, please reapply for permission.
- requires a full credit (Kluwer Academic Publishers book/journal title, volume, year of publication, page, chapter/article title, name(s) of author(s), figure number(s), original copyright notice) to the publication in which the material was originally published, by adding: with kind permission of Springer Science and Business Media.

Material may not be republished until at least one year after our publication date.

Permission free of charge on this occasion does not prejudice any rights we might have to charge for reproduction of our copyrighted material in the future.

Sincerely yours,

Inge Weijman
Special Licensing Department
Tel.nr.: +31-78-6576130
Fax nr.: +31-78-6576-300
E-mail: Inge.Weijman@springer-sbm.com
<http://www.springeronline.com>
<http://www.springer-sbm.com>

PS.PLEASE BE CERTAIN TO INCLUDE OUR REFERENCE IN ALL CORRESPONDENCE

Dear Dr. Neer,

Thank you for your email. We grant you permission to use the article in an electronic form, if password protected and only as a whole (not separately downloadable). We herewith also waive the condition that material may not be republished until at least one year after our publication date.

Best regards

Inge Weijman

Inge Weijman

Springer

Indexing and Abstracting Coordinator | Special Licensing Department

Van Godewijckstraat 30 | 3311 GX

Office Number: 04C16b

P.O. Box 17 | 3300 AA

Dordrecht | The Netherlands

tel +31 (0) 78 657 6130

fax +31 (0) 78 657 6744

Inge.Weijman@springer-sbm.com

www.springeronline.com

www.springer-sbm.com

-----Original Message-----

From: Julie A Neer [<mailto:Julie.Neer@noaa.gov>]

Sent: Wednesday, March 09, 2005 4:46 PM

To: Weijman, Inge, Springer NL

Subject: copyright permission EBFi MS-3775-04

Dear Inge-

I received your reprint permission letter for my upcoming manuscript (EBFi MS-3775-04) in the mail today. (The original request is pasted below.) Unfortunately, I see that the permission excluded use in an electronic form. All theses and dissertations at my University (Louisiana State University - Baton Rouge, Louisiana, USA) are electronic. It is a University requirement and paper copies are not acceptable. The University requires all dissertations to be available electronically to registered students and faculty of LSU immediately, and to the public after one year. I'm writing to determine what needs to be done to get the electronic exclusion removed.

Also, the letter indicates that the "Material may not be republished until at least one year after our publication date". I do not know when my manuscript will be published but I am aware that EBFi has a long backlog from acceptance to publication. (A colleague's paper took over a year.) However, my dissertation must be turned in by 20 May 2005, which will most likely be BEFORE my manuscript is even published by the Journal. I'm not sure what to do about this.

Your help with these matters will be greatly appreciated. My contact information is listed below.

Thank you.

Julie A. Neer

Hi Ingrid,

Could you please handle Dr. Neer's request? Thanks! Best, Suzanne

From: Julie A Neer [<mailto:Julie.Neer@noaa.gov>]

Sent: vrijdag 4 februari 2005 17:50

To: Mekking, Suzanne, SV NL

Subject: copyright permission

Dear Suzanne-

Lynn Bouvier informed me that I need to contact you regarding copyright permission for my In Press manuscript in Environmental Biology of Fishes (MS-3775-04). The research presented in the manuscript is part of my dissertation research at Louisiana State University. Since the manuscript has now been accepted and is In Press, I am required to get permission to include it as part of my dissertation, even through it is not published yet. I require a letter for Permission from the journal to be included in the dissertation as an Appendix, and to add text stating "Reprinted with permission from Environmental Biology of Fishes". If this email request is not sufficient, please let me know what I need to do to acquire this permission.

If you have any further question, please contact me via email, or at the phone number or address below. Thanks you for your help in this matter. I look forward to hearing from you.

Julie A. Neer

Julie A. Neer

Graduate Research Fellow

3500 Delwood Beach Road

Panama City, FL 32408

(850) 234-6541 ext. 240 julie.neer@noaa.gov

VITA

Julie Ann Neer was born on 5 February 1970, in Chicago, Illinois. She is the daughter of Dr. David D. and Carol R. Neer and older sister of R. Jeffery Neer. She attended Glenbrook North High School in Northbrook, Illinois, graduating in 1988. Julie graduated from California State University – Long Beach in August 1993 with a Bachelor of Science degree in marine biology. She earned her Master of Science degree in marine science at Moss Landing Marine Laboratories (MLML) through San Jose State University in August 1998. She worked as a Research Technician at MLML examining the artisanal elasmobranch fishery in the Gulf of California before entering the doctoral program in the Department of Oceanography and Coastal Sciences at the Louisiana State University in the summer of 1999. Her major professors were Dr. Kenneth A. Rose and Dr. Bruce A. Thompson. Julie was awarded a three-year National Marine Fisheries National (NMFS) - Sea Grant Fellowship in Population Dynamics and Marine Resource Economics, which funded her dissertation research and allowed her to conduct the majority of her research at the NMFS lab in Panama City, Florida. Her NMFS Mentors were Drs. Enric Cortés and John K. Carlson. She will earn her doctoral degree in oceanography and coastal sciences in August 2005.